

UNIVERSIDADE FEDERAL DO PARANÁ

BRUNO GOMES DE SOUZA

REGISTRO SEDIMENTAR DE UM SISTEMA GLÁCIO-MARGINAL DA FORMAÇÃO
RIO DO SUL (NEOPALEOZOICO DA BACIA DO PARANÁ, SUDOESTE DO
GONDWANA): TRANSIÇÕES DE FLUXOS E IMPLICAÇÕES DEPOSICIONAIS

CURITIBA

2021

BRUNO GOMES DE SOUZA

REGISTRO SEDIMENTAR DE UM SISTEMA GLÁCIO-MARGINAL DA
FORMAÇÃO RIO DO SUL (NEOPALEOZOICO DA BACIA DO PARANÁ,
SUDOESTE DO GONDWANA): TRANSIÇÕES DE FLUXOS E IMPLICAÇÕES
DEPOSICIONAIS

Dissertação apresentada ao Programa de Pós-Graduação em Geologia, Setor de Ciências da Terra, Universidade Federal do Paraná, como requisito parcial à obtenção do título de Mestre em Geologia.

Orientadora: Prof(a). Dr(a). Carolina Danielski Aquino

Coorientador: Prof. Dr. Fernando Farias Vesely

CURITIBA

2021

Catálogo na Fonte: Sistema de Bibliotecas, UFPR
Biblioteca de Ciência e Tecnologia

S729r

Souza, Bruno Gomes de

Registro sedimentar de um sistema glácio-marginal da formação Rio do Sul (neopaleozoico da Bacia do Paraná, sudoeste do Gondwana): transições de fluxos e implicações deposicionais [recurso eletrônico] / Bruno Gomes de Souza. – Curitiba, 2021.

Dissertação - Universidade Federal do Paraná, Setor de Ciências da Terra, Programa de Pós-Graduação em Geologia, 2021.

Orientador: Carolina Danielski Aquino – Coorientador: Fernando Farias Vesely.

1. Análise de sedimentação. 2. Sedimentos (Geologia). 3. Período glacial. I. Universidade Federal do Paraná. II. Aquino, Carolina Danielski. III. Vesely, Fernando Farias. IV. Título.

CDD: 551.303

Bibliotecário: Elías Barbosa da Silva CRB-9/1894



MINISTÉRIO DA EDUCAÇÃO
SETOR DE CIÊNCIAS DA TERRA
UNIVERSIDADE FEDERAL DO PARANÁ
PRÓ-REITORIA DE PESQUISA E PÓS-GRADUAÇÃO
PROGRAMA DE PÓS-GRADUAÇÃO GEOLOGIA -
40001016028P5

TERMO DE APROVAÇÃO

Os membros da Banca Examinadora designada pelo Colegiado do Programa de Pós-Graduação GEOLOGIA da Universidade Federal do Paraná foram convocados para realizar a arguição da Dissertação de Mestrado de **BRUNO GOMES DE SOUZA** intitulada: **REGISTRO SEDIMENTAR DE UM SISTEMA GLÁCIO-MARGINAL DA FORMAÇÃO RIO DO SUL (NEOPALEOZOICO DA BACIA DO PARANÁ, SUDOESTE DO GONDWANA): TRANSIÇÕES DE FLUXOS E IMPLICAÇÕES DEPOSICIONAIS**, sob orientação da Profa. Dra. CAROLINA DANIELSKI AQUINO, que após terem inquirido o aluno e realizada a avaliação do trabalho, são de parecer pela sua APROVAÇÃO no rito de defesa.

A outorga do título de mestre está sujeita à homologação pelo colegiado, ao atendimento de todas as indicações e correções solicitadas pela banca e ao pleno atendimento das demandas regimentais do Programa de Pós-Graduação.

CURITIBA, 29 de Outubro de 2021.

Assinatura Eletrônica

03/11/2021 14:52:26.0

CAROLINA DANIELSKI AQUINO

Presidente da Banca Examinadora

Assinatura Eletrônica

04/11/2021 15:58:35.0

CLAUS FALLGATTER

Avaliador Externo (UNIVERSIDADE FEDERAL DE PERNAMBUCO)

Assinatura Eletrônica

03/11/2021 15:12:56.0

VICTORIA VALDEZ BUSO

Avaliador Interno Pós-Doc (UNIVERSIDADE FEDERAL DO PARANÁ)

DEPARTAMENTO DE GEOLOGIA-CENTRO POLITÉCNICO-UFPR - CURITIBA - Paraná - Brasil

CEP 81531-990 - Tel: (41) 3361-3365 - E-mail: posgeol@ufpr.br

Documento assinado eletronicamente de acordo com o disposto na legislação federal Decreto 8539 de 08 de outubro de 2015.

Gerado e autenticado pelo SIGA-UFPR, com a seguinte identificação única: 124236

Para autenticar este documento/assinatura, acesse <https://www.prppg.ufpr.br/siga/visitante/autenticacaoassinaturas.jsp> e insira o código 124236

Dedico este trabalho aos meus pais Rosméri e Joaquim.

AGRADECIMENTOS

Agradeço primeiramente aos meus pais Rosméri e Joaquim por seu amor incondicional e por sempre me incentivarem a ir atrás dos meus sonhos e objetivos.

A minha orientadora, professora Carolina Danielski Aquino por compartilhar todo o seu vasto conhecimento, pela oportunidade de realizar esse trabalho, e por me apoiar nos momentos difíceis que passei durante a dissertação. Com certeza, será uma convivência que jamais esquecerei.

Ao meu Coorientador, professor Fernando Farias Vesely, por compartilhar seu conhecimento vasto, e principalmente por me conceder diversas oportunidades desde meu tempo de graduação, que com certeza me qualificaram como pesquisador para que eu chegasse nesse momento melhor preparado. Agradeço muito.

Ao Programa de Pós-Graduação em Geologia da Universidade Federal do Paraná pela oportunidade de realizar um projeto de mestrado em alto nível.

Ao Laboratório de Análise de Bacias (LABAP) por me acolher desde a época que era um graduando de outra universidade e por me proporcionar toda a estrutura para a realização deste trabalho. Agradeço também aos meus colegas e amigos de laboratório Leonardo, Thammy, Hugo, Deise, Ronaldo, Aurora, Mérolyn, Lara, Bruno e Nicole. Especialmente aos colegas Deise, Ronaldo e Lara por me auxiliarem nos trabalhos de campo.

À Universidade Federal do Paraná, pela oportunidade e por toda a estrutura para a realização deste trabalho. Confesso que poder estudar na universidade de maior excelência do estado do Paraná foi um sonho realizado.

À Petrobrás pelo financiamento desta pesquisa e pela concessão de bolsa de estudos através do Termo de Cooperação 2016/00284-7.

Aos meus amigos da república da Lindinha: Brita, Hugo, Jun, Maciel e Catarina. Ter a sua amizade e parceria durante todos esses meses foi essencial para que esse projeto fosse realizado. Um agradecimento especial a Lindinha, mascote da casa, que infelizmente nos deixou esse ano. Ela era um ser de muito amor e luz e com certeza está cuidando de nós em um outro lugar.

A todos os cientistas brasileiros por toda a sua luta e perseverança durante períodos tão sombrios, dominados pelo negacionismo.

***“A wizard is never late, Frodo Baggins. Nor is he early.
He arrives precisely when he means to”***

Gandalf, the Grey

Lord of the Rings: The Fellowship of the Ring

By J.R.R Tolkien

RESUMO

Embora o conhecimento acerca de sistemas glácio-marginais seja extenso, o reconhecimento de algumas formas de leito no registro antigo destes ambientes ainda é escasso, especialmente aquelas que se referem ao regime de fluxo supercrítico. Este trabalho visa portanto, colaborar com a caracterização destas formas de leito no registro antigo, assim como as transições de fluxo intrínsecas a elas. Foi selecionada uma sucessão cascalhosa de 60 m de espessura localizada no município de Presidente Getúlio – SC, composta por: conglomerados, arenitos e diamictitos depositados durante a Glaciação Neopaleozoica (GNP) na Bacia do Paraná, na unidade conhecida como Formação Rio do Sul (topo do Grupo Itararé). O foco central do estudo se dá na caracterização faciológica destas litologias, visando identificar a possibilidade de ocorrência de formas de leito relacionadas a fluxos supercríticos nestes depósitos da GNP. Para realizar tal estudo foram descritas as fácies sedimentares, levantados perfis sedimentológicos de detalhe e medidas paleocorrentes ao longo do intervalo de interesse. Na base da sucessão, foram descritos diamictitos foliados que foram interpretados como produto de gláciotectônica. Acima deste substrato gláciotectonizado se depositam conglomerados, diamictitos e arenitos que foram interpretados como produto de sedimentação glácio-marginal compartimentada em duas partes, uma porção subglacial restrita (*grounding-zone wedge*) e uma porção subaquática (*grounding-line fan*) depositada sobre um talude submarino. Na porção subaquática observa-se que o principal mecanismo de deposição são os *wall-jets*. Em termos de faciológicos, foram observadas formas de leito que representam desde o salto hidráulico (estruturas de corte e preenchimento, *backsets*, e aglomerados de clastos), o estabelecimento de um fluxo supercrítico (antidunas lenticulares), a transição para um fluxo subcrítico (*humpback dunes*), e o estabelecimento de um fluxo subcrítico (dunas subcríticas). Distalmente os jatos tendem a transicionar de fluxos dominados por momento para fluxos gravitacionais depositando antidunas sinusoidais e *climbing ripples*. Fluxos de detritos também contribuíram para a arquitetura do leque. Muitas vezes eles podem apresentar uma componente de hidroplanagem que leva a deposição de turbiditos do tipo *surge* associados a estes fluxos coesivos. A acumulação de diamictitos com feições de ressedimentação no topo da sucessão é interpretada como um depósito de transporte em massa (DTM) com diferentes níveis de homogeneização. A intercalação entre produtos relacionados aos *wall-jets* e fluxos de detritos ao longo da sucessão é interpretada como uma sedimentação bimodal construída a partir de múltiplos eventos únicos de sedimentação. A partir da análise de paleocorrentes (tendência de transporte para NW), sugere-se que a fonte glacial dos sedimentos esteja localizada na Namíbia. Em conjunto a isso, de acordo com o contexto deposicional observado, propõe-se que esse avanço glacial se deu em um ambiente marinho.

Palavras chave: Fluxos supercríticos; *Wall-jets*; *Grounding-line fans*; Era glacial Neopaleozoica.

ABSTRACT

Although the knowledge of glacial-marginal systems is extensive, recognizing some of their bedforms in the ancient record still needs to be improved, especially those related to supercritical flows. Therefore, this work aims to collaborate with the characterization of these bedforms in the ancient record and the flow transitions linked to them. To execute this work, we selected a gravelly succession located in the region of Presidente Getúlio – SC, composed of conglomerates, sandstones, and diamictites. This succession was deposited during the Late Paleozoic Ice Age (LPIA) in the Paraná Basin, at the Rio do Sul Formation (the basal portion of the Itararé Group). The main focus of this study is the faciological characterization of these lithologies, aiming to the recognition of supercritical flow bedforms at these deposits of the LPIA. Were described the sedimentary facies, raised sedimentological logs, and collected paleocurrent measures when available. At the base of the succession were described foliated diamictites that were interpreted as a product of glaciotectonics. Directly above the glaciotectonized conglomerates, sandstones, and diamictites occur. These facies were interpreted as the result of glacial-marginal sedimentation subdivided into two parts: a restricted subglacial portion (grounding-zone wedge) and a subaquatic portion (grounding-line fan) that was deposited in a submarine slope. It was observed that the primary mechanism of deposition in the subaquatic context is the wall-jets. In faciological terms were observed bedforms that represent the entire specter of flow transition in a wall-jet context: The hydraulic jump (scour-fill structures, backsets, and clast clusters), the establishment of a supercritical flow (lenticular antidunes), the transition into a subcritical flow (humpback dunes), and the establishment of a genuine subcritical flow (subcritical dunes). Distally, the jets tend to evolve from momentum-dominated flows to gravity-flows depositing sinusoidal antidunes and climbing ripples. Debris flows also contributed to the fan architecture. They can present a hydroplaning component that could lead to the deposition of surge-type turbidites associated with these debris flows. The accumulation of diamictites with ressedimentation features at the top of the succession is interpreted as a mass-transport deposit (MTD) containing different levels of homogenization. The interbedding of products related to the wall-jets and the debris flows along the record is interpreted as bimodal sedimentation built from multiple single flood events. From our paleocurrent analysis (NW paleotransport tendency), it is suggested that the glacial source of the sediments is located in Namibia. Following that, according to our depositional context are proposed that this glacial advance took place in a marine environment.

Keywords: Supercritical flows; Wall-jets; Grounding-line fans; Late Paleozoic Ice Age.

LISTA DE FIGURAS

Figura 1 – Localização e contexto geológico da área de estudo. A) Localização da área aflorante do Grupo Itararé e da área de estudo na Bacia do Paraná (Modificado de Vesely & Assine, 2006). B) Contexto Geológico e estratigráfico da área de estudo. No mapa geológico estão dispostos os pontos mapeados e os perfis sedimentológicos levantados por esse estudo. As unidades de mapeamento expostas no mapa e no perfil sedimentológico foram adaptadas de Schemiko <i>et al.</i> (2019).....	19
Figure 2 - Localization and geological setting of the study area. A) Localization of the outcrop belt of the Itararé Group and the study area in the Paraná Basin (adapted from Vesely and Assine, 2006). B) Stratigraphical and geological setting of the study area. In the geological map are disposed of the mapped points and the sedimentological logs raised in this study. The map units on the sedimentological log and the geological map were adapted from Schemiko et al. (2019).....	27
Figure 3 - Stratigraphic logs of the study interval. A) Composite log of the study interval. B) There are seven logs that were raised for the study of the interval. In the legend, we have the described structures, the five facies associations, and the substrate of the succession. The locations of the sedimentary logs are in figure 2. ...	39
Figure 4 – Main features of the glaciotectionized substrate and the basal lithologies of the Rio do Sul Formation. A) Ressedimented diamictites on the base of the study interval. In the bottom part of the outcrop, we can observe the shales. B) Basal shales. In the upper portion of the picture, they have deformed bedding. C) Disposition of the glaciotectionized substrate in relation to the early-stage fan deposits. We can observe an erosive contact between the substrate and the first deposits of the fan. D) Detail of figure 4C. We can keep in detail the erosive contact between the two facies associations. Also important to note is the occurrence of scratched boulder-sized clasts composing the Dfl facies. E) Detail of figure 4C. In this figure, we can observe in detail the features which comprise the Dfl facies. Firstly, we see how the foliation is more prominent in portions with a higher mud content. In contrast, parts with more extensive sand and gravel tend to be more massive and not develop foliation. Another critical aspect is how the foliation tends to be more folded around larger clasts (cobble and Boulder size). In the right portion of the figure, we see the foliation presenting recumbent folds. The boudins have a sandy composition and a massive structure. Finally, look at how some clasts show fractures. They are	

mainly pebble-sized. F) Details of the interpretations of figure 4E. For the composition of the clasts - SM: Sand massive; CR: Crystalline.39

Figure 5 – Features related to the Gbd facies. A) Oversized boulder of 6m length. This boulder presents polished surfaces with some angular edges as well. B) Folded bedding of stratified portions of the Gbd facies, that portion of the Gbd facies could present some imbricated boulders with lenticular deformed beds of clast-supported conglomerates associated (Gmc facies). C) Interpretation of the figure 5B.44

Figure 6 – Variability of the the basal deposits of the ESFD. A) Interbedding of between massive sandstones (Sm facies), clast-supported conglomerates (Gmc facies) and lenticular sandstones with antidunes (Slad facies). Note the scoured bases at the contacts between the facies. B) Interpretation of the figure 6A. C) Detail a lenticular antidune deposit (Slad facies). Look how are irregular the contacts between the surrounding facies. D) Interpretation of the figure 6C. E) Heterolithes (Ht facies) composed of the intercalation of lenticular beds of sandstones and mudstones which are deformed. F) Folded beds containing the deformed heterolithes (Ht facies). G) Massive diamictites (Dmm facies) interbedded with lenticular sandstones with antidunes (Slad facies) containing some through-stratified sandstones representing backsets (Gt facies). H) Detail of the Gt facies backset of figure 6G.46

Figure 7 – General features of the scoured conglomerates and sandstones of the ESFD. A) Photomosaic of the outcrop of Gruta da Pimenta, located on the southern sector of the study area. Here we can observe how the scours are disposed of, their fills, and the deformation structures associated with these deposits. B) Interpretation of the figure 7A. Here we can observe the different order of scours. In red, the second-order scours, which are related to contacts between individual strata. In green, the first order scours corresponding to more extensive surfaces which subdivide groups of individual scours. If we observe the strata between the two first-order scours, we can see beds dipping to SE. These beds have a similar dip angle and direction and are associated with the deposition of an unic macroform. Above the second first-order scour, we see that the beds don't dip in the same direction as those located under the first-order scour surface. These differences in the dip direction of the beds are attested for the deposition of sigmoidal through-cross bedded conglomerates (Gt facies) above the second first-order scour surface.....48

Figure 8 – Feature details of the scoured conglomerates and associated facies in the ESFD. A) Deep incised scours in through-cross bedded conglomerates (Gt facies).

Here we observe a set of deep scours containing through cross stratifications dipping to both sizes, indicating that some of the stratifications are backsets. We measure the paleoflow from climbing-rippled sandstones located at the base of the outcrop. B) Sigmoidal through-cross bedded conglomerates (Gt facies), here we attest a change in the paleoflow at the outcrop, this change in the occur above the second high order scour (fig. 7). C) Metric flame structure located in the contact between some sandstones and fine-grained facies. D) Decametric bed of clast-supported conglomerates (Gmc facies). In the figure 6, we can see that these conglomerates extend for more than 10 meters along the outcrop. E) Sinusoidal sandstones with antidunes (Ssad facies). This sandstones were described at the foresets of the macroform stablished between the two high-order scours exposed in figure 7.49

Figure 9 – Mainly features of the massive diamictites (Dmm facies). A) Main fabric of the Dmm facies. The diamictites are characterized by a muddy matrix containing dispersed clasts and a massive structure. A common aspect is the deposition of lenticular sandstone beds, which are commonly deformed. B) Clast-supported conglomerates and antidune sandstones associated with the Dmm facies. C) Huge massive clast-supported conglomerate bed. D) Here, we can see a portion where the conglomerates are deformed, containing an injected aspect and, in some cases mixing yourself with the matrix of the diamictite. We also observe that associated with the conglomeratic beds, coarse-grained sandstones with antidunes occur. E) Detail of an injected bed of conglomerate a fluidized sandstone with antidune lamination. F) Faults and boudins are associated mainly with fine-grained sandstones interbedded with the diamictite matrix. We highlighted the major fault plans which are related to the fault genesis and consequently the boudins.....50

Figure 10 – Features related to clast organization and deposition at the ESFD. A) Metric granite clast deposited along a bed of a massive diamictite. This clast is described as a lonestone. Hammer for scale. B) Striated granite clast in a massive conglomerate bed (Gm facies). C) Clast cluster deposited at the top of an massive matrix-supported conglomerate (Gm facies). D) Organization of a set of beds of normally graded conglomerates (Gn facies).....52

Figure 11 – Features related to sandstone deposition along the ESFD. A) Massive sandstone bed containing tool marks at your base. B) Groove and Chevron marks are presented in the massive sandstone bed of figure 11A. C) Lenticular bed of climbing-rippled sandstone (Sr facies) deposited between beds of massive diamictite

(Dmm facies). D) Association of beds of climbing-rippled sandstones (Sr facies) and through cross-stratified sandstones (St facies), the contact between the beds are transitional, containing small scours between them. E) Continuous set of sandstones containing sinusoidal antidunes (Ssad facies). Look how the antidunes are extensive, containing a metric length.53

Figure 12 - Facies and features described in the late-stage fan deposits (LSFD). A) Larger exposer to the LSFD in a road cut in the southern sector of the study area (CT log). Here we can observe the main character of the LSFD with the irregular interbedding between massive diamictites and massive sandstones. Firstly, we can see that the sandstones vary from a tabular to a lenticular geometry, with some beds containing a chaotic geometry (upper portion of the outcrop). Another character to observe is the presence of scoured bases in the lenticular sandstone beds. The Dmm beds also present multiples geometries varying from tabular to lenticular and sometimes are sandwiched between the sandstone beds. B) Contact between massive diamictites and massive sandstones. We highlighted the occurrence of lonestones in the diamictite bed. Another essential feature that remains similar to those massive diamictites deposited in the ESFD is sheared sandstone beds dispersed among the diamictites' matrix. C) Detail to the sheared sandstone beds in figure 12B. D) Centimetric bed of clast-supported conglomerates deposited between two horizons of diamictites. E) Aspect of the normally graded conglomerates deposited in the LSFD.62

Figure 13 – Mainly features of the Dm(r-ht) facies. A) WT-2 outcrop showing the main fabric of the heterogeneous diamictites. In this outcrop, we can observe some critical features that compose these facies. Firstly at the base of the outcrop, we have relicts of the LSFD that remains almost undeformed. Laterally we observe how the rate matrix/clasts tend to increase to the upper portion of the outcrop. B) Internally deformed block of sandstone containing boudins, faults, and sheared beds. C) Highlighted conglomerate block in the WT-2 outcrop. D) Outcrop of the SCD in the southern sector of the study area. Here we can observe how the sandstone blocks tend to become smaller and discontinuous towards the upper portion of the outcrop, increasing the matrix content.66

Figure 14 – Main Features of the Dm(r-hm) facies. A) Picture of the WT-1 outcrop showing a thoroughly homogenized diamictite with a high matrix content. B) Fabric of the homogenized diamictites. Here we can observe a homogeneous muddy-matrix

with dispersed clasts ranging from granule to cobble-size. Note that some of the clasts are angular. C) Centimetric sheared sandstone bed deposited in the homogeneous diamictites.....67

Figure 15 – Rose diagrams with the paleocurrent data analyzed for the ESFD succession. The locations of the outcrops are available in figure 1, with the mean direction of each rose diagram. A) Directions of the NSF outcrop. B) Directions of the BT outcrop. C) Directions of the PT outcrop. D) Directions of the AE outcrop. E) Directions of the CT outcrop. F) Compose diagram containing all the paleocurrent data collected in the ESFD succession.71

Figure 16 – Schematic depositional model proposed for the evolution of the grounding-line fan system at the Presidente Getúlio region (out of scale).83

LISTA DE TABELAS

Table 1– Facies table with the main characteristics of the described lithologies, their frequency, and the interpreted processes related to their genesis.	37
---	----

LISTA DE ABREVIATURAS OU SIGLAS

GNP – Glaciação Neopaleozoica

DTM – Depósito de transporte em massa

LPIA – Late Paleozoic Ice Age

MTD – Mass-transport deposit

ESFD – Early-stage fan deposits

LSFD – Late-stage fan deposits

SCD – Slope collapsed deposits

LISTA DE SÍMBOLOS

Fr – Froude Number

SUMÁRIO

1. INTRODUÇÃO E ÁREA DE ESTUDO	18
1.1 Objetivo Geral e Específicos	20
2. CONTEXTO GEOLÓGICO	20
3. MATERIAIS E MÉTODOS	22
4. ANÁLISE E DISCUSSÃO DOS RESULTADOS	24
4.1 Introduction	26
4.2 Wall-jets in Grounding-Line Fans	28
4.3 Geological Setting	30
4.4 Methods	31
4.5 Results	32
4.5.1 Facies associations	32
4.5.1.1 Glaciotectonized substrate	32
4.5.1.2 Early-stage fan deposits	41
4.5.1.3 Late-stage fan deposits	60
4.5.1.4 Slope collapsed deposits	64
4.5.2 Paleocurrents	70
4.6 Discussion	73
4.6.1 Depositional environment and flow transitions	73
4.6.2 Depositional events and sediment source	83
4.7 Conclusions	85
5. CONSIDERAÇÕES FINAIS	86
6. REFERÊNCIAS	88

1. INTRODUÇÃO E ÁREA DE ESTUDO

Diversos autores tem desenvolvido trabalhos de cunho faciológico com foco em estudos paleogeográficos e paleoambientais em sistemas glácio-marginas do Grupo Itararé (registro da Glaciação Neopaleozoica (GNP) da Bacia do Paraná (fig. 1A) (Vesely, 2001; Vesely *et al.*, 2015; Aquino *et al.*, 2016; Mottin *et al.*, 2018; Fallgatter & Paim, 2019; Fedorchuk *et al.*, 2019; Rosa *et al.*, 2019). Porém, ainda são escassos, trabalhos que relacionem as descargas de água de degelo produzidas durante a sedimentação desses sistemas com a morfodinâmica desses fluxos e suas respectivas formas de leito dentro da unidade. Dentro de sistemas glácio-marginais, sistemas do tipo *grounding-line fan* possuem uma dinâmica intrínseca com descargas de águas de degelo, sendo alvo desse tipo de estudo em registros mais recentes (Russell & Arnott, 2003; Hornung *et al.*, 2007; Russell, 2007; Winsemann *et al.*, 2009; Lang & Winsemann, 2013; Lang *et al.*, 2017).

Tais sistemas são alimentados por túneis englaciais/subglaciais que desaguam em um corpo d'água a montante (Powell & Molnia, 1989; Powell, 1990; Lønne, 1995). Esse tipo de dinâmica, onde os túneis de água de degelo previamente confinados deságuam em um corpo d'água faz com que o fluxo se expanda e desalecere passando de um fluxo supercrítico ($Fr > 1$) para um fluxo subcrítico ($Fr < 1$) (Powell, 1990; Russell & Arnott, 2003; Hornung *et al.*, 2007; Winsemann *et al.*, 2009). Devido a esse tipo de comportamento, a visualização das fácies relacionadas a esse tipo de sistema deposicional se faz essencial para que se possa compreender a relação entre os eventos de descarga glacial, as transições de fluxo e suas respectivas formas de leito.

Porém, dentro desse tipo de contexto, apenas o trabalho de Aquino *et al.* (2016) se propôs a compreender as formas de leito relacionadas a esse tipo de sistema no contexto da GNP na Bacia do Paraná. Dentro do trabalho foram identificadas algumas características que poderiam ser relacionadas a ação de fluxos supercríticos como estruturas de corte e preenchimento, e mudanças abruptas de granulometria (Aquino *et al.*, 2016). Porém, não foram evidenciadas formas de leito como antidunas, *cyclic-steps* ou *chute and pools*, tipicamente associadas a fluxos supercríticos nestes tipos de sistema deposicional (Lang *et al.*, 2021b).

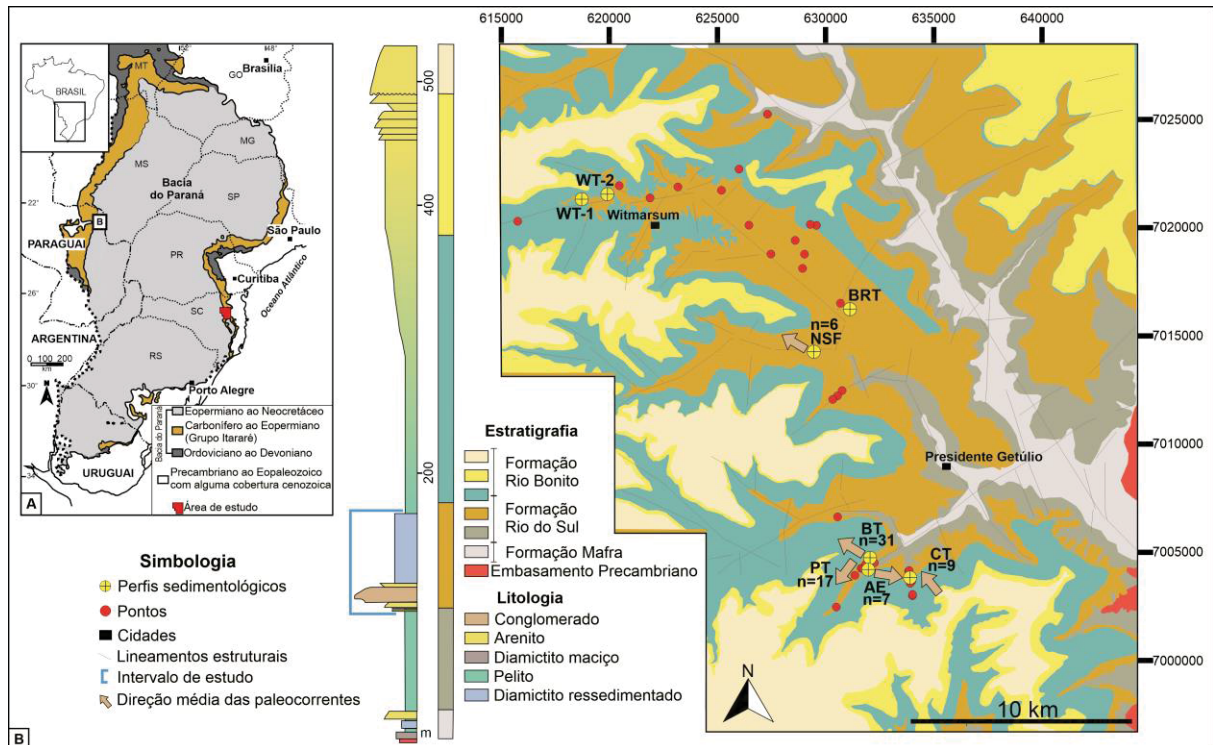


Figura 1 – Localização e contexto geológico da área de estudo. A) Localização da área aflorante do Grupo Itararé e da área de estudo na Bacia do Paraná (Modificado de Vesely & Assine, 2006). B) Contexto Geológico e estratigráfico da área de estudo. No mapa geológico estão dispostos os pontos mapeados e os perfis sedimentológicos levantados por esse estudo. As unidades de mapeamento expostas no mapa e no perfil sedimentológico foram adaptadas de Schemiko *et al.* (2019).

Tendo isso em vista, o presente trabalho visa auxiliar na compreensão destes fluxos dentro do contexto da GNP na bacia. Tal estudo, tem como foco uma sucessão de cerca de 60m localizada na região de Presidente Getúlio, centro-leste do estado de Santa Catarina (Fig. 1B). Essa sucessão heterogênea é composta por conglomerados, arenitos e diamictitos, onde alguns desses diamictitos apresentam feições de ressedimentação. Tais depósitos foram alvo do estudo de Schemiko *et al.* (2019), que relacionaram esses depósitos a fluxos gravitacionais canalizados em um talude submarino alimentado por uma costa não glaciada. Porém, muitos dos depósitos arenosos e conglomeráticos analisados por Schemiko *et al.* (2019), são similares a aqueles interpretados por Aquino *et al.* (2016) como registros de um *grounding-line fan*. Devido a isso, o presente estudo visa detalhar esses depósitos, tentando compreender se sua gênese pode estar ou não relacionada com a deposição de um sistema glácio-marginal.

1.1 Objetivo Geral e Específicos

O principal objetivo desse trabalho é investigar se essa sucessão representa a deposição de um sistema glácio-marginal ou um sistema que não possui uma relação direta com o gelo (e.g., leques submarinos ou leques deltaicos). Considerando que esse sistema pode representar a deposição de um sistema do tipo *grounding-line fan*, é proposto também uma série de questões acerca do comportamento deste sistema deposicional: 1) Se observa a presença de formas de leito relacionadas a fluxos supercríticos? 2) Se sim, quais delas? 3) Como é a transição de fluxo partindo de um regime supercrítico para um regime subcrítico? 4) Qual é o espectro de fluxos gravitacionais de sedimentos observados na área de estudo? 5) Existe alguma relação entre a concentração de sedimentos nos fluxos gravitacionais e as respectivas formas de leito? 6) Foi observado alguma deformação glacioteclônica ao longo da sucessão? 7) Qual é o significado da deposição de diamictitos com feições de ressedimentação no topo da sucessão? 8) Qual é o caráter dos eventos deposicionais (múltiplos ou único) que construíram a arquitetura deposicional do sistema? 9) Onde está localizada a fonte glacial que proveu sedimentos para o sistema?

2. CONTEXTO GEOLÓGICO

A bacia do Paraná é uma das maiores bacia intracratônicas da América do Sul. A bacia ocupa uma área de 1.500.000 km² no Brasil, Argentina, Paraguai e Uruguai e pode atingir até 7.000 m de espessura em seu depocentro (Zalán *et al.*, 1987; Milani *et al.*, 2007). O Grupo Itararé, depositado entre o Carbonífero e o Permiano tem seu registro estratigráfico controlado por avanços glaciais vindo de áreas circundantes em direção a Bacia do Paraná (Eyles *et al.*, 1993; Santos *et al.*, 1996; Vesely *et al.*, 2015; Rosa *et al.*, 2016; Mottin *et al.*, 2018). Essa dinâmica de avanços e recuos, resulta em um arquitetura composta por ciclos de granodecrescência ascendente, abrigando ambientes deposicionais continentais, transicionais e marinhos com diversos níveis de influência glacial (Franca & Potter, 1988; Vesely & Assine, 2006). Nesses ciclos a base é composta por conglomerados e arenitos que tendem a gradar para diamictitos maciços e pelitos no topo das sucessões (Schneider *et al.*, 1974; Franca & Potter, 1988; Vesely & Assine, 2004, 2006). Vesely (2001), compreende que esses ciclos granodecrescentes, poderiam

representar uma deposição glácio-marinha. Além disso, por representar ambientes marinhos, o autor propõe que a base conglomerática representaria a deposição de *grounding-line fan* (leques de *outwash* subaquosos na nomenclatura do referido trabalho).

Para a região sudeste do estado do Paraná e para todo o estado de Santa Catarina uma estratigrafia baseada em afloramentos propõe dividir esses ciclos granodescrescentes em três unidades (da base para o topo): Formação Campo do Tenente, Formação Mafra, e Formação Rio do Sul (Schneider et al., 1974). Dentro da área de estudo, de acordo com Schemiko *et al.* (2019), apenas duas dessas formações afloram, Mafra e Rio do Sul. A exposição da Formação Mafra é bastante limitada e é restrita a alguns poucos metros. Já a Formação Rio do Sul é bem exposta e pode atingir até 500 m de espessura (Schemiko *et al.*, 2019). Sobre o preenchimento, trabalhos prévios propõe que a deposição dessa unidade se deu em uma bacia marinha relativamente restrita (Castro, 1980; Canuto, 1993; Santos *et al.*, 1996). A porção basal e mediana da unidade representaria a deposição de um sistema marinho profundo e a porção superior relataria a progradação de um sistema deltaico sobre essa sub-bacia (Castro, 1980; Canuto, 1993; Santos *et al.*, 1996; Schemiko *et al.*, 2019).

O alvo deste trabalho é uma sucessão de 60 m de espessura depositada na porção interpretada previamente como marinho profunda (Castro, 1980; Canuto, 1993; Schemiko et al., 2019). Dentro desse pacote, observam-se conglomerados, arenitos e diamictitos. A afinidade desses depósitos com um ambiente marinho profundo se dá pelo contexto estratigráfico onde estas fácies estão depositadas. Acima e abaixo desses depósitos ocorrem espessos pacotes de folhelhos, sugerindo um contexto marinho profundo (Castro, 1980; Canuto, 1993; Schemiko *et al.*, 2019). A partir do contexto da deposição dos folhelhos adjacentes e das características destas fácies grossas, interpretações prévias sugerem fluxos gravitacionais em um talude submarino (Schemiko *et al.*, 2019) e leques submarinos (Canuto, 1993) (ambos contendo influência glacial) como as possíveis origens desses depósitos. Contudo, nenhuma pesquisa prévia estudou esses depósitos em detalhe. As publicações anteriores trabalharam com essa sessão como parte da sucessão completa da Formação Rio do Sul, estudando a área de estudo em um contexto

regional, com o enfoque no preenchimento e paleogeografia da sub-bacia como um todo (Castro, 1980; Canuto, 1993; Santos et al., 1996; Schemiko et al., 2019).

Porém, a principal questão envolvendo as interpretações prévias é a distância dos ambientes deposicionais propostos para a margem glacial. As características descritas nas fácies como matacões de dimensões métricas, *lonestones*, e clastos facetados e estriados poderiam ser indícios de que a margem da geleira não estaria tão distante do local de deposição como previamente proposto. Contudo, a ocorrência de folhelhos acima e abaixo da sucessão é interessante por sugerir uma configuração marinho profunda para a deposição, o que de certa forma é raramente associada com sistemas glácio-marginais.

3. MATERIAIS E MÉTODOS

O presente estudo é baseado em um mapeamento geológico dentro do pacote de interesse na região de Presidente Getúlio, centro-leste do estado de Santa Catarina. A área de estudo envolve cerca de 800 km². Foram visitados um total de 40 afloramentos, onde foram descritas as fácies e coletadas paleocorrentes quando possível. Devido a vegetação, a disposição dos afloramentos ao longo da área de estudo heterogênea, sendo difícil realizar o mapeamento dentro de uma malha regular de pontos. As melhores exposições estão concentradas em cavernas, grutas, cortes de estrada e cachoeiras. Dentro da área de mapeamento foram levantados um total de 7 perfis sedimentológicos em uma escala de 1:100 visando descrever os padrões de empilhamento faciológicos, e a variação vertical e lateral de fácies.

Em afloramentos extensos foram gerados fotomosaicos para analisar as variações laterais de fácies em conjunto com a disposição de formas de leito de maiores dimensão. Esse critério é importante, pois, algumas formas de leito geradas em contextos relacionados a fluxos supercríticos tendem a ter dezenas de metros de comprimento devido a magnitude dos fluxos (Russell & Arnott, 2003; Hornung *et al.*, 2007; Winsemann et al., 2009; Lang *et al.*, 2017, 2021a).

Visando uma normalização textural entre conglomerados e diamictitos, foi estabelecido um critério para diferenciar estas fácies. Aquelas que possuem uma matrix com uma razão areia/lama >1 foram descritas como conglomerados, já as

que possuem valores <1 foram descritas como diamictitos. Esse critério é importante devido a frequente similaridade entre essas litologias em afloramento. Em conjunto, foi utilizada a nomenclatura proposta por Mulder & Alexander (2001) para a interpretação de fluxos gravitacionais de sedimentos. Essa nomenclatura é baseada na concentração de sedimentos que compõe o fluxo gravitacional.

4. ANÁLISE E DISCUSSÃO DOS RESULTADOS

Os resultados, discussões e conclusões referentes a este trabalho serão apresentados na forma de um artigo científico que posteriormente será submetido para publicação em uma revista nacional ou internacional.

SEDIMENTARY RECORD OF A GLACIAL-MARGINAL SYSTEM OF THE RIO DO SUL FORMATION (NEOPALEOZOIC OF THE PARANÁ BASIN, SOUTHWESTERN GONDWANA): FLOW TRANSITIONS AND DEPOSITIONAL IMPLICATIONS

Abstract

The recognition of supercritical flow bedforms in grounding-line fan settings is still poorly constrained in the ancient record. Trying to improve the characterization of these bedforms and their flow transitions in Paleozoic deposits, we worked on a 60m gravel-rich succession composed of conglomerates, sandstones, and diamictites (including deformed ones at the top) deposited during the Late Paleozoic Ice Age (LPIA) in south-eastern Paraná Basin, Brazil. In this study, we want to test if we can identify bedforms related to supercritical flows in this LPIA succession and what is the meaning of these bedforms in terms of flow transitions and depositional architecture. To investigate this succession, we conducted a geological mapping in the region of Presidente Getúlio, center-east of the Santa Catarina state. The record is composed at the base by a glaciotectionized substrate overlaid by the deposition of a glacial-marginal system formed by a restrict subglacial segment (grounding-zone wedge) and a subaquatic portion (grounding-line fan) deposited in a slope break setting. During the deposition of the fan, we interpreted that the primary mechanism of deposition of the environment is the wall-jets. In terms of flow transitions, we described bedforms represents since the hydraulic jump (scour-fills, backsets, and clast clusters), supercritical flows (lenticular antidunes), the transition to a subcritical flow (humpback dunes), and the establishment of a genuine subcritical flow (subcritical dunes). Distally the jets tend to transit from momentum-dominated to gravity-dominated flows, depositing sinusoidal antidunes and climbing ripples. Debris flow is also an essential contribution to the deposition of the fan. These cohesive flows could contain a hydroplaning component, leading to the deposition of surge-like turbidites at the head of the debris flow. The accumulation of ressedimented diamictites at the top of succession is interpreted as mass-transport deposits (MTD), representing the collapse of the fan. The intercalation between wall-jet (conglomerates and sandstones) and debris flow (massive-diamictites) are interpreted as a bimodal sedimentation. We suggested that the architecture of the fan is built by multiple single-flood events, which leads to this bimodality and the vertical intercalation of bedforms during the sedimentary succession. From our paleocurrent analysis (NW transport trend), we suggest that the source of the sediments is located in Namibia, following several glacial records in the Itararé Group. Furthermore, according to the context of deposition, we suggested that this glacial advance took place in a marine environment.

Keywords: Supercritical flows; Wall-jets; Grounding-line fans; Late Paleozoic Ice Age.

4.1 Introduction

During the Carboniferous and Permian, multiple glaciation episodes during the Late Paleozoic Ice Age (LPIA) deposited glacial-influenced sediments in Gondwana basins (Crowell and Frakes, 1970; Isbell et al., 2003, 2012; Limarino et al., 2014). The Paraná Basin (southwestern Gondwana) contains one of the complete records of this glaciation, the Itararé Group (Fig. 2A) (Franca and Potter, 1988; Eyles et al., 1993; Santos et al., 1996; Vesely and Assine, 2006; Vesely et al., 2015; Valdez Buso et al., 2020). Some of the Itararé Group deposits are records of glacial margins reaching the Paraná Basin. These advances from the glaciers towards the basin create favorable conditions for the deposition of grounding-line fans, which several authors related (Vesely, 2001; Vesely and Assine, 2004, 2006; Aquino et al., 2016; Mottin et al., 2018; Fedorchuk et al., 2019; Rosa et al., 2019).

Despite recognizing several systems with characteristics of grounding-line fans in the Itararé Group, just the work of Aquino et al. (2016) identifies faciological features related to hydraulic jumps and the actions of supercritical flows (abrupt changes from gravel to sand-rich deposits and scour fills). However, still, they don't recognize bedforms like antidunes and cyclic steps, typically associated with the upper flow regime (Lang et al., 2021b).

According to Lang et al. (2021b), bedforms that represent the deposition of an upper flow regime in glaciogenic settings are widespread, along with the geological record. However, in grounding-line fans, these records are restricted to the quaternary, more specifically to Pleistocene deposits (Brennand, 1994; Russell and Arnott, 2003; Hornung et al., 2007; Russell, 2007; Winsemann et al., 2009; Lang and Winsemann, 2013; Lang et al., 2017). Lang et al. (2021b) propose that the non-existence of bedforms in the ancient geological record is associated not with the small potential of preservation of these bedforms but with the failures in recognizing these deposits. Our study tries to improve the characterization of these bedforms in the grounding-line fan ancient record, working on deposits of the Late Paleozoic Ice Age (LPIA) in southwestern Gondwana.

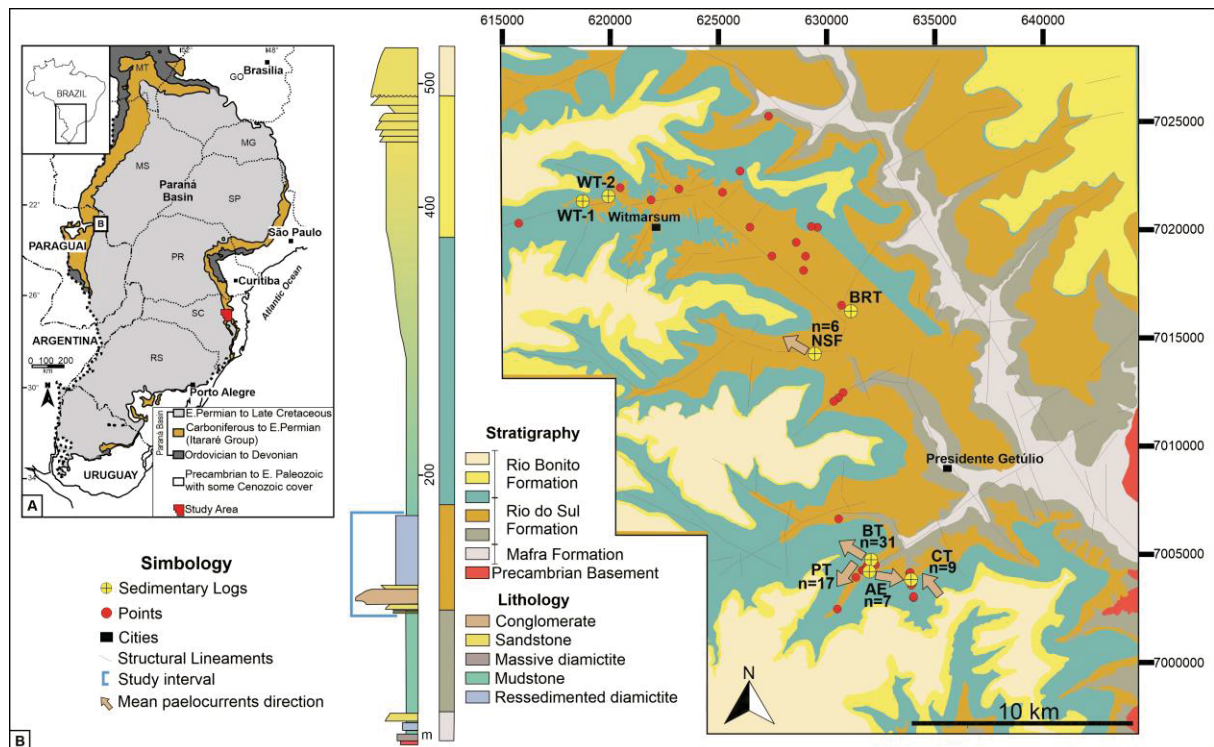


Figure 2 – Regional and local geological setting of the study area. A) Localization of the outcrop belt of the Itararé Group and the study area in the Paraná Basin (adapted from Vesely and Assine, 2006). B) Stratigraphical and geological setting of the study area. In the geological map are disposed of the mapped points and the sedimentological logs raised in this study. The map units on the sedimentological log and the geological map were adapted from Schemiko et al. (2019).

To improve the characterization of these flows and their bedforms in the LPIA record, we will study a 60 m gravel-rich succession (Fig. 2B) deposited in the south-eastern Paraná Basin. This record was the subject of study from Schemiko et al. (2019) and is composed of conglomerates, diamictites (including deformed ones on the top of succession), and sandstones with characteristics similar to those interpreted by Aquino et al. (2016) as grounding-line fan deposits. Schemiko et al. (2019) analyzed the succession as a deepwater turbidite system fed by a non-glaciated shoreline. However, the study of Schemiko et al. (2019) examined this gravel package as part of an interval of 500m in the upper portion of the Itararé Group. So, our study is the first to detail these deposits.

The central objective is to understand if these deposits could represent the deposition of a glacial marginal system or a system that doesn't have a relationship with the ice during their deposition instead (e.g., coarse-grained submarine fans or fan deltas). Considering that these deposits could represent a grounding-line fan, we want to propose a series of questions about the depositional aspects of the system. 1) Do we observe the presence of supercritical flow bedforms? 2) If yes, which of them? 3) How is the transition of the flow from a supercritical to a subcritical regime.

4) What is the specter of density flows observed in the area? 5) Do we keep a relationship between the sediment concentration and the bedforms related to them? 6) Do we see some glaciotectionic deformation in the record of the system? 7) What is the meaning of the accumulation of ressedimented diamictites on the top of the succession? 8) What is the character of the depositional events (multiple or singular events) that build up the depositional architecture of the system? 9) Where is located the glacial source that provides the sediments to the system?

4.2 Wall-jets in Grounding-Line Fans

Grounding-line fans are systems controlled by subglacial and englacial momentum jets that reach a water body (Eyles et al., 1989; Powell and Molnia, 1989; Powell, 1990; Lønne, 1995; Powell and Alley, 1997; Russell and Arnott, 2003; Hornung et al., 2007; Winsemann et al., 2009; Koch and Isbell, 2013; Lang and Winsemann, 2013; Aquino et al., 2016; Lang et al., 2017, 2021b). The jet causes a high-velocity flow that expands and decelerates when it gets to the water body (Rajaratnam and Subramanyan, 1986; Long et al., 1990, 1991; Roberts et al., 2001; Hoyal et al., 2003; Russell and Arnott, 2003; Hornung et al., 2007; Lang et al., 2021a). Due to the nature of these jets, buoyancy plumes could ascend, causing the deposition of fine-grained sediments (Powell, 1990; Lønne, 1995). Despite the high velocity flows, other mechanisms are common along these glacial margins. Gravity-flows can also occur. They trigger on the diamict wedges from basal portions of the glaciers, moved by gravity from the grounding zone to the water body, generating mass and sedimentary gravity flows (e.g., debris flow) (Eyles et al., 1985, 1989; Powell, 1990; Lønne, 1995). Another contributor to the sedimentation on these systems is the calving icebergs which can deposit sediments over the water body by ice-rafting (Eyles et al., 1985; Thomas and Connell, 1985; Powell, 1990; Lønne, 1995). Besides that, the glacial margins are still subject to their dynamics (advances and retreats), with your deposits being prone to be eroded by the glacier or deformed by glaciotectionics (Van der Wateren, 2002; McCarroll and Rijdsdijk, 2003; Phillips, 2018).

Despite all those essential processes on a glacial margin, one mechanism stands out in the sedimentation of these systems, the wall-jets (Powell, 1990; Lønne, 1995; Russell and Arnott, 2003; Hornung et al., 2007; Winsemann et al., 2009; Lang et al., 2021b, 2021a). Wall-jets are flows that emerge from confined conditions to

ambient body water. When the flow entrains the body water, it decelerates and expands. (Rajaratnam and Subramanyan, 1986; Long et al., 1990, 1991; Russell and Arnott, 2003; Winsemann et al., 2009; Lang et al., 2021b). These jets present a transition from momentum-dominated flows (nearby the orifice) to gravity flows (fading away from the orifice) during their evolution along the body water (Powell, 1990; Lønne, 1995; Roberts et al., 2001; Hoyal et al., 2003; Lang et al., 2021a).

Due to the nature of the jets in grounding-line fans, the flows tend to pass from supercritical (Froude number > 1) to subcritical (Froude number < 1) flows quickly, as the jet entrains into the body water and decelerates (Rajaratnam and Subramanyan, 1986; Long et al., 1990, 1991). This transition can or cannot involve a hydraulic jump. Still, typically they are attributed to these conditions being responsible for the genesis of typically proximal grounding-line fans facies (e.g., scour-fill deposits and backsets) (Russell and Arnott, 2003; Hornung et al., 2007; Winsemann et al., 2009; Lang and Winsemann, 2013; Lang et al., 2017, 2021b). However, recent work from Lang et al. (2021a) contested that hydraulic jumps are always responsible for forming scour-fills. In their view, in some cases, other internal flow factors as complex recirculations, turbulent eddies, bursts, and waves are responsible for developing these features (Lang et al., 2021a). After the hydraulic jump, tend to deposit bedforms related to the action of supercritical flows like chute and pools and antidunes (Winsemann et al., 2009; Lang and Winsemann, 2013; Cartigny et al., 2014; Lang et al., 2017). As long as the jet loses velocity, the flows progressively transit again to a subcritical regime, depositing transitional bedforms (e.g., humpback dunes) and pure subcritical flow bedforms like dunes and ripples in more distal settings (Lang and Winsemann, 2013; Lang et al., 2017).

As said before, the flows tend to lose momentum, moving away from the proximal region of the jet (Roberts et al., 2001; Hoyal et al., 2003; Russell and Arnott, 2003; Hornung et al., 2007; Lang et al., 2021a). This loss of velocity generates a transition from turbulence-dominated flows to gravity-dominated underflows in distal areas of the jets (Roberts et al., 2001; Hoyal et al., 2003; Lang et al., 2021a). All those processes (proximal and distal) in grounding-line fans are very dynamic, always subject to glacier dynamics, and their understanding can provide us a better interpretation of ancient and modern glacial deposits.

4.3 Geological Setting

The Paraná Basin is one of the largest intracratonic basins in South America. The basin occupies an area of 1.500.000 km² in Brazil, Argentina, Paraguay, and Uruguay, reaching 7.000 m of thickness on his depocenter (Zalán et al., 1987; Milani et al., 2007). The Itararé Group is deposited between the Carboniferous and Permian with their record reflecting the multiple advances and retreats from glaciers in surrounding areas towards the Paraná basin (Crowell and Frakes, 1970; Eyles et al., 1993; Vesely et al., 2015; Rosa et al., 2016; Mottin et al., 2018). The dynamics of advances and retreats result in an architecture composed of fining-upward sequences formed by continental, transitional, and marine deposition containing different levels of glacial influence (Franca and Potter, 1988; Vesely and Assine, 2006). Generally, these packages are composed of conglomerates and sandstones in the base of the sequences that grade to diamictites and mudstones at their top (Schneider et al., 1974; Franca and Potter, 1988; Vesely and Assine, 2004, 2006). Vesely (2001) understands that these fining-upward sequences represent a glaciomarine deposition. In their proposition, the conglomerates and sandstones on the base of the sequences represent the deposition of grounding-line fans (*subaqueous outwash fans* on their sense).

For the Southern area of Paraná state and the whole Santa Catarina state, an outcrop-based stratigraphy split the Itararé Group into three formations (from the base to the top): Campo do Tenente, Mafra, and Rio do Sul (Schneider et al., 1974). In our study area, two of these formations are represented according to Schemiko et al. (2019), the Mafra and Rio do Sul. The exposition of the Mafra Formation is restricted. However, the Rio do Sul Formation is very well exposed, reaching a thickness of 500 m (Schemiko et al., 2019). About the infill, the Rio do Sul Formation represents a restricted marine basin, according to some authors (Castro, 1980; Canuto, 1993; Santos et al., 1996). The basal and middle portion represents deep-marine sedimentation, and the upper portion the progradation of a deltaic system over this sub-basin (Castro, 1980; Canuto, 1993; Santos et al., 1996; Schemiko et al., 2019).

This article deals with a sedimentary succession located in the portion interpreted as deep-marine sedimentation. The facies comprehend conglomerates, diamictites, and sandstones, for many authors interpreted as deep-marine deposition

(Castro, 1980; Canuto, 1993; Santos et al., 1996; Schemiko et al., 2019). This affinity with gravitational and deep-water sedimentation is arguable due to the context where these facies occur. These coarse-grained facies are embedded in thick packages of shales, interpreted by many authors as deep marine (Castro, 1980; Canuto, 1993; Schemiko et al., 2019). Due to the context of the surrounding shales and the characteristics of the coarse-grained ones, previous interpretations suggest slope-induced gravity-flows (Schemiko et al., 2019) and submarine-fans (Canuto, 1993) (both containing glacial influence) as the possible genesis for these deposits. However, neither of these articles worked in this coarse-grained succession in detail. All the previous publications deal with this section as a portion of the Rio do Sul Formation, studying the area in a regional context and trying to understand the infill and paleogeography of the entire sub-basin (Castro, 1980; Canuto, 1993; Santos et al., 1996; Schemiko et al., 2019).

Our main divergences with these interpretations are the distance of the proposed depositional environments to the glacial margin. The characteristics in the facies, like metric boulders, limestones, faceted and striated clasts, could suggest that the glacial margin was not so far from the local of deposition. However, the occurrence of shales above and below the coarse-grained facies could be associated with a deep-water character, rarely associated in proximal contexts with glacial margins.

4.4 Methods

The base of our study was a geological mapping in the region of Presidente Getúlio, Santa Catarina state (eastern outcrop belt of the Paraná Basin) in a total area of 800 km² focused only in the 60m package. We visit a total of 40 outcrops describing the sedimentary facies and taking paleocurrents measurements. The disposition of the outcrops along the study area is heterogeneous, where the better exposures are in caves, roadcuts, and waterfalls. However, the high amount of vegetation difficult for a homogeneous geological mapping of this unit. In 7 locations, we measured sedimentary logs on a 1:100 scale to describe the vertical stacking and the vertical and lateral facies variations. To correlate our sedimentary logs, we utilize the basal shales where they are available.

In more extensive outcrops, we generate photo mosaics to analyze lateral facies variations and the disposition of larger bedforms. This criterion is essential because bedforms formed in supercritical context tend to have meters of length due to the magnitude of the flows (Russell and Arnott, 2003; Hornung et al., 2007; Winsemann et al., 2009; Lang et al., 2017, 2021b).

To create a textural normalization between conglomerates and diamictites, we establish criteria to differentiate these facies. Those which contain a matrix with a sand/mud ratio >1 we described as conglomerates and, those with a <1 we described as diamictites. This criterion is essential because massive diamictites and conglomerates facies occur frequently and could be similar in outcrop. Additionally, we follow the terminology of Mulder and Alexander (2001) for the interpretation of density flows, which their nomenclature is based on the sediment concentration of the flows.

To establish the sense of depositional transport, we collected paleocurrents when available. The main facies which show preserved sedimentary structures are the climbed-rippled sandstones. We also collected few measures from cross-stratifications, but these structures could represent backsets in supercritical contexts (Lang et al., 2021b), so the analysis of these structures needs to be careful.

4.5 Results

4.5.1 Facies associations

We described 16 sedimentary facies (tab. 1) and subdivided them into four different facies associations. The division of the associations it's accorded to each stage of evolution of our sedimentary succession. Each phase of the sedimentary record is associated with different processes explored in detail in the following sections. In 7 locations, we raised 1:100 logs to understand how the facies associations are distributing along our study area (fig. 3).

4.5.1.1 Glaciotectonized substrate

- Description

This association is composed of ressedimented diamictites (fig. 4A), shales (fig. 4B), and foliated diamictites (fig. 4C,4D,4E,4F). The shales and ressedimented

diamictites are included in our logs due to being our study succession substrate. Still, the sedimentary process of these deposits will not be the target of interpretations in this article. The foliated diamictites (Dfl) are analyzed and interpreted in this study because their character is linked to the following facies associations. We observe an erosive contact between the Dfl facies and the first deposits of the subsequent facies association (fig. 4C).

The Dfl facies (tab. 1) has a localized occurrence, being exposed only on the base of the CT log (fig. 2,3; fig. 4C). The muddy-sandy matrix has a similar grain size to the shales and ressedimented diamictites, with considerable mud over the sand (fig 4D, 4E, 4F). The more significant sand content is restricted to some deformed sandstone clasts, which are described as boudins (fig. 4E, 4F). Other granulometric heterogeneities are attributed to more gravelly portions (fig. 4E, 4F). These parts of the diamictite are composed of granules and small pebbles and have a massive structure.

Facies code	Description	Geometry	Structures	Frequency	Interpretation
Gms	Matrix-supported conglomerates with matrix ranging from medium to very coarse sand. The clasts range from sub-rounded to sub-angular and vary from granule to boulder size. The composition is varied but mainly composed of granitic, low and high-grade metamorphic, and volcanic rocks. Fine-grained sandstone beds, which sometimes are deformed, occur embedded in the matrix. The sandstones could show climbing-ripple lamination. These massive conglomerates can also show clast clusters of pebble and cobble sizes.	Lenticular or generally containing scoured bases. The beds range from cm to m in size.	Massive.	+++++	Disorganized conglomerates with scoured bases represent local hydraulic jumps in a proximal fan context (concentrated density flows). The deposition of fine-grained sandstone beds inside the conglomerates is interpreted as surge-like turbidites originated by diluting the concentrated density flows. The clast clusters are formed by hydraulic segregation induced by supercritical flow conditions.
Gmc	Clast-supported conglomerates with the matrix composed of coarse to very coarse-grained sand. The clasts range from sub-angular to angular, with size ranging from granule to boulder. These conglomerates are polymictic, mainly composed of granitic, high-grade metamorphic, and volcanic rocks.	Lenticular with scoured bases (cm to m bed size).	Massive.	+++	The occurrence of massive clast-supported conglomerates is interpreted as the deposition of hyperconcentrated density flows. The lenticular aspect of the beds and their scoured bases indicates supercritical flow conditions.
Gt	Matrix and clast-supported conglomerates containing through cross-stratifications. The matrix range from medium to very coarse-grained sand. The clast range from sub-rounded to angular and can show imbrication. The composition is similar to other conglomeratic facies. In matrix-supported conglomerates, the bigger clast tends to be in the bottom part of the stratifications.	Lenticular or sigmoidal, mainly with scoured bases. Beds ranging from cm to m size.	Through stratifications, it was sometimes showing imbrication.	+++	The interpretation of the Gt facies is associated with their geometry and the sense of the structures, respectively. Beds containing only foresets are interpreted as progradational subcritical gravelly dunes. Beds containing both foresets and backsets could be interpreted as local hydraulic jumps. Finally, the beds with sigmoidal geometry are interpreted as humpback dunes.
Gbd	Matrix-supported conglomerates containing oversized boulders. The matrix range from medium to coarse-grained sand. The clasts are angular and are mainly from boulder size reaching up to 6m. These boulders have a granitic composition, and some of them are imbricated. Centimetric beds of massive clast-supported conglomerates are associated with these facies.	Lenticular. Beds with m size.	Massive. It could have clast imbrication.	++	The deposition of metric boulders, where some of them are imbricated among a restricted sedimentary bed, is interpreted as the product of concentrated density flows in a subglacial conduit.
Gn	Matrix-supported conglomerates showing normal grading. The matrix range from medium to very coarse-grained sand. The clasts range from sub-rounded to angular and vary from granule to pebble in size. The composition is similar to the massive conglomeratic facies.	Mainly tabular but could be lenticular as well (cm bed size).	Normal graded.	+++	Normally graded deposits are interpreted as the product of concentrated density flows.
Sm	Fine-grained to conglomeratic sandstones with massive structure. These sandstones range from	Lenticular or tabular showing scoured bases—	Massive. It could show groove marks on the	+++	Massive sandstones are interpreted as Ta Bouma facies product of

	moderate to poorly sorted. The sandstones could have intracasts of mudstones embedded in their textural framework. The base of the beds could have groove marks.	beds ranging from cm to m size.	base of the beds.		concentrated density flows. The occurrence of tool marks in the base of some beds is a consequence of laminar flows containing a turbulent base (stratified flows).
Sr	Fine to very-coarse grained sandstones with climbing-ripple lamination. They are moderate to very poorly sorted and, in some cases, could show granules on their laminations. The beds with climbing ripples sometimes are associated with cm beds of trough cross-bedded sandstones. In these occasions, the sandstones tend to be coarser.	Lenticular or tabular. In the lenticular ones, they tend to present scoured bases—beds with cm size.	Climbing-ripple lamination.	++++	The deposition of the Sr facies represents the migration of climbing-ripple bedforms under waning subcritical flows in a distal fan setting.
St	Fine to very-coarse grained sandstones with trough cross-stratification. They range from moderate to poorly sorted sandstones and could have granules on the bottom of the strata. As said before, it's common the association between facies St and Sr. In these cases, the facies St tends to be in the base of the beds and the Sr in the upper portion of the strata.	Lenticular with scoured bases. Beds ranging from cm to m size.	Climbing-ripple lamination.	+++	We interpret Gt facies as the migration of subcritical dunes in a waning jet context.
Sp	Poorly sorted conglomeratic sandstones with planar cross-stratifications. The matrix of the sandstones ranges from medium to very-coarse grained sand. They have a certain content of granules and some small pebbles embedded in the matrix.	Tabular. Beds with cm size.	Planar cross-stratification.	++	Sp facies are interpreted as small architectural elements of subcritical flows in a mouth bar setting.
Ssad	Fine-grained sandstones with sinusoidal antidunes. These deposits represent metric lateral continuous well-sorted sandstones showing sinusoidal trends of antidunes. The bedforms are characterized by their similar ondulal aspect along the outcrops.	Sinusoidal. Beds with cm size.	Sinusoidal antidunes.	+++	Sinusoidal antidunes are interpreted as waning stages of supercritical flows in a wall-jet context. These deposits are generally deposited as underflows in the lee side of prograding clinoforms.
Slad	Fine to coarse-grained sandstones with antidunes and a lenticular aspect. This facies represent moderate to poorly sorted sandstones with a lenticular geometry. We describe the stratification of the sandstones as antidunes.	Lenticular. Beds with a cm size.	Lenticular antidunes.	+++	Lenticular antidunes are interpreted as surge supercritical flows associated with density flows (concentrated and hyperconcentrated density flows).
Dmm	Muddy-sandy diamictites. These diamictites have a muddy-sandy matrix containing dispersed clasts ranging from granule to boulder size. The rounding of the clasts ranging from sub-rounded to angular, showing no textural maturity for these diamictites. The composition of the clasts is varied and similar to the massive conglomeratic facies. Some of the boulders are described as lonestones. The Dmm facies it's characterized for the occurrence of lenticular	Tabular or lenticular, containing centimetric stratified sandstone beds inside the diamictite. Beds of the diamictites range from cm to m in size.	Massive.	+++++	We interpret the main fabric of the Dmm facies as a product of debris flow expelled by basal portions of the glacier. Surge-like turbidity currents are responsible for the deposition of lenticular sandstone beds in the diamictite fabric. The depositional process is similar to the sandstones described in the Gms facies. Still, some described ones in the Dmm

	<p>sandstone beds inside the matrix of the diamictite. Some of these sandstones are described as antidunes. In some cases, these sandstone beds are deformed (boudins, faults, and folds). Clast-supported conglomerates are described embedded in the matrix as well. These conglomerates, in some cases, are deformed and have an injected aspect.</p>				<p>facies indicate supercritical conditions due to associated lenticular antidunes. However, the beds of sandstones interpreted as a product of diluting of the debris flow are much more common here than in the Gm facies. We understand that episodic floods also contribute to these facies, responsible for the deposition of the described clast-supported conglomerates (hyperconcentrated flows). Despite that, the presence of limestones among the diamictite matrix is interpreted as a product of ice-rafted debris.</p>
Dfl	<p>Diamictites with foliation. These diamictites have a muddy foliated matrix with dispersed clasts ranging from granule to boulder size. The composition is varied but is mainly composed of granitic rocks. The foliation tends to be folded and follow the edges of larger clasts. The matrix in some portions of the diamictite contains more rigid content composed of sand, which is also deformed but tends to be lesser than the muddy portions. In some portions, the diamictite has a higher content of gravel which is also deformed. Some of the folds are described as recumbent with internally parasitic folds. The occurrence of dispersed centimetric beds of deformed sandstones among the matrix is described as boudins. We also detected that some of the clasts were fractured.</p>	<p>Lenticular. The bed varies from cm to m in size.</p>	<p>Foliation, folds, boudins and fractured clasts.</p>	<p>+</p>	<p>The Dfl facies is a product of glacier advance over the previous marine deposits of the Rio do Sul Formation. The fabric and deformational structures indicate glaciotectionic deformation in a subglacial shear zone.</p>
Dm(r-ht)	<p>Heterogeneous diamictite with ressedimentation features. The diamictites have a muddy-sandy matrix with allochthonous blocks of sandstones and conglomerates dispersed in the matrix. In some parts of these diamictites, we can observe remnants of the protolith. These portions are composed of massive sandstones interbedded with massive matrix-supported diamictites, still presenting some of their original aspects but still containing deformation. The allochthonous sandstone blocks are folded and show internal deformation (penecontemporaneous faults, boudins, and internal shearing). We also describe clasts ranging from granule to boulder size dispersed in the matrix. They have a similar composition to other nondeformed facies, and some of the clasts are striated.</p>	<p>Chaotic.</p>	<p>Massive, containing ressedimentation features like allochthonous blocks, penecontemporaneous faults, boudins, folds, and sheared beds.</p>	<p>++++</p>	<p>First stage of slump deposition (low to mid-grade of homogenization) in a submarine slope.</p>

Dm(r-hm)	Homogeneous diamictite with ressedimentation features. The matrix of the diamictite is muddy and homogeneous. We describe a few dispersed clasts which vary from granule to pebble size. These clasts vary from sub-rounded to angular and have similar compositions compared to the other facies. In this diamictite, the only ressedimentation feature described are sheared beds of fine to medium-grained sandstones that reach a maximum thickness of 2 cm. Despite these small beds of sandstones, the diamictite is completely homogeneous.	Tabular.	Sheared sandstone beds.	+++	Late stage of slump deposition (high-grade of homogenization) in a submarine slope.
Ht(d)	Very fine-grained sandstones and mudstones with heterolithic bedding. These facies comprises the interbedding of cm beds of fine-grained sandstones and cm to mm beds of mudstones. The sandstones are well-sorted. The Htd facies is deformed, with the strata presenting small folds and stretch. The beds of the Htd facies are deformed not only in a bed scale but also compose more prominent folds with metric scale.	Lenticular.	Stretched and folded beds.	++	We interpreted this facies as turbidites originated by the expelling of low-density gravity flows in a glacial margin.

Table 1– Facies table with the main characteristics of the described lithologies, their frequency, and the interpreted processes related to their genesis.

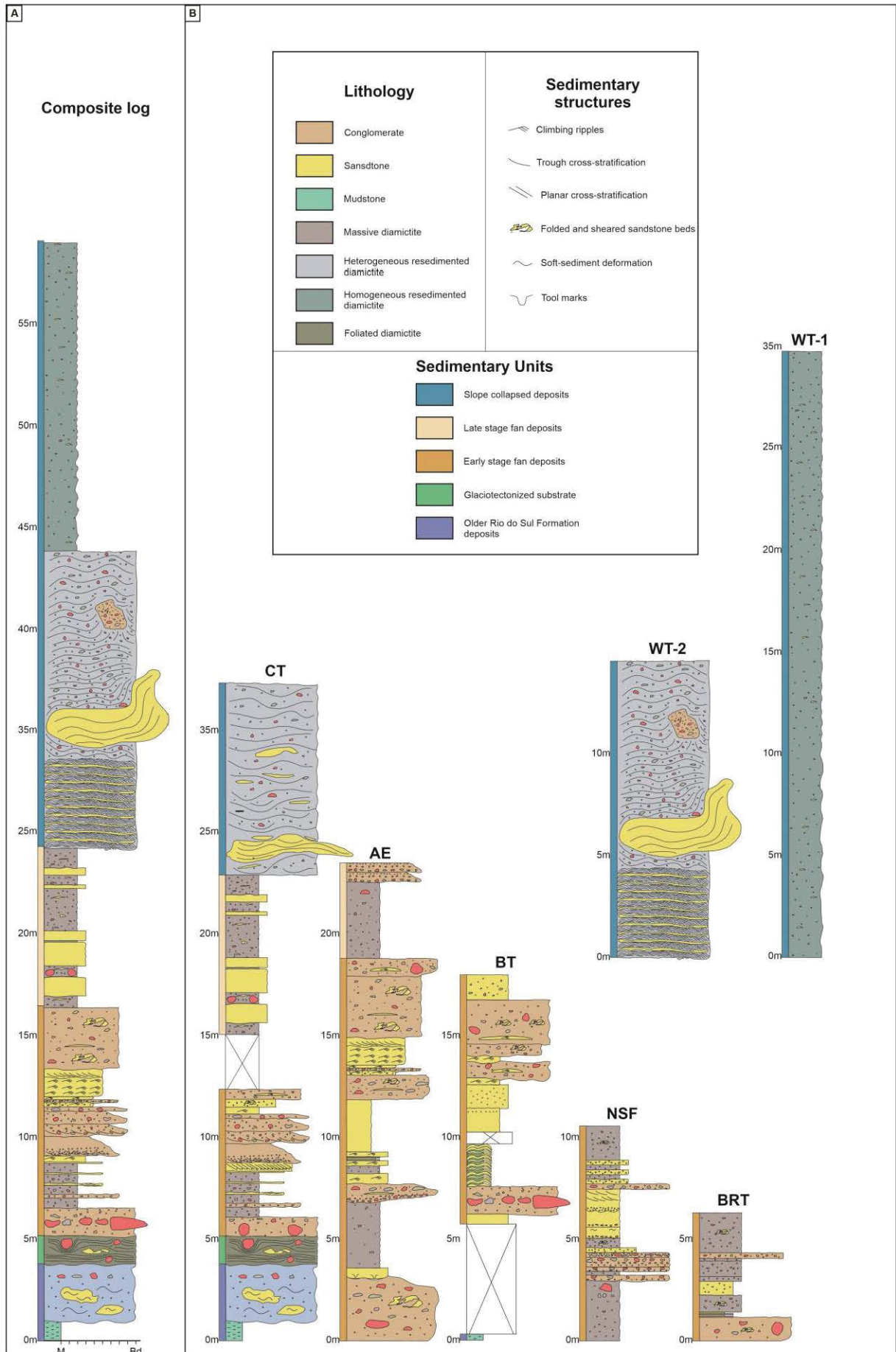


Figure 3 - Stratigraphic logs of the study interval. A) Composite log of the study interval. B) There are seven logs that were raised for the study of the interval. In the caption, we have the described structures, the five facies associations, and the substrate of the succession. The locations of the sedimentary logs are in figure 2.



Figure 4 – Main features of the glaciotectionized substrate and the basal lithologies of the Rio do Sul Formation. A) Ressedimented diamictites on the base of the study interval. In the bottom part of the outcrop, we can observe the shales. B) Basal shales. In the upper portion of the picture, they have deformed bedding. C) Disposition of the glaciotectionized substrate in relation to the early-stage fan deposits. We can observe an erosive contact between the substrate and the first deposits of the fan. D) Detail of figure 4C. We can keep in detail the erosive contact between the two facies associations. Also important to note is the occurrence of scratched boulder-sized clasts composing the Dfl facies. E) Detail of figure 4C. In this figure, we can observe in detail the features which comprise the Dfl facies. Firstly, we see how the foliation is more prominent in portions with a higher mud content. In contrast, parts with more extensive sand and gravel tend to be more massive and not develop foliation. Another critical aspect is how the foliation tends to be more folded around larger clasts (cobble and Boulder size). In the right portion of the figure, we see the foliation presenting recumbent folds. The boudins have a sandy composition and a massive structure. Finally, look at how some clasts show fractures. They are mainly pebble-sized. F) Highlighted features of figure 4E. For the composition of the clasts - SM: Sand massive; CR: Crystalline.

However, the massive character is restricted to some portions with a more extensive gravel content. In parts with more mud, the Dfl facies presents almost entirely foliated (fig. 4E, 4F). This foliation is visible macroscopically and is marked due to granulometric heterogeneities. The foliation has a significant amount of folds, but they tend to be more prominent where the foliation encircles clast of cobble and boulder size (fig. 4E, 4F). Beyond these folds, we also described recumbent ones containing parasitic folds internally (fig. 4E, 4F).

About the clasts on the Dfl facies, the composition of the crystalline ones are mainly composed of granitoids. The larger clasts (cobbles and boulders) are scratched and could have angular edges (fig. 4D, 4E, 4F). Finally, another feature interesting on the Dfl facies is the occurrence of fractures on clasts of crystalline composition (fig. 4E, 4F). The clasts containing these fractures are mainly pebble-sized.

- Interpretation

The presence of the Dfl facies over the previous ressedimented diamictites and shales of the Rio do Sul Formation bring us several questions about the genesis of the Dfl facies. Firstly, the foliated diamictites share a very similar muddy matrix with the shales, which are one of the facies that compose the substrate previously to the deposition of the Dfl facies. It's important to note that these diamictites don't present sedimentary structures. Instead, the features described at the Dfl facies are only deformational, denoting that the genesis of these diamictites is related to deformation.

We infer that the Dfl facies was generated from the action of deformation agents over the substrate (shales and ressedimented diamictites). In our analysis, the deformational structures like foliation, folds, boudins, and fractured clasts are commonly related to the action of shearing forces. Glaciers could be an agent of shearing deformation over sedimentary sequences, responsible for the generation of soft sediment shear zones (SSSZ) over the glacier bed, producing similar products compared to tectonics shear zones at different scales (Van der Wateren, 2002; Phillips, 2018).

In the Dfl facies, we observe different products of the action of shearing over the Rio do Sul Formation substrate. This variety of products suggests different levels of deformation due to the movement of the glacier over the bed. The description of recumbent folds shows in a first moment lower rates of deformation compared to other structures, which need higher rates to develop. (Phillips, 2018). However, the genesis of features with higher strain rates as boudins as foliations attest to a progressive increase in strain rates over the bed (Van der Wateren, 2002; McCarroll and Rijdsdijk, 2003; Phillips, 2018). We interpret that this increase in the shearing forces was responsible for a relative homogenization of the Dfl facies generating the foliation and the boudins (Phillips, 2018).

Foliations are generally the final product of glaciotectionic deformation (Phillips, 2018). But some factors acted as facilitators for the genesis of this fabric. We observe that the foliation of the Dfl facies is mainly composed of fine-grained sediments. We suggest that shearing forces acted preferentially at the bedding planes of the previously deposited shales, facilitating the formation of the foliated diamictites.

Other features which suggest the action of glaciers over the previously deposited sediments are the clasts. We described clasts with angular edges and some scratches on their surfaces. These characteristics are generally related to processes at the base of glaciers like abrasion and plucking (Boulton, 1979). We also observe that some pebbles are fractured, which can be associated with the action of glaciers as well (Boulton, 1979).

Therefore, we interpreted the deposition of the Dfl facies as a product of a glacier advance over the previously deposits of the Rio do Sul Formation. This advance was responsible for deforming the substrate and generating a deformational product related to glaciotectionic deformation, which is overlayed by the subsequent facies.

4.5.1.2 Early-stage fan deposits

- Description

The Early-stage fan deposits (ESFD) are the facies association with the higher frequency of occurrence in the entire interval, described in almost the whole study

area. We logged this association in five (fig.3) of our seven logs (CT, AE, BT, NSF and, BRT). The ESFD has an erosive contact with the older deposits of the Rio do Sul Formation (mainly shales) and with the glaciotectionized substrate (fig. 4C).

In the ESFD association, we describe a total of thirteen sedimentary facies (tab.1). The facies in the ESFD comprise conglomerates, sandstones, and diamictites, containing differences in the stacking patterns along with the study area. Firstly, conglomerates and sandstones are less frequent in the middle and northern sectors (NSF and BRT logs) than in the southern sector (CT, AE, BT logs).

The basal portion is deposited in disconformity with the shales and ressedimented diamictites of the Rio do Sul Formation, which could be deformed by glaciotectionics (fig. 3, 4C). Directly above this substrate, we have the record of the Gbd facies (fig. 5). These conglomerates have very particular features because they present the enormous boulders of the entire succession, reaching up to 6m (fig 5A). These facies were described in the southern sector of the study area, most precisely in the BT log (fig. 2). The boulders in the Gbd facies could present angular edges and some scratches (fig. 5B). In the 6m clast, we describe these same angular edges but containing some polished surfaces (fig. 5A). It is important to note that some of the clasts in the Gbd facies present imbrication (fig. 5B). The conglomerates with more enormous boulders could have some portions with deformation associated with more stratified strata (fig. 5B, 5C).

In the same stratigraphical level of the Gbd facies, we observe a significant variability of lithologies in a short area (fig. 6). Only in two logs (fig. 3), we mapped the contact between the base of the ESFD and the substrate (BT and CT log). In the BT log, this basal portion is composed by the Gbd facies, but not only by that. Laterally to the conglomerates with boulders, we describe a high variability of facies in the same outcrop (fig. 6) This variability presents a complex architecture (fig 6A to 6D) composed of lenticular beds of massive sandstones (Sm), clast supported conglomerates (Gmc), sandstones with lenticular antidunes (Slad), and sandstones with sinusoidal antidunes (Ssad). Directly above the Gbd facies in the BT outcrop, we described some heterolithes (Htd facies) that could be deformed (mainly folded) (fig. 6E, 6F).

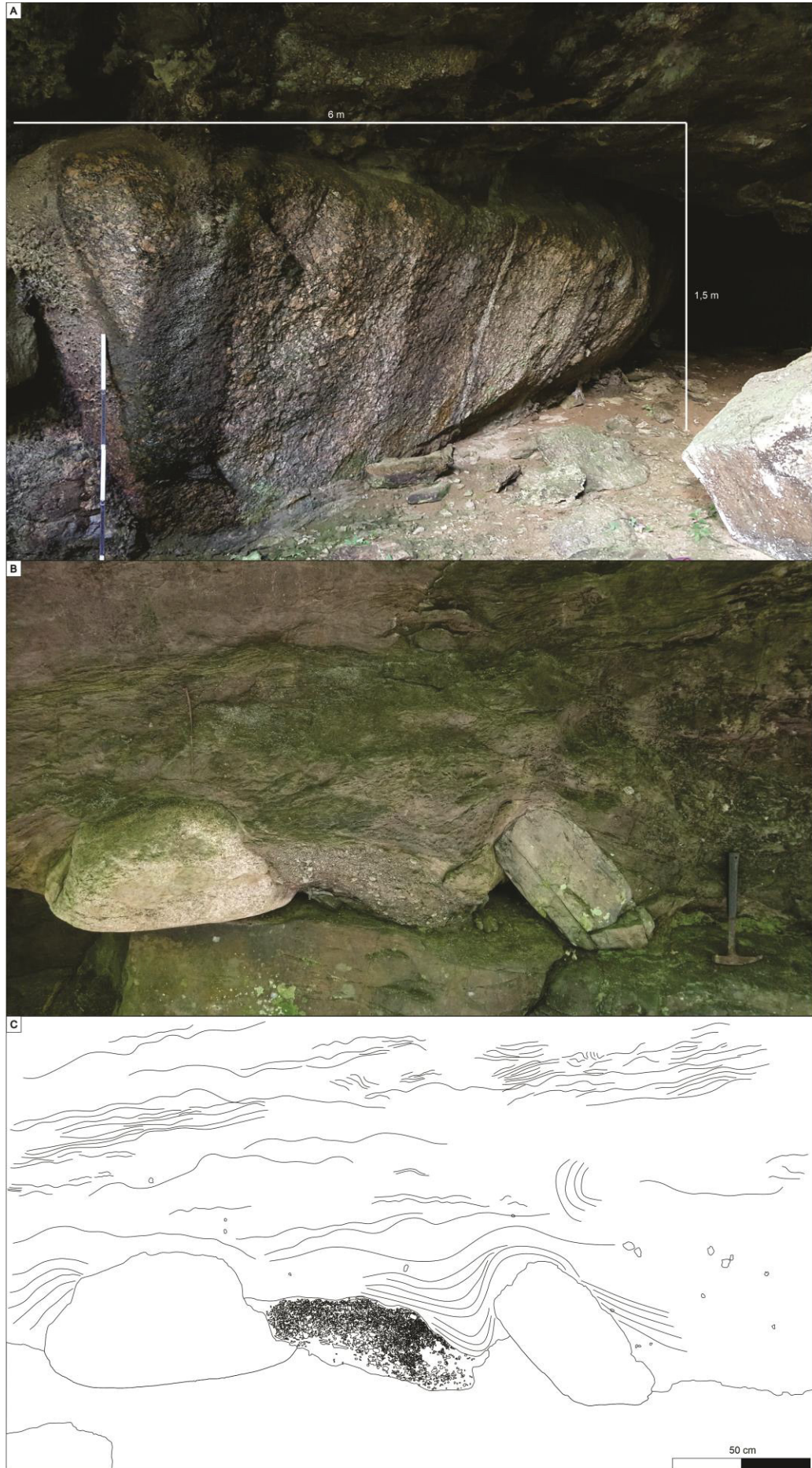


Figure 5 – Features related to the Gbd facies. A) Oversized boulder of 6m length. This boulder presents polished surfaces with some angular edges as well. B) Folded bedding of stratified portions of the Gbd facies, that portion of the Gbd facies could present some imbricated boulders with lenticular deformed beds of clast-supported conglomerates associated (Gmc facies). C) Interpretation of the figure 5B.

However, in the CT outcrop, this variability is less prominent (fig. 6G, 6H). Oppositely, in this outcrop, we described neither the Gbd nor facies with highly scoured bases. The facies at the base of the CT outcrop show some scoured bases but are mainly composed of massive conglomerates (fig. 4C, 4D) (Gm facies), massive diamictites (Dmm facies), some centimetric beds of lenticular sandstones with antidunes (Slad facies), and sandstones with backsets of through cross-stratifications (St facies) (fig. 6G, 6H).

Above the basal deposits, we describe mainly conglomerates and sandstones with some massive diamictites as well. This architecture is the main component of the ESDF. In the southern sector, we can observe in perspective how are disposed of the geometry of the sedimentary succession (fig. 7). The outcrop has almost 50m of lateral extension, and there we can realize how the architecture of the deposits are mainly composed of conglomerates and sandstones (fig. 7, 8). At this scale, we observe that the deposits have scoured bases which represents scour-fill deposits (fig. 7). These deposits could be massive (Gm, Gmc, and Sm) or stratified (Gt, St, Sr, and Ssad). It is important to note that some stratified (Gt, and St) deposits present stratifications dipping to both sides of the beds, some of them representing backsets (fig. 7, 8). Another feature in stratified deposits is the occurrence of metric sets of facies St with sigmoidal geometry (fig. 7, 8B).

About the scours, we create a hierarchy to distinguish different surfaces at the outcrop (fig. 7B). These surfaces represent two orders of scours. Firstly, we have scoured surfaces that subdivide groups of beds (first-order scours). Generally, this group of beds tends to behave similarly at the outcrop, so the beds between two first-order surfaces represent a similar genetic context (fig. 7B). On the other hand, the second-order surfaces represent contacts between single beds, so they result from contact between individual strata. We also observe that some of the beds show deformation. This deformation is described as flame structures (fig 7, 8C).

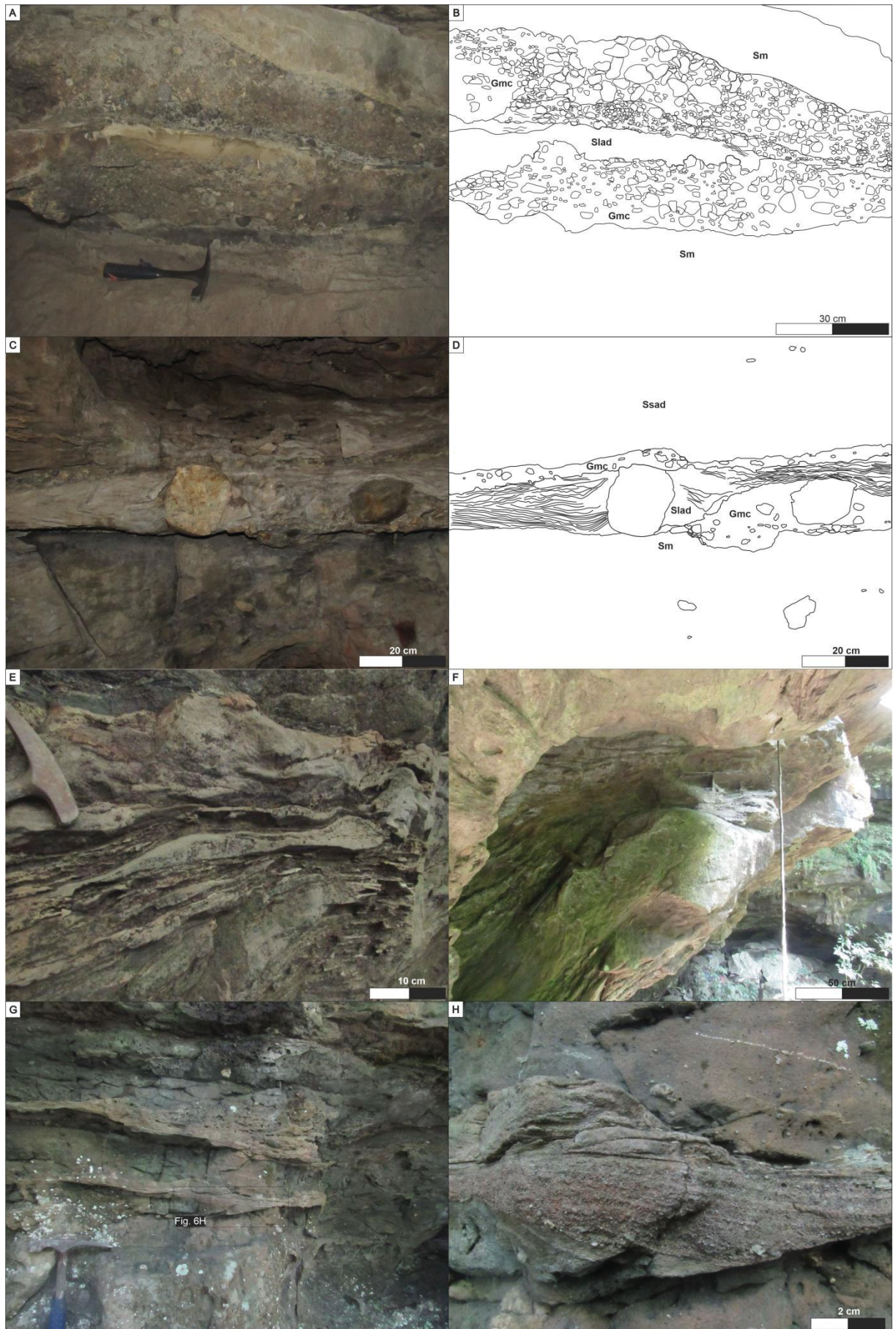


Figure 6 – Variability of the the basal deposits of the ESFD. A) Interbedding of between massive sandstones (Sm facies), clast-supported conglomerates (Gmc facies) and lenticular sandstones with antidunes (Slad facies). Note the scoured bases at the contacts between the facies. B) Interpretation of the figure 6A. C) Detail of a lenticular antidune deposit (Slad facies). Look how are irregular the contacts between the surrounding facies. D) Interpretation of the figure 6C. E) Heterolithes (Ht facies) composed of the intercalation of lenticular beds of sandstones and mudstones which are deformed. F) Folded beds containing the deformed heterolithes (Ht facies). G) Massive diamictites (Dmm facies) interbedded with lenticular sandstones with antidunes (Slad facies) containing some through-stratified sandstones representing backsets (Gt facies). H) Detail of the Gt facies backset of figure 6G.

Generally, the the second-order scours-fill deposits which compose the ESFD vary from one meter to tens of meters (fig. 7). Typically, these scours are related to the Gm, Gmc, Gt, or St facies (fig. 7, 8). The exception is restricted to some climbing-rippled sandstones (Sr facies) and some lenticular sandstones with antidunes (Slad) (fig. 8E, 11C, 11E). These deposits present scours with dimensions ranging from cm to 1-3 meter scale.

But is not the entire architecture of the ESFD that is related to scour-filled deposits. Some facies do not present an architecture related to beds with erosional aspects and tend to be tabular but could be lenticular in exceptional cases. The main facies associated with this character is the massive diamictites (Dmm facies) (fig. 9). The massive diamictites tend to be more tabular, but in some exceptions, they could present scours. This facies is mainly composed of a muddy-sandy matrix showing dispersed clast varying from granule to boulder size, where some of these boulders are described as lonestones (fig. 9A, 10A). But a significant characteristic of these facies is the occurrence of sandstone beds interbedded along with the Dmm fabric (fig. 8). These sandstones are mainly fine-grained, lenticular, with a frequent presence of deformation (fig. 9A). These sandstones are well-sorted, contrasting with the massive diamictites fabric, generally poorly sorted (fig. 9A). These sandy beds could be stratified in some cases, presenting bedforms like antidunes (fig. 9B, 9D, 9E). Those with antidunes present moderately to poorly sorted. Another essential feature is the occurrence of clast-supported conglomerate beds. These beds are usually chaotic and can show an injected-like geometry (fig 9B, 9C, 9D).

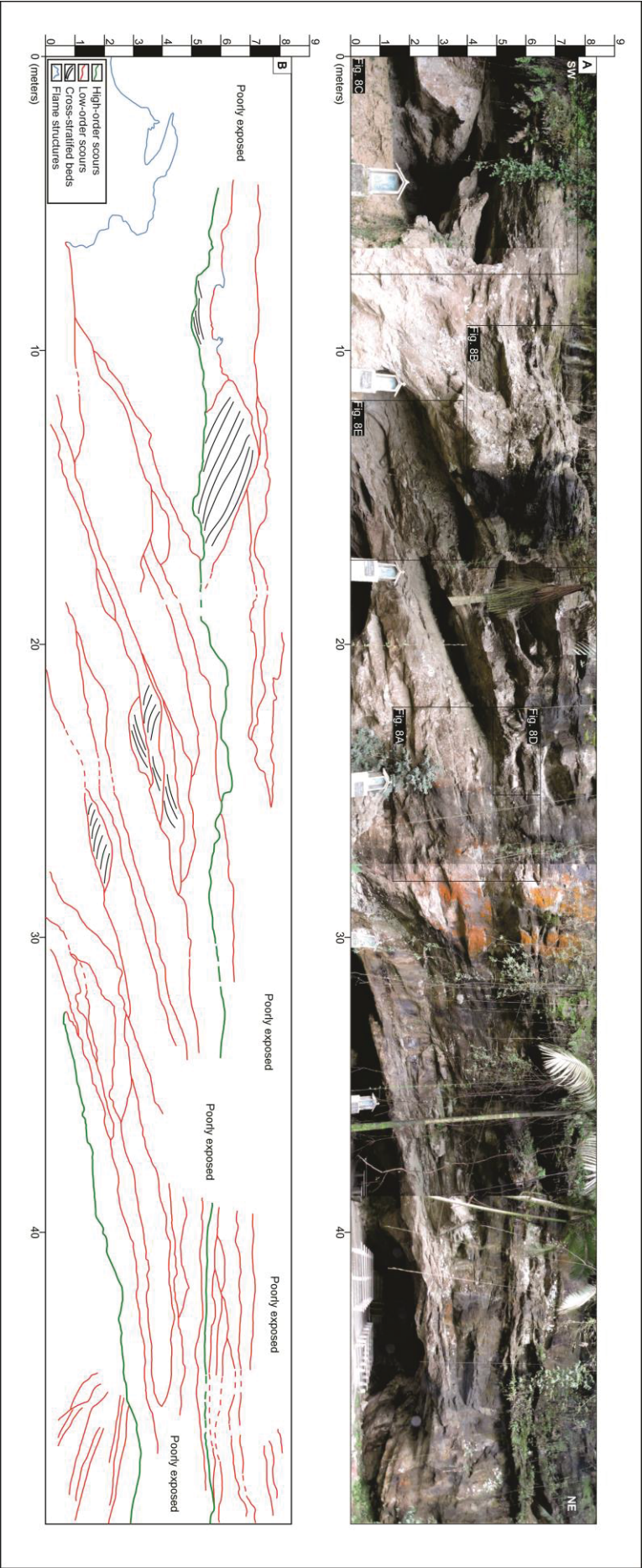


Figure 7 – General features of the scoured conglomerates and sandstones of the ESFD. A) Photomosaic of the outcrop of Gruta da Pimenta, located on the southern sector of the study area. Here we can observe how the scours are disposed of, their fills, and the deformation structures associated with these deposits. B) Interpretation of the figure 7A. Here we can observe the different order of scours. In red, the second-order scours, which are related to contacts between individual strata. In green, the first order scours corresponding to more extensive surfaces which subdivide groups of individual scours. If we observe the strata between the two first-order scours, we can see beds dipping to SE. These beds have a similar dip angle and direction and are associated with the deposition of an unic macroform. Above the second first-order scour, we see that the beds don't dip in the same direction as those located under the first-order scour surface. These differences in paleocurrents direction of the beds are attested for the deposition of sigmoidal through-cross bedded conglomerates (Gt facies) above the second first-order scour surface.



Figure 8 – Feature details of the scoured conglomerates and associated facies in the ESFD. A) Deep incised scours in through-cross bedded conglomerates (Gt facies). Here we observe a set of deep scours containing through cross stratifications dipping to both sizes, indicating that some of the stratifications are backsets. We measure the paleoflow from climbing-rippled sandstones located at the base of the outcrop. B) Sigmoidal through-cross bedded conglomerates (Gt facies), here we attest a change in the paleoflow at the outcrop, this change in the occur above the second high order scour (fig. 7). C) Metric flame structure located in the contact between some sandstones and fine-grained facies. D) Decametric bed of clast-supported conglomerates (Gmc facies). In the figure 6, we can see that these conglomerates extend for more than 10 meters along the outcrop. E) Sinusoidal sandstones with antidunes (Ssad facies). This sandstones were described at the foresets of the macroform established between the two high-order scours exposed in figure 7.

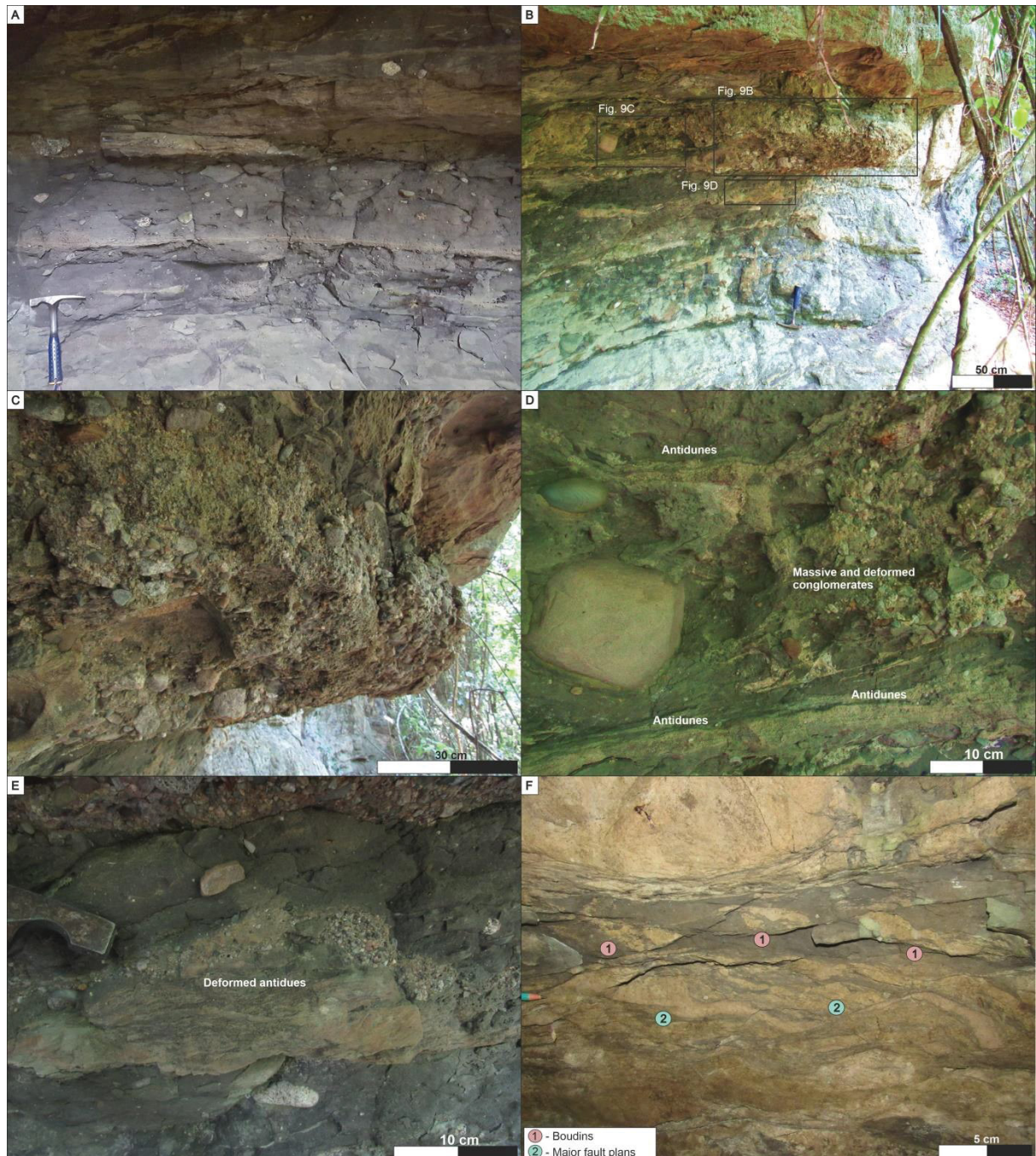


Figure 9 – Mainly features of the massive diamictites (Dmm facies). A) Main fabric of the Dmm facies. The diamictites are characterized by a muddy matrix containing dispersed clasts and a massive structure. A common aspect is the deposition of lenticular sandstone beds, which are commonly deformed. B) Clast-supported conglomerates and antidune sandstones associated with the Dmm facies. C) Huge massive clast-supported conglomerate bed. D) Here, we can see a portion where the conglomerates are deformed, containing an injected aspect and, in some cases, mixed with the diamictite matrix. We also observe that associated with the conglomeratic beds, coarse-grained sandstones with antidunes occur. E) Detail of an injected bed of conglomerate a fluidized sandstone with antidune lamination. F) Faults and boudins are associated mainly with fine-grained sandstones interbedded with the diamictite matrix. We highlighted the major fault plans which are related to the fault genesis and consequently the boudins.

As early exposed, some of the sandstone beds along the Dmm are deformed. The most common style of deformation are the faults (fig. 9F). The faults vary from an mm to cm dimension and could be normal or inverse. Another significant

deformation structure is the boudins (fig. 9F). It is essential to expose that the different deformation structures are usually associated. Another frequent structure is the sheared beds of sandstones (fig 9A, 9F). This structure is widespread due to the difficulty of these sandstones showing continuous beds, creating a standard feature along with the Dmm fabric (fig. 9A).

Despite the diamictites, two other facies groups are widespread, along with the ESFD, the conglomerates (which we already exposed some characteristics), and the sandstones. We will show some of the features of these facies in detail. All the conglomerates of the ESFD have a similar composition of clasts, comprising mainly granitoids, high and low-grade metamorphic rocks, and volcanic (fig. 5, 6A, 6C, 8D, 9C, 10). Some of the clasts in the conglomerate facies are faceted, scratched, and can also be striated (fig. 5, 6A, 6C, 8D, 10B, 10C). We saw that the clasts are aligned in some facies, forming clusters of clasts from pebble and cobble size (fig. 10C). In some cases, the Gm facies can show deformed fine-grained sandstone beds, similar to those in the Dmm facies. As early exposed, the conglomerates tend to have scoured bases, and this characteristic remains even in the graded conglomerates (Gn facies) (fig. 10D).

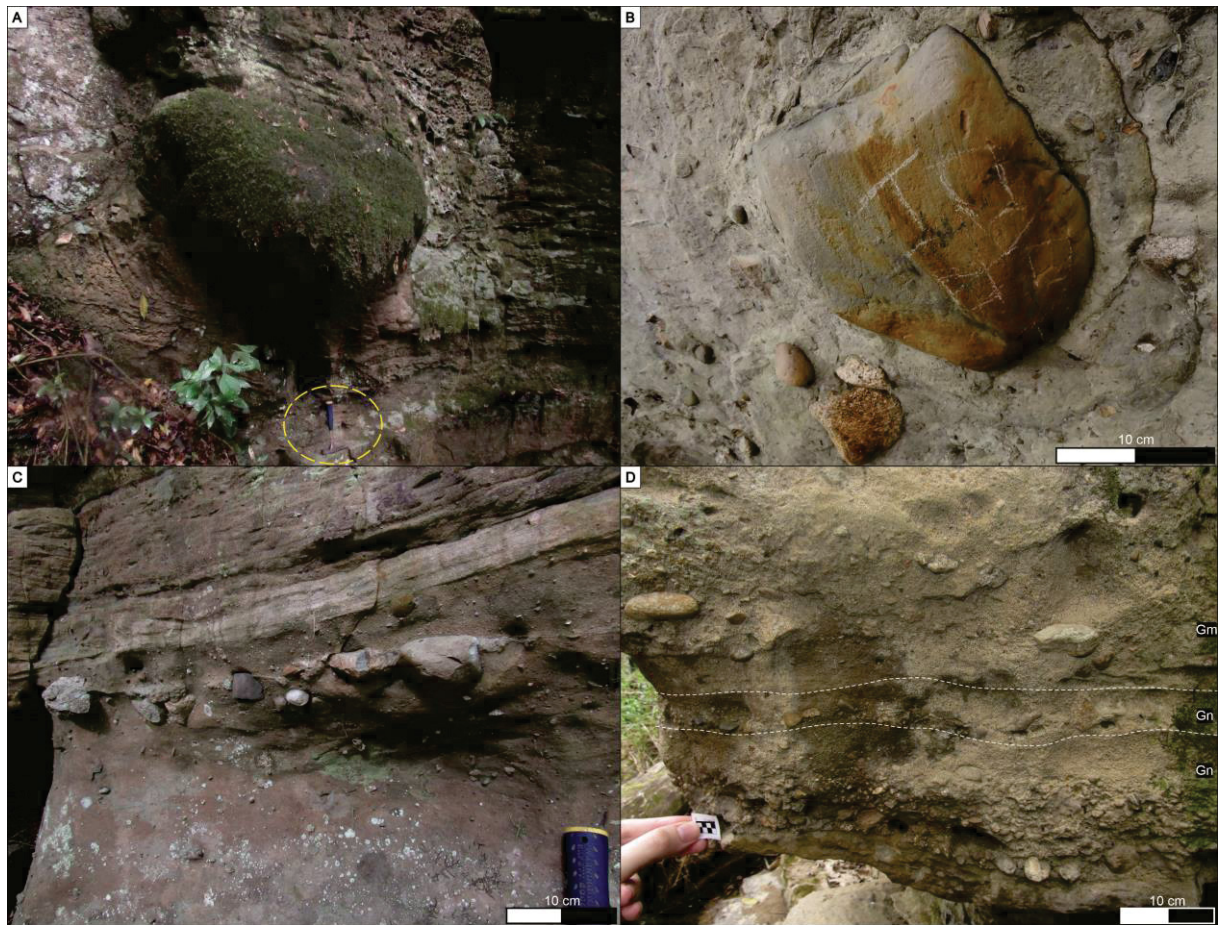


Figure 10 – Features related to clast organization and deposition at the ESFD. A) Metric granite clast deposited along a bed of a massive diamictite. This clast is described as a lonestone. Hammer for scale. B) Striated granite clast in a massive conglomerate bed (Gm facies). C) Clast cluster deposited at the top of an massive matrix-supported conglomerate (Gm facies). D) Organization of a set of beds of normally graded conglomerates (Gn facies).

The sandstone deposits show a variety of facies at the record of the ESFD (fig. 10). Sandstone facies in this facies association vary from well to poorly-sorted. The well-sorted sandstones contain climbing ripples (Sr facies) or sinusoidal antidunes (Ssad facies) (fig. 11C, 11E). Oppositely, the moderate and poorly-sorted are those with massive structures (Sm facies) or cross-stratifications (St and Sp facies) (fig. 11A, 11D). The sandstones frequently represent scour-fill deposits due to their scoured bases (fig. 7, 11D). The Sm facies could be conglomeratic and can contain mud intraclasts. Another feature of these facies is the occurrence of tool marks (grooves and chevrons) at the base of the beds (fig. 11A, 11B). These sole marks are disposed between the interface of sandstones (Sm facies) and conglomerates (Gm facies) (fig. 11A, 11B).



Figure 11 – Features related to sandstone deposition along the ESFD. A) Massive sandstone bed containing tool marks at your base. B) Groove and Chevron marks are presented in the massive sandstone bed of figure 11A. C) Lenticular bed of climbing-rippled sandstone (Sr facies) deposited between beds of massive diamictite (Dmm facies). D) Association of beds of climbing-rippled sandstones (Sr facies) and through cross-stratified sandstones (St facies), the contact between the beds are transitional, containing small scours between them. E) Continuous set of sandstones containing sinusoidal antidunes (Ssad facies). Look how the antidunes are extensive, containing a metric length.

The other group of sandy facies is the stratified ones. The main stratified sandstones are climbing-rippled (Sr facies) ones (fig. 11C, 11D). These facies are composed of sandstones which vary from well to poorly sorted, with the beds could be tabular or lenticular with a centimetric size (fig. 11C, 11D). We note that beds of Sr can almost reach metric sizes in exceptional cases (fig. 11D). The Sr are moderately sorted in beds with larger thickness and don't present a large lateral continuity, restricted to a few meters (fig. 11D). Still, about these large beds, they are generally associated with St, Gm, or Dmm facies. Through cross-bedded sandstones (St facies) could be related to these facies (fig. 11D). The St facies have scoured bases and vary from cm to m in size. Equally to the conglomeratic Gt facies, the St facies could have backsets (fig. 6H). Sandstones with planar cross-stratification are rare and have a lenticular geometry.

The sandstones with antidunes are mainly represented by sinusoidal sandstones (Ssad facies) (fig. 8E, 11E). The Ssad facies are described as trains of well-sorted sandstones with a low angle stratification (fig. 8E, 11E). Each bed of the Ssad facies has a centimetric size, but those beds tend to form sets reaching a metric thickness. These facies do not present scoured bases and have a metric extension along the outcrops (fig. 8E, 11E). The beds of the Ssad facies generally have a low dip angle that could be horizontal. It was detected that these facies could be deposited at the base of some macroforms foresets, tending to horizontalize at the bottom of them (fig. 8E). Other sandstones with antidunes are the lenticular ones (Slad facies) (fig. 6A, 6C, 6G). These facies are moderate to poorly sorted and are represented by antidunes with lower amplitudes compared to the Ssad facies. Oppositely to the Ssad, these are lenticular and are generally associated with Dmm facies (fig. 6G).

- Interpretation

Along with the deposition of the ESFD, we described a great variety of sedimentary facies composing a complex architecture. The sedimentary facies vary from massive to stratified, changing their sediment concentration, indicating different processes of genesis in the ESFD.

Firstly, we need to understand the meaning of the deposition of conglomerates with outsized boulders (Gbd facies) in the basal portion of the ESFD. These gravel

deposits don't have large lateral continuity and are restricted to the BT log (fig. 3). Due to their content with the more enormous boulders containing angular edges and polished surfaces, we interpret these clasts as ice transported (Boulton, 1979). However, we also observe stratifications and imbricated clasts in some of the Gbd facies. These structures could indicate that we have a flow component on the genesis of these deposits. We interpret that the Gbd facies represent a transition between a subglacial conduit and the external portion to the conduit. This context of sedimentation is common in ice-marginal deposits when the grounding zone sediments advance towards the water body depositing subglacial debris in a wedge geometry (Batchelor and Dowdeswell, 2015; Dietrich and Hofmann, 2019). These characteristics fit with our sedimentary record due to the geometry of the Gbd facies.

The deposition of conglomerates and diamictites along the ESFD with the facies being poorly organized suggests that the dominated processes at this succession are related to density flows. We observe the facies compose a vast spectrum of density flows due to these differences in sediment concentration and the structures in each facies. The conglomerates present a fabric comprising medium to very coarse-grained sand and clasts ranging from granule to boulder-size. This textural component suggests flows with a high density of sediments. We evaluate that the flows which form the conglomerates vary from concentrated to hyperconcentrated (Mulder and Alexander, 2001). This observation is attested by the range of conglomeratic facies that compose the ESFD.

Other facies with a disorganized character representing the deposition of density flows are the massive diamictites (Dmm facies) (fig. 9). This facies has a lesser sand and gravel concentration compared to the conglomerates. As early exposed, their higher mud content characterizes these facies. The matrix is composed of a mixture of mud and fine to medium-grained sand (fig. 9A). The content of clasts is considerable at this facies (granule to boulder size) but is also lesser if compared to the conglomerates. At our analysis, a constituent of the massive diamictites that cannot be despised is the prominent deposition of sandstone beds, which are interbedded with the massive diamictites (fig. 9A). The occurrence of these beds along the Dmm facies sedimentation exposes that these facies suffer dilution along with their deposition (Mohrig et al., 1998). We interpret that the Dmm facies represents debris flows due to their higher mud content (Mulder

and Alexander, 2001). This mud attests that these diamictites respond to more cohesive flows, characterizing another specter of density flows along the ESFD (Mulder and Alexander, 2001; Tripsanas and Piper, 2008). The sandstone beds are deposited due to the diluting of some portions around the head of the debris flow (Mohrig et al., 1998; Sohn, 2000). This diluting is a response to basal hydroplaning between the debris flow body and the bed (Mohrig et al., 1998). The hydroplaning generates an increase in the velocity of the flow. Due to this velocity increment, the water around the body is incorporated, causing a diluting of some portions of the debris flow. This dilution generates a response to the flow behavior allowing the formation of surge-like turbidite flows in the head of the debris flows, causing the deposition of sandstone beds (Mohrig et al., 1998).

Another essential aspect in the entire facies spectrum analyzed in the ESFD is defining in which flow regime the facies are deposited. We also want to know if different flux regimes can transition from one another during the deposition of the ESFD and how this transition occurs. The most typical feature, along with the deposition of the conglomerates, is their scoured bases. Scoured bases are attributing to multiple geneses but are generally related to the action of hydraulic jumps (Russell and Arnott, 2003; Hornung et al., 2007; Winsemann et al., 2009; Lang and Winsemann, 2013; Aquino et al., 2016; Lang et al., 2017). These bases could be generated for local hydraulic jumps (Russell and Arnott, 2003; Russell, 2007; Winsemann et al., 2009; Lang and Winsemann, 2013; Aquino et al., 2016; Lang et al., 2017) and most recently been attributed to complex recirculations with not necessarily the need for a hydraulic jump (Lang et al., 2021a). We interpret that these scoured bases are attributed to the action of local hydraulic jumps due to the infilling of some of these scours for lenticular antidunes formerly to the scoured conglomerates (fig 6A to 6D). Other features that in our interpretation is related to hydraulic jumps is the deposition of conglomerates with backsets (Winsemann et al., 2009; Lang and Winsemann, 2013; Lang et al., 2021b) (fig. 6H, 7, 8) and the deposition of some clast clusters, which can also be related to hydraulic sorting (Carling, 1990) (fig. 10C).

We understand that the stacking of beds of conglomerates, diamictites, and sandstones could form macroforms. One example of these macroforms is revealed in the figure 7. In that figure, we see a group of beds that tend to dip in a similar

direction between the two high-order surfaces described in the outcrop. We understand that these similar patterns represent the progradation of a unit macroform, a mouth bar (Hornung et al., 2007; Winsemann et al., 2009; Lang and Winsemann, 2013). The main architecture is composed of massive conglomerates, and some containing through-cross stratifications could mean local hydraulic jumps (those with backsets) and subcritical dunes (those which contain only foresets). We identify that in the foresets of the mouth-bar, we have most fine-grained sediments being deposited, mainly sandstones with sinusoidal antidunes (fig 8E). These facies are interpreted as supercritical flows generated by gravity-dominated underflows (Hoyal et al., 2003; Hornung et al., 2007; Winsemann et al., 2009; Lang and Winsemann, 2013; Lang et al., 2021a, 2021b). Another feature that highlights the deposition of fine-grained in the foresets of the mouth-bar is the occurrence of flame structures (fig. 7, 8C). These flames are interpreted as a product of loading a bed of higher density over the fine-grained sediment. This excessive load causes the liquefaction of the sediment and generates the structure (Lowe, 1975). In the upper portion of the mouth-bar (above the second high-order scour) (fig. 7), we observe a change of the paleoflow, attested by the presence of sigmoidal conglomerates through cross-stratified (fig. 8B). The deposition of these conglomerates is interpreted as humpback dunes. The occurrence of these bedforms generally represents a transition between supercritical and subcritical flow regimes (Lang and Winsemann, 2013; Lang et al., 2021b).

We also described the action of supercritical flow during the deposition of some massive diamictites (Dmm facies). We detected some lenticular sandstones with antidunes (fig. 6G, 9B, 9D, 9E). These facies are associated with beds of clast-supported conglomerates. This type of association between antidunes and clast-supported conglomerates is interpreted as hyperconcentrated episodic flows contemporaneously to the debris flow that generates the Dmm facies. This contemporaneity between these two types of flows is suggested by the conglomerates' injected aspect (fig. 9D, 9E) and the antidunes' geometry (which could be fluidized (fig. 9E)), indicating a quick interval of deposition.

An important aspect that helps elucidate the diversity of flows in the ESFD is understanding the genesis of some sole marks (fig. 11A, 11B) in the basal portion of massive sandstones (Sm facies). The sole marks described in our succession are

tool marks, interpreted as grooves and chevrons. To understand the role of these marks in the flow behavior, we need to know how density flows transit between a turbulent flow to a cohesive flow. Recent models trying to understand density flows subdividing them relative to their level of turbulence (Baas and Best, 2008). In these models, we have a flow thoroughly turbulent in one extreme. On the opposite side, the flow is almost entirely supported by cohesive strength, only containing a thin basal bed with turbulence. But during the flow evolution, we have intermediate portions with less turbulence and a more cohesive force (transitional flows) (Baas and Best, 2008). In these visions, the flows tend to become progressively more cohesive due to the incorporation of mud along the way (Baas and Best, 2008). So along with their path, the flow tends to become increasingly cohesive as it incorporates mud. They were passing from a thoroughly turbulent flow to a debris flows (Baas and Best, 2008). This understanding is essential to comprehend how the tool marks were generated at the base of our massive sandstone beds. To a tool (clast) became fixed and leave a mark on the basal bed of a flow, these clasts need a certain cohesive strength to be there (Peakall et al., 2020). If the flow doesn't have these cohesive forces around the clast, they will be transported and don't will leave a mark like a groove or a chevron on the basal portion of a bed (Peakall et al., 2020). So base on these stratified flows, we understand that some of these sandstones represent flows with a high level of cohesive strength with only a basal bed of turbulence, thus generating the tool marks (Peakall et al., 2020). It is important to note that we described lots of mud intraclasts inside these sandstones, which helps validate these models.

Despite features related to supercritical flows in a proximal context (concentrated and hyperconcentrated density flows), we also described facies representing the transition and the subcritical flow regimes. Along with the formation of the mouth bars, we have bedforms related to a transitional context (humpback dunes) (fig. 8B) and strata interpreted as pure subcritical flow regimes (subcritical dunes) (fig. 7, 8A, 11D). Despite that bedforms, another group of facies is related to more distal subcritical facies. We already explained that sinusoidal antidunes (fig. 8E, 11E) are deposited as underflows in the lee side of our mouth bars. We imagine a similar context to the climbing-rippled sandstones (fig. 11C, 11D). In their recent paper, Lang et al. (2021a) expose how the facies that compose mouth bars transit to

underflows generating similar features to those described by us in the ESFD. In a proximal context, the facies tend to be scoured and could also present backsets and subcritical dunes (Russell and Arnott, 2003; Hornung et al., 2007; Winsemann et al., 2009; Lang and Winsemann, 2013; Lang et al., 2017, 2021a). But as the flow loses momentum, it evolves to an underflow depositing antidunes and ripples in a more distal context (Powell, 1990; Hoyal et al., 2003; Lang et al., 2021a).

In terms of our density flows concentration, we still have one facies unrelated to high concentrations of sediments, the heterolithes (Ht facies). These facies (fig. 6E, 6F) present sets of well-sorted sandstones interbedded with thin beds of mudstones and present almost entirely deformed. But we will not explain their deformation right now. We interpreted these deposits as turbidity currents (Lowe, 1982; Mulder and Alexander, 2001). These turbidity currents are rare and restricted to the basal portion of the ESFD, probably deposited between intervals where the density flows with high concentration ceased bring space to low-density currents be deposited.

Finally, we also observe features that give us the perception that these flows could be glacially derived. Firstly, a general characteristic along with the conglomerates and diamictites in the morphology of the clasts. Many of these clasts (fig. 5, 6C, 8D, 10) are faceted and could present polished surfaces and even striations. These characteristics suggest a glacial action based on the morphometry of the sediment (Boulton, 1979). Another characteristic that could attest to the glacial action is the deposition of oversized boulders (fig. 5) in the Gbd facies. As early exposed, these sediments have been interpreted as a part of a grounding zone (Batchelor and Dowdeswell, 2015; Dietrich and Hofmann, 2019). Finally, another glacial feature related to our interpretation is the occurrence of oversized clasts (fig. 10A) in some massive diamictite beds. We interpret the occurrence of these clasts as ice-rafted (Powell, 1990; Eyles et al., 1998; Koch and Isbell, 2013; Ives and Isbell, 2021). Features related to deformation could also be a product of glaciotectonics, like the faults and boudins (fig. 9F) in some diamictite beds and the folds that deformed the fine-grained heterolithes (fig. 6F). However, we interpreted that these deformations do not have a direct relationship with the ice. Firstly, the faults and boudins are interpreted as the product of an excessive load of sediment above fine-grained beds, causing an extension, disrupting the fine-grained sandstones, and

generating the faults and boudins (Goscombe et al., 2004; Rodrigues et al., 2020). The deformation on the heteroliths is interpreted as the product of small slumps in the glacier's front, generating the folds and the deformation in the fine-grained facies.

4.5.1.3 Late-stage fan deposits

- Description

The Late-stage fan deposits (LSFD) are the facies association deposited directly above the ESFD, where we observe a transitional contact between these units in the outcrops. Oppositely to the deposits of the ESFD, the LSFD was not mapped in the whole study area, with the outcrops being restricted to the southern sector (AE and CT logs (fig. 3)). The lithologies which compose this unit are less diverse if compared to the ESFD. If in the ESFD we have a great specter of facies with a great diversity of structures and fabrics, here the facies are mainly massive diamictites (fig. 12A, 12B, 12C) (Dmm facies) and sandstones (fig. 12A, 12B) (Sm facies). Beyond that, we described a minor number of conglomerates that are restricted to cm beds of normally graded (fig. 12E) conglomerates (Gn facies) and some lenses of clast-supported (fig. 12D) conglomerates (Gmc facies) embedded in the diamictites.

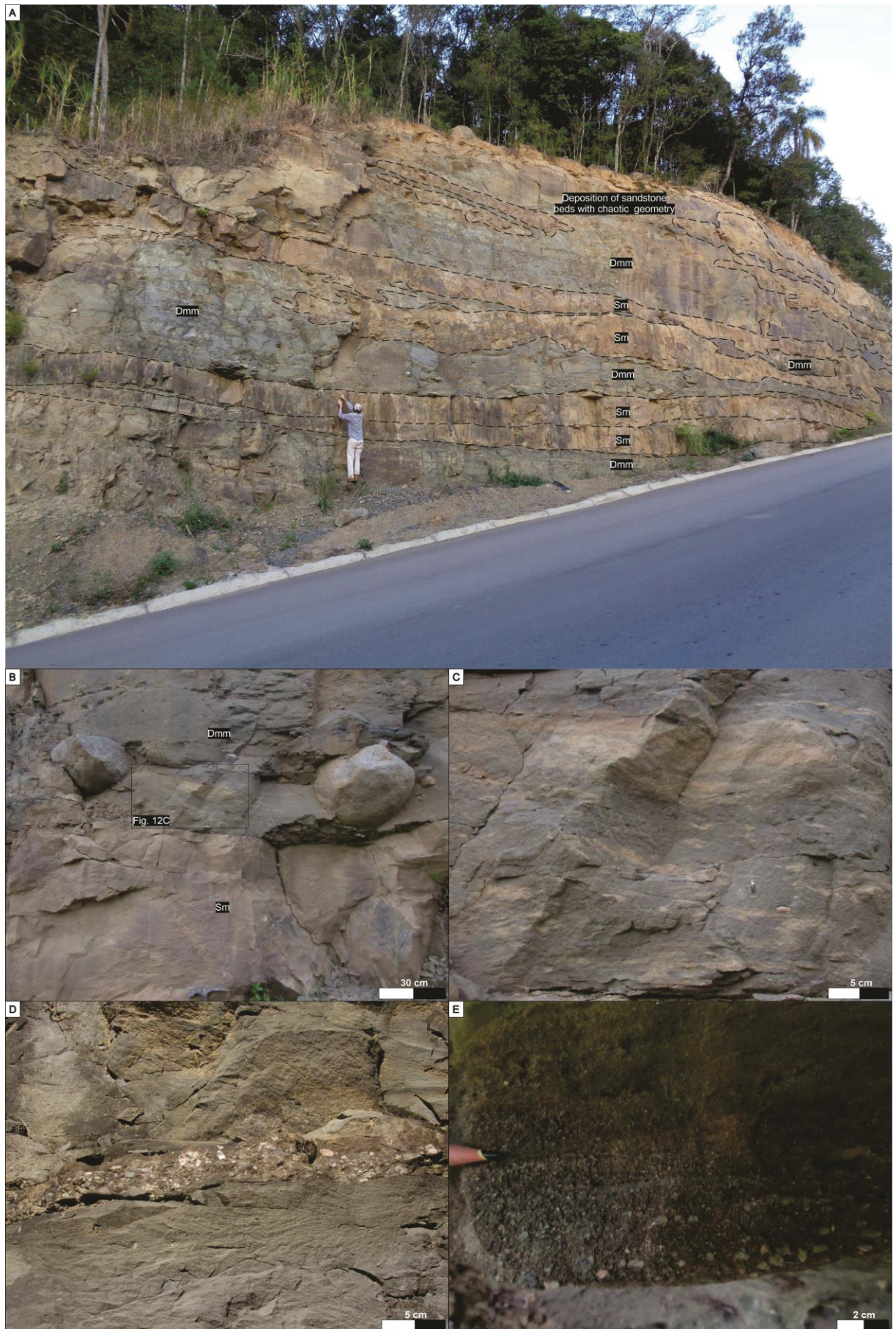


Figure 12 - Facies and features described in the late-stage fan deposits (LSFD). A) Larger exposure to the LSFD in a road cut in the southern sector of the study area (CT log). Here we can observe the main character of the LSFD with the irregular interbedding between massive diamictites and massive sandstones. Firstly, we can see that the sandstones vary from a tabular to a lenticular geometry, with some beds containing a chaotic geometry (upper portion of the outcrop). Another character to observe is the presence of scoured bases in the lenticular sandstone beds. The Dmm beds also present multiple geometries varying from tabular to lenticular and sometimes are sandwiched between the sandstone beds. B) Contact between massive diamictites and massive sandstones. We highlighted the occurrence of lonestones in the diamictite bed. Another essential feature that remains similar to those massive diamictites deposited in the ESFD is sheared sandstone beds dispersed among the diamictites' matrix. C) Detail to the sheared sandstone beds in figure 12B. D) Centimetric bed of clast-supported conglomerates deposited between two horizons of diamictites. E) Aspect of the normally graded conglomerates deposited in the LSFD.

The main fabric of the LSFD is composed of massive sandstones and diamictites as early exposed (fig. 12A). The sandstones are moderately sorted with varying from fine to medium-grained sand. The structure of the sandstones is massive, and they have a geometry ranging from tabular to lenticular, with some having a chaotic one (fig. 12A). In some cases the sandstone beds can also be amalgamated. A common feature is the borders of some lenticular beds. These beds tend to expand to inside the surrounding diamictite beds (Dmm facies) and, in some cases, mix with the diamictites (fig. 12A). Some borders with a vertical expansion toward the diamictite beds could represent flame structures.

The diamictites are slightly different from those described in the ESFD, where the difference remains that these have a higher mud content and fewer boulders and cobbles than the previous ones. Without that, these diamictites present the same massive structure and dispersed clasts ranging from granule to boulder-sized (fig. 12A, 12B). Another similar aspect is the occurrence of sheared beds of fine to medium-grained sandstones deposited inside the diamictite beds (fig. 12C). About the clasts inside the diamictites, they have various formats ranging from sub-rounded to angular. Some of them contain angular edges or polished surfaces. The occurrence of outsized boulders dispersed in the matrix is interpreted as lonestones (fig. 12B). It's important to note that lonestones were previously described in the ESFD, but those in the LSFD are smaller, reaching almost 30 cm.

We describe a restricted number of conglomerate facies in the LSFD (Gmc and Gn facies). The clast-supported conglomerates (Gmc facies) are limited to some cm lenticular beds (fig. 12D). These conglomerates present angular clasts that range from granule to pebble-sized. The normally graded conglomerates (Gn facies) also have a cm thickness and have angular clasts ranging from granule to small pebbles (Fig. 12E).

- Interpretation

In the LSFD, we observe some changes in the facies architecture if we compared these facies association with the ESFD. The first significant change in the facies genesis is the abrupt change in the abundance in the conglomeratic facies. In the LSFD, the only facies related to conglomerates are restricted to some normally graded conglomerates (Gn facies) (fig. 12E) and lenticular deposits of clast-supported (fig. 12D) conglomerates (Gmc facies). We interpreted this small amount of gravelly deposition to the action of episodic concentrated and hyperconcentrated density flows (Mulder and Alexander, 2001).

The diamictites deposited in the LSFD are a response to multiple combined processes of deposition (fig. 12A, 12B, 12C, 12D). Firstly the matrix of these diamictites is muddy, containing a small amount of sand. The fabric of these diamictites is compatible with those deposited by upwelling plumes in the front of grounding-line fans (Powell, 1990; Lønne, 1995; Powell and Alley, 1997). Grounding-line fans are known for expelling jets from subglacial tunnels to body water, and these jets could generate multiple density flows (which their specter was explored in the ESFD deposits). Some of the jet's mixtures of fluid and sediment could be less dense than the ambient body water. If these conditions happen, a plume ascends in the water, settling fine-grained sediment and generally create massive diamictite facies (Powell, 1990). Furthermore, we understand that processes like debris flow expelled by the grounding-line and fall-out of ice-rafted debris (lonestone deposition) could also contribute to these diamictites' genesis. This contribution by debris flow is suggested by the similarities between the sheared sandstone beds (fig. 9A, 9E, 12C) in the LSFD and those described in the ESFD, which were attributed to the hydroplaning of debris flows (Mohrig et al., 1998; Sohn, 2000).

If the LSFD does not present many conglomeratic facies, it shows massive sandstones (Sm facies). These beds of these sandstones show different geometries (fig. 12A), suggesting that we can have depositional and post-depositional processes that are influenced in the genesis and the disposal of the beds. We interpreted that the sandstone beds' with tabular geometry are related to the action of concentrated flows expelled by glacial jets (Powell, 1990; Mulder and Alexander, 2001; Russell and Arnott, 2003). However, we observe that many of these beds don't have a

tabular geometry. Oppositely, the disposal of the majority of the beds varies from lenticular to chaotic. We interpreted that these beds' dispositions could be related to deformational processes that deformed previously tabular beds.

These deformations are attested by how some parts of the beds entrains the surrounding diamictites vertically and laterally (fig. 12A). Processes like fluidization could generate these edges of the deformed sandstones (Lowe, 1975). The fluidization allows that the sediment flows to the surrounding lithologies causing this deformed aspect. But which processes could cause fluidization in such different levels as observed in the LSFD? Similar facies were described in LPIA deposits of Antarctica. In that deposits, the fluidization in the sandstone bodies is attributed to slumps in the front of grounding-line fans (Koch and Isbell, 2013; Ives and Isbell, 2021). In our study, we understand that slumps can contribute to generating these structures, observing an increase in the rate of deformation towards the top of the succession. This growth in the fluidization in the LSFD could be related to an increment in the slope angle, creating more significant slumps in the top of the succession. In our analysis, these features indicate that the deposition of this system could be related to a sloped surface.

4.5.1.4 Slope collapsed deposits

- Description

The slope collapsed deposits (SCD) is the last facies association described in our study interval. The SCD is deposited directly above the facies of the LSFD, where we observe a transitional contact between these two units. We suggest that these contacts are transitional because of two factors. Firstly, we see that at the top of the LSFD, the sandstones and diamictites already present deformational features. Despite that, we described relicts (fig. 13A) of the LSFD deposits in the base of some SCD outcrops, which suggests less deformed portions inside this facies association. About the frequency in the study area, we described outcrops in the southern and northern sectors.

The facies which compose the SCD are diamictites with ressedimentation features (tab. 1). We separate these diamictites into two facies. The first facies is the heterogeneous massive diamictites with ressedimentation features (Dm(r-ht) facies).

They are composed of a muddy matrix containing basinal (sandstones and conglomerates) and extrabasinal (granites and high-grade metamorphic rocks) clasts. The basinal clasts as early exposed are sandstones and conglomerates. These clasts were described as rafted blocks that are dispersed in the muddy-sandy matrix. The sandstone blocks have more significant dimensions that could reach almost 10 m in length. Inside the blocks, we observe an internally deformed aspect, which could contain faults, boudins, and sheared beds (fig 13B). The conglomerate blocks are smaller, reaching dimensions lesser than one meter. The conglomerates described as blocks are clast-supported with composition and morphometry of the clasts similar to those described in the ESFD and LSFD facies associations (fig. 13C). The extrabasinal clasts show multiple grades of rounding varying from rounded to angular and ranging from granule to boulder size.

The second facies composing the SCD are homogeneous diamictites (fig. 14) with ressedimented aspects (Dm(r-hm) facies). These diamictites present a homogeneous muddy matrix containing some dispersed intrabasinal and extrabasinal clasts. The extrabasinal clasts have a similar composition and morphometry to those described in the heterogeneous diamictites (fig. 14B). However, they are considerably less frequent and range from granule to cobble size. In terms of intrabasinal clasts, we described some fine to medium-grained sandstone beds dispersed along with the matrix of the diamictites (fig. 14C). It's widespread that these sandy beds present themselves with a sheared aspect with a centimetric thickness.

An important characteristic to note in the outcrops of the SCD is how the matrix content changes (fig. 13,14). If we observe the outcrops containing the Dm(r-hm) facies, the zones that contain larger intrabasinal blocks (metric ones) tend to have a lesser matrix content (fig. 13A, 13D). Oppositely, in areas where the matrix is more widespread, the rafted blocks are smaller or not even present (fig. 13A, 13D). These increases in the matrix appear to be progressive, reaching the higher peak in the Dm(r-hm) facies (fig. 14). In the homogeneous diamictites, we don't observe rafted blocks anymore, with the sand content being restricted to the sheared sandstone beds (fig. 14C).

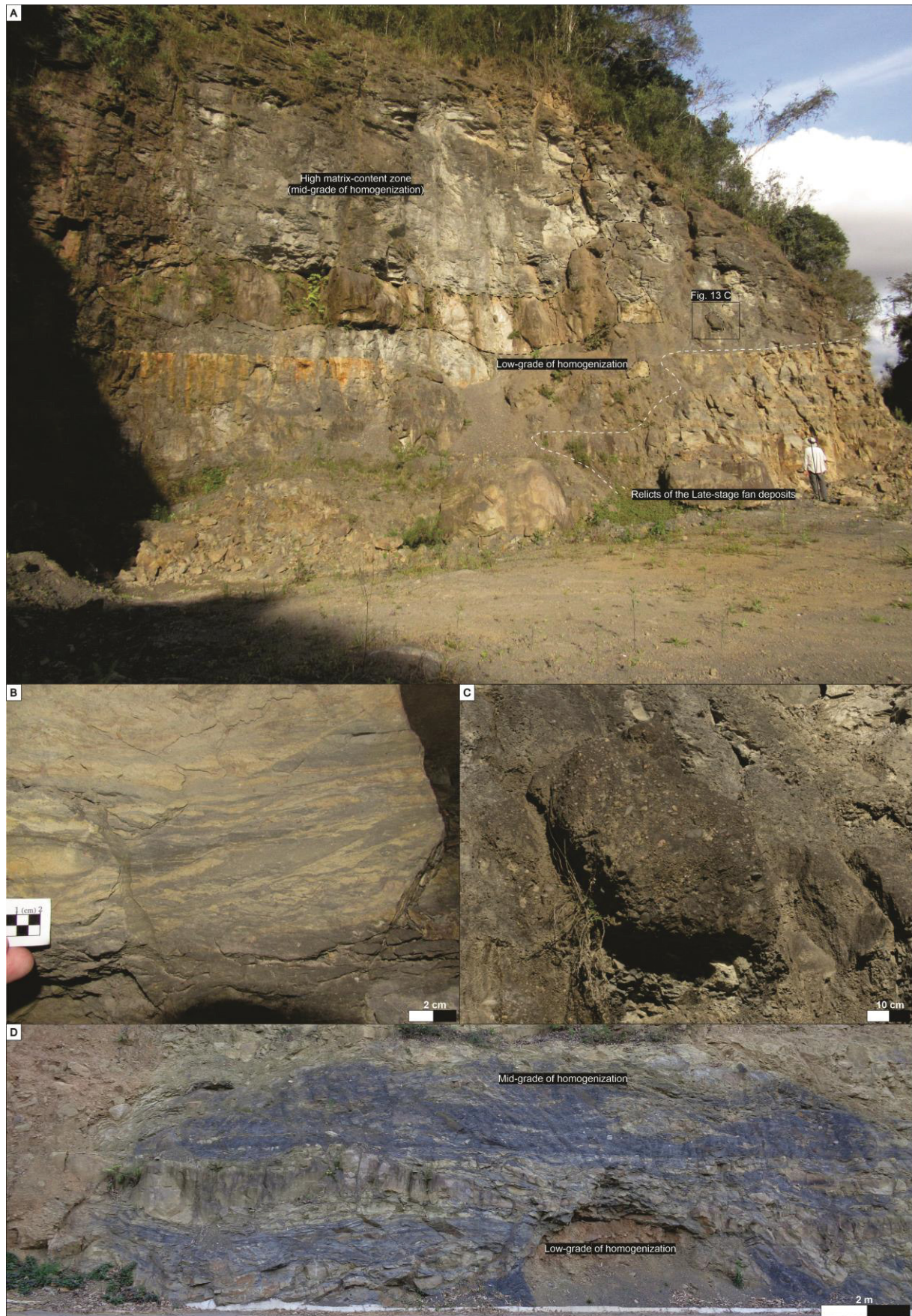


Figure 13 – Mainly features of the Dm(r-ht) facies. A) WT-2 outcrop showing the main fabric of the heterogeneous diamictites. In this outcrop, we can observe some critical features that compose these facies. Firstly at the base of

the outcrop, we have relicts of the LSFD that remains almost undeformed. Laterally we observe how the rate matrix/clasts tend to increase to the upper portion of the outcrop. B) Internally deformed block of sandstone containing boudins, faults, and sheared beds. C) Highlighted conglomerate block in the WT-2 outcrop. D) Outcrop of the SCD in the southern sector of the study area. Here we can observe how the sandstone blocks tend to become smaller and discontinuous towards the upper portion of the outcrop, increasing the matrix content.



Figure 14 – Main Features of the Dm(r-hm) facies. A) Picture of the WT-1 outcrop showing a thoroughly homogenized diamictite with a high matrix content. B) Fabric of the homogenized diamictites. Here we can observe a homogeneous muddy-matrix with dispersed clasts ranging from granule to cobble-size. Note that some of the clasts and angular. C) Centimetric sheared sandstone bed deposited in the homogeneous diamictites.

- Interpretation

Analyzing the facies deposited inside the SCD association, we observe that the entire specter of lithologies has a particular grade of affinity with ressedimentation processes. This link is suggested by the characteristics described in the diamictites. Firstly, in the Dm(r-ht) facies, we observe many features that could be correlated with deformational processes. The most prominent is the occurrence of rafted blocks of sandstones and conglomerates that are dispersed in a sandy mud matrix. The existence of these blocks spread among the matrix suggested remobilization and ressedimentation of a previously deposited sediment (Dott, Jr, 1963; Nemec, 1990; Posamentier and Martinsen, 2011). Another aspect that suggested ressedimentation is the internal fabric of these heterogeneous diamictites. The deformed blocks of sandstones and diamictites are similar in texture and structure to those described inside the previously deposited facies associations (ESFD and LSFD). Despite that, we saw relicts of the LSFD inside the heterogeneous diamictites, which also suggests a genetic link between these two facies associations.

Another facies represents a second stage where the deformation tends to create a significant amount of matrix over the basinal clasts, creating a more homogenized product. In the Dm(r-hm) facies, we observe that the features like larger allochthonous blocks are not present anymore. Even the matrix was homogenized. If in the heterogeneous diamictites we have a matrix with a significant quantity of sand, in these ones, the fabric is entirely muddy. The only sand content is restricted to sheared beds of sandstones. In our view, some processes were capable of progressively homogenizing these sedimentary products, decreasing the sand content, and creating more matrix in the diamictites (Nemec, 1990; Martinsen, 1994; Eyles and Eyles, 2000; Strachan, 2008).

In our perception, these facies could represent the deposition of mass-transport deposits (MTD) due to the features described among the diamictites (Dott, Jr, 1963; Martinsen, 1989, 1994; Nemec, 1990; Moscardelli et al., 2006; Strachan, 2008; Posamentier and Martinsen, 2011; Rodrigues et al., 2020). The deposition of MTD is related to mass-flows. In these conditions, the sediment tends to be transported “*en masse*” during the evolution of the flow (Dott, Jr, 1963; Martinsen, 1994). This means that the sediment inside the flow is transported together, mainly supported by the cohesion between the grains. The group of mass-flows includes debris flow, slumps, and slides (Dott, Jr, 1963). However, the mass-flows with more

capability to cause remobilization, ressedimentation, and, consequently, deformational structures on a large scale are the slumps and slides (Dott, Jr, 1963; Martinsen, 1994; Posamentier and Martinsen, 2011). A decollement surface generally generates the slides at their upper portion of the mass flow (Nemec, 1990; Posamentier and Martinsen, 2011). Their products are related to a small internal deformation (rotation and translation of the beds), which could generate brittle deformation (faults) at the distal portion of the deposits (Dott, Jr, 1963; Nemec, 1990; Martinsen, 1994; Moscardelli et al., 2006; Posamentier and Martinsen, 2011).

The slumps are another specter of the mass-flows. They could also be created by a decollement surface or evolve from slides (Nemec, 1990; Martinsen, 1994; Posamentier and Martinsen, 2011). These flows are characterized by moving together as a coherent mass and, different from the slides, present significant internal deformation. In slumps, processes like fluidization, liquefaction, mixing, and desegregation are active and could generate multiple deformational products (Dott, Jr, 1963; Martinsen, 1989, 1994; Eyles and Eyles, 2000; Strachan, 2008; Rodrigues et al., 2020). Several studies suggested that these processes could be increasingly more prominent along with the evolution of the slumps. The increment in the disaggregation and mixing cause a progressive homogenization of the protolith, increasing the matrix content and decreasing the size of intrabasinal clasts (Nemec, 1990; Martinsen, 1994; Eyles and Eyles, 2000; Strachan, 2008; Rodrigues et al., 2020).

Recent studies in the ressedimented diamictites of the Itararé Group (which include the analyzed outcrops) by Rodrigues et al. (2020) suggested that these are the mechanisms capable of creating a homogeneous product coming from an initial little or non-deformed protolith. In this study, the authors explore how processes like mixing, desegregation, fluidization, and liquefaction can create multiple deformational products like the allochthonous blocks, boudins, faults, and sheared beds observed in our outcrops (Rodrigues et al., 2020). We suggest that similar processes were capable of deforming and homogenizing the initial sandstones and massive diamictites of the LSFD and create the products observed in the SCD association.

In terms of sedimentary environment, we interpreted that this deformation is associated with a submarine slope (Nemec, 1990; Moscardelli et al., 2006;

Posamentier and Martinsen, 2011; Rodrigues et al., 2020). We suggested that because of two factors. Firstly, our initial observations in the deposition of the LSFD indicated that along with their sedimentation, the deformation increases toward the top of the succession. These deformations could be caused by slumps contemporaneously to the sedimentation of the LSFD (Dott, Jr, 1963; Martinsen, 1989, 1994; Nemec, 1990; Posamentier and Martinsen, 2011). Furthermore, we understand that the occurrence of ressedimented diamictites (which are progressively homogenized) could result from the collapse of the previously deposited sediments (LSFD) in a submarine slope (Nemec, 1990; Eyles and Eyles, 2000; Moscardelli et al., 2006; Strachan, 2008; Posamentier and Martinsen, 2011; Rodrigues et al., 2020).

4.5.2 Paleocurrents

As previously mentioned in the methods and facies associations sections, a cross-stratification in supercritical contexts could represent backsets, representing a structure that goes in the opposite direction of the flow. To maintain control about these flow directions in these stratifications, we need to measure associate structures or bedforms that represent the deposition in the subcritical flow regime most of the time (Lang et al., 2021b). It is essential to follow these parameters to create greater security about the directions of our paleocurrents and have a great certainty that these cross-stratifications don't represent backsets.

In our analysis, these parameter is complicated to be followed in our outcrops. The main problem that we detected is that we don't observe sandstones with ripples or climbing-ripple lamination (representing a genuinely subcritical flow regime) associated with the cross-stratification in all the outcrops. So, we opted to utilize only paleocurrents from climbing ripples in our study, which granted us a reliable analysis of the paleotransport. Another essential aspect to consider is that the data were collected from the ESFD association, the only succession with sedimentary structures indicating the paleoflow.

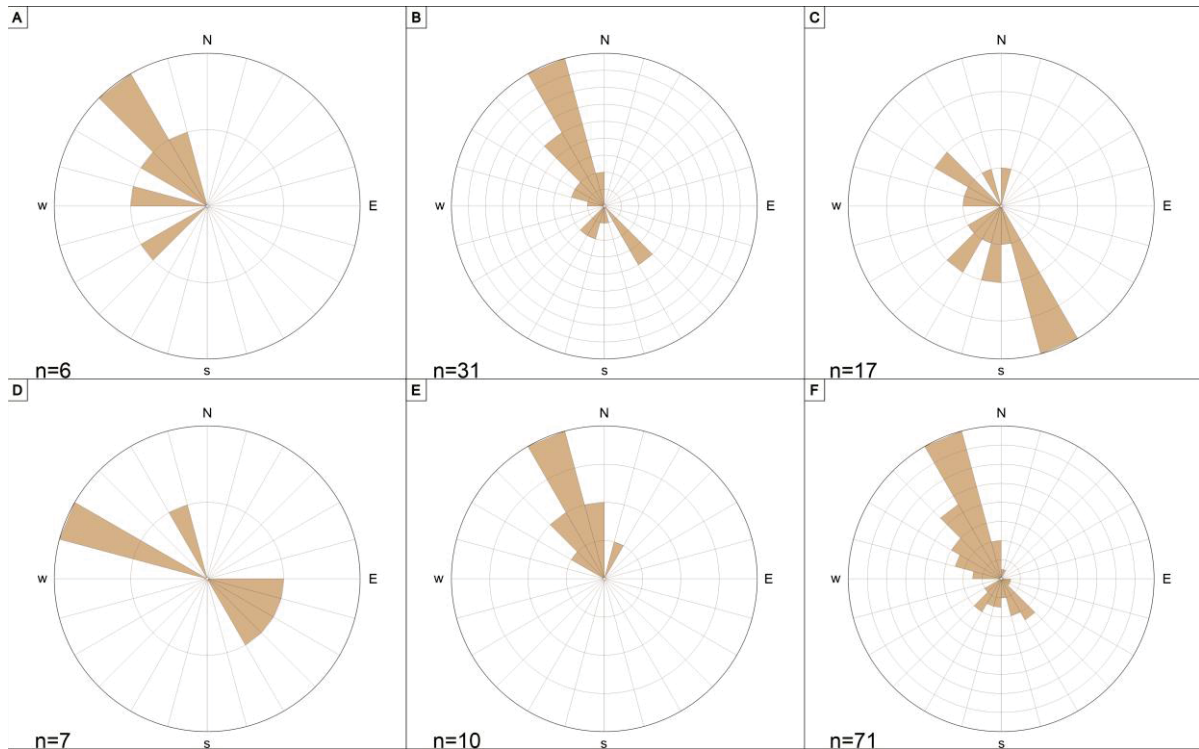


Figure 15 – Rose diagrams with the paleocurrent data analyzed for the ESFD succession. The locations of the outcrops are available in figure 1, with the mean direction of each rose diagram. A) Directions of the NSF outcrop. B) Directions of the BT outcrop. C) Directions of the PT outcrop. D) Directions of the AE outcrop. E) Directions of the CT outcrop. F) Compose diagram containing all the paleocurrent data collected in the ESFD succession.

In total, we analyzed 71 paleocurrent measures in sandstones with climbing ripple laminations in 5 different outcrops. In four of these outcrops, we raised sedimentary logs (fig. 3). In one of these outcrops (PT), we don't raise a sedimentary log, but you can observe their architecture in the photomosaic of figure 7. In a general analysis, we can keep that three of our five individual rose diagrams (fig. 15A, 15B, 15E) presents a primary trend to NW with secondary trends for SW and SE. Only in the PT outcrop (fig. 15C) do we observe a primary trend to the south. If we note that is the direction where we see the progradation of the mouth bar in figure 6. Despite that, we suggest that these directions could indicate a slight change in the paleocurrent directions, indicating a readjustment of the system. But, if we observe at the top of the outcrop (fig. 7), the humpback dunes suggest a new change in the paleoflow, changing their flow direction and migrating towards the north. Another explanation to some paleocurrents towards the south could be related to the action of some hydraulic jumps. Some field studies in glacial deltas suggest that their activity could generate an up-slope migration of the ripples, generating some bedforms migrating opposite to the flow direction (Winsemann et al., 2007, 2018).

However, if we observe the total amount of paleocurrents, they indicate a direction to NW. These directions became more consistent if we analyze the paleocurrents together (fig. 15F). In general, the deposition of the ESFD indicates a general trend of paleotransport to NW, which is compatible with many successions in of the Itararé Group in the Santa Catarina state (Barbosa, 1940; Carvalho, 1940; Rocha-Campos et al., 1988; Santos et al., 1992; Puigdomenech et al., 2014; Aquino et al., 2016; Rosa et al., 2016, 2021; Fallgatter and Paim, 2019). These trends of paleocurrents suggest a disagreement with the previous work in the study area. Schemiko et al. (2019) also analyzed the paleocurrents in the ESFD association, indicating a general trend of paleotransport toward the South (SSE and SSW). We imagine that in their analysis, some of the measure structures could represent backsets changing than the downflow direction of the paleoflow. We opted to utilize only climbing ripples in our analysis for that reason. If we measure backsets in cross-stratification, our paleocurrents could become polluted with measures that does not indicate the real paleoflow direction but the opposite direction instead. Even knowing that climbing ripples could migrate up-slope, the occurrence of these settings in the geological record is rare (Winsemann et al., 2007, 2018), so we understand that these structures are reliable as paleotransport indicators.

In our view, the trend of paleotransport associated with the several glaciogenic features described in our facies suggests a glacier advance from the adjacent areas (SE) as the source of sediments to the deposition of the study succession. According to these directions of paleoflow, these sediments could be supplied by glacial paleovalleys located in the Windhoek Highlands in Namibia (Martin, 1981; Visser, 1987; Santos et al., 1996). These paleovalleys were interpreted by several authors as the glacial source of the Itararé Group in the eastern and south-eastern border of the Paraná Basin (Santos et al., 1996; Vesely et al., 2015; Aquino et al., 2016; Fallgatter and Paim, 2019; Rosa et al., 2019). However, evidence from the action of the Namibian glacial source in the Santa Catarina state is restricted to strata deposited below the Lontras shale (base of the Rio do Sul Formation). So, these could be the first evidence of a new advance of these glaciers towards Paraná Basin in the last stages of deposition of the Itararé Group in Santa Catarina state.

4.6 Discussion

4.6.1 Depositional environment and flow transitions

In our understanding, each of our facies associations represents a different stage of evolution of a depositional system related to ice action. At the base of our succession, we identify shales and ressedimented diamictites of the Rio do Sul Formation (fig. 4A,4B). These sediments were previously interpreted as deposited below the wave base level (Castro, 1980; Canuto, 1993; Puigdomenech et al., 2014; Schemiko et al., 2019). Directly above these facies, we describe the Dfl facies (fig. 4C to 4F), which represent a glaciotectionic deformation over the previous substrate. We interpreted that this glaciotectionic deformation over the Rio do Sul Formation sediments occur due to a glacier advance towards the Paraná Basin. However, it is essential to note that the sediments which are deposited below the Dfl facies represent the deposition of mainly turbidites (and ressedimented associated facies), deposited in a marine basin, as discussed by several authors (Castro, 1980; Canuto, 1993; Puigdomenech et al., 2014; Fallgatter and Paim, 2019; Schemiko et al., 2019; Vesely et al., 2021). In our view, the deposition of the glaciotectionites of the Dfl facies over the marine sediments of the Rio do Sul Formation corroborates that these glacial advances took place over a marine environment.

Above the glaciotectionized substrate, we observe that the products generated by the deposition of the ESFD association are varied and represent multiple processes along a glacial margin. The products deposited directed above the substrate vary along with the study area. However, in our sedimentary logs, the most proximal facies over the substrate (Dfl facies or mudstones) are the Gbd facies (fig. 5). The Gbd facies are interpreted as a combining of subglacial transport with a current component due to the imbrication of the clasts and the stratifications in some portions of the deposits. In our view, the deposition of the Gbd facies represents a portion of the ESFD generated underneath the glacier. Due to the limited and lenticular occurrence of the Gbd facies, we interpreted that these deposits represent the transition between the subglacial conduit and the water body, probably deposited in a wedge shape (Batchelor and Dowdeswell, 2015; Dietrich and Hofmann, 2019).

However, most of the facies in the ESFD association are not deposited underneath the ice but deposited towards the water body. These facies are

composed of massive diamictites (Dmm facies), conglomerates (Gms, Gmc, Gt, and Gn facies), and sandstones (Sr, St, Sm, Ssad, and Slad facies) and Heterolites (Ht facies). The sub-aquatic deposits of the ESFD represent a wide specter of density flows related to multiple support mechanisms that vary according to the sediment concentration and the distance to the ice margin.

The facies with a higher mud content on their matrix are the massive diamictites (Dmm facies) (fig. 9). These facies are interpreted as products of cohesive density flows (debris flows). It's common, along with the deposition of the Dmm facies, the occurrence of fine-grained sandstone beds (fig. 9A). We interpreted that these sandstone beds are related to surge-like turbidite flows triggered on the heads of the debris flows. To generate these currents on the head of the flows, some diluting needs to occur to create portions with less density inside the flow. We suggested that the process responsible for generating this dilution is the hydroplaning of the debris flows (Mohrig et al., 1998; Sohn, 2000). The hydroplaning of the flow is a response to a high lubricated base with high water content. These lubricated bases cause an increment in the velocity of the flow. Along with the evolution of the flow, they tend to incorporate some adjacent water as the velocity increases, causing a progressive dilution and triggering turbidity currents at the head of the debris flows (Mohrig et al., 1998; Sohn, 2000).

In our understanding, these debris flows are generated through sediments accumulated in the grounding zone the slumps towards the body water (Eyles et al., 1985; Powell and Molnia, 1989; Powell, 1990; Lønne, 1995). These slumps cause the generation of cohesive flows in the front of the glacier margin in some portions that could hydroplane and generate the sandstone beds that we discussed previously. We also observe other processes that lead to the deposition of lonestones, clast-supported conglomerates, and sandstones with antidunes associated with the massive diamictites. These other processes will be discussed further in this section.

However, in the ESFD association, we also described facies that are related to the deposition of concentrated and hyperconcentrated density flows. We observe that these facies varies along the study area, comprehending massive and scoured conglomerates and sandstones (Gms, Gmc, Sm facies), graded gravels (Gn facies),

and stratified conglomerates that could contain foresets or backsets (Gt facies). In our description, along with the study area, we observe that these facies vary laterally, representing different stages of the flow behavior.

These patterns were observed in several successions of glacial-marginal systems and are attributed to a wall-jet model (Powell, 1990; Russell and Arnott, 2003; Hornung et al., 2007; Winsemann et al., 2009; Lang and Winsemann, 2013; Aquino et al., 2016; Lang et al., 2017). In hydraulics, the wall-jets are represented as a flow with capability for expansion (Rajaratnam and Subramanyan, 1986; Long et al., 1990, 1991). In glacial contexts, the flow is confined to a single or a group of subglacial (or englacial) conduits until reaching a body of water. When the flow gets the body water, they tend to expand due to the loss of confinement. During this expansion, the flow transits from a subcritical ($Fr < 1$) to a supercritical ($Fr > 1$) flow (Rajaratnam and Subramanyan, 1986; Long et al., 1990, 1991; Roberts et al., 2001; Hoyal et al., 2003; Russell and Arnott, 2003). This transition generally involves a hydraulic jump, generating scours in the facies more proximal to the jump (Russell and Arnott, 2003; Hornung et al., 2007; Winsemann et al., 2009; Lang and Winsemann, 2013; Aquino et al., 2016; Lang et al., 2017). However, recent work attributed that the scours in the proximal regions of the jets could be attributed to other factors like complex recirculations, bursts, and waves as the genesis of the scours, with no need for a hydraulic jump (Lang et al., 2021a).

In our succession, we observed several features that indicate a similar mechanism of deposition. We described several facies compatible with a jet sedimentation, showing an entire specter from proximal to distal deposits. In the most proximal portion, we characterized matrix-supported (fig. 7, 8A, 10C, 10D) and clast-supported conglomerates (fig. 6A, 6B, 6C, 6D, 7, 8D) (Gms and Gmc facies) and trough-cross stratified conglomerates with backsets (fig. 6H, 8D) (Gt facies). These facies are interpreted as the deposits of the hydraulic jump zone due to the characteristics like deep-scour fills (fig. 7, 8A), backsets (fig. 7, 8A), and clast clusters (fig. 10C) that could be generated by hydraulic segregation (Carling, 1990; Russell and Arnott, 2003; Hornung et al., 2007; Winsemann et al., 2009; Lang and Winsemann, 2013; Lang et al., 2017, 2021a).

Still, in the proximal region of the jet, we described facies that represent the action in the upper flow regime (Winsemann et al., 2009; Lang and Winsemann, 2013; Cartigny et al., 2014; Lang et al., 2017, 2021b). They are characterized by the deposition of lenticular antidunes (Slad facies) (fig. 6A, 6B, 6C, 6D, 6G, 9B, 9D, 9E) that are associated with the deposition of clast-supported conglomerates (Gmc facies) or massive diamictites (Dmm facies). These antidunes have small length and were described together with clast-supported conglomerates, which suggest an association between concentrated and hyperconcentrated flow and the deposition of these upper flow regime bedforms. The association of these bedforms (where some are fluidized) with the massive diamictites suggests some contemporaneity between the jet events (hyperconcentrated flows) and the debris flow slumped from the grounding zone.

Distancing from the proximal region of the jet, we observe some bedforms that show us a transitional behavior of the flow from supercritical to subcritical flow, the humpback dunes (fig. 7, 8B) (Lang and Winsemann, 2013; Lang et al., 2017). These bedforms are characterized as conglomerates with a sigmoidal geometry and a metric dimension (fig. 7, 8B). In wall-jet contexts, these bedforms are considered a stage of transition from the deposition of antidunes and subcritical dunes (Lang and Winsemann, 2013).

As long the jet loses velocity distancing from the proximal zone, the flow tends to pass from supercritical to a subcritical regime (Russell and Arnott, 2003; Hornung et al., 2007; Winsemann et al., 2009; Lang and Winsemann, 2013). As the end member of the jet facies, we identify the deposition of foresets (fig. 8A, 11D) trough cross-stratified sandstones (Gt facies). These facies, in our view, are subcritical dunes, being them the returning of the flow to a subcritical regime (Russell and Arnott, 2003; Winsemann et al., 2009; Lang and Winsemann, 2013; Lang et al., 2021a).

The architecture of the deposits in wall-jet settings tends to form mouth-bars (fig. 6), which are facies that are related to momentum-dominated flows. In the study area, the mouth bars are composed of scoured matrix-supported conglomerates that could contain foresets or backsets (Gms and Gt facies); scoured clast-supported conglomerates (Gms facies); graded conglomerates (Gn facies), sigmoidal

conglomerates (Gt facies); trough-cross bedded sandstones (St facies); and massive sandstones (Sm facies).

However, during the flow evolution in a wall-jet context, it tends to lose momentum during its pathway. During this loss of velocity, the flow transit from a momentum-dominated in the most proximal region of the jet to a gravity-dominated flow in their distal portion (Powell, 1990; Roberts et al., 2001; Hoyal et al., 2003; Winsemann et al., 2009; Lang et al., 2021a). This transformation in the flow tends to deposit the gravity-driven flows into the lee side of the mouth-bars. Works with flume experiments revealed that these density flows deposit as underflows after their transformation due to the loss of momentum (Roberts et al., 2001; Hoyal et al., 2003; Lang et al., 2021a). Recent work from Lang et al. (2021a) showed that these underflows could deposit both antidunes and climbing ripples, indicating that the gravity-flows, like the proximal jet facies, could also transit from a supercritical to a subcritical regime. In the study area, we verified the deposition of sandstones with sinusoidal antidunes (Ssad facies) (fig. 7, 8E, 11E) in the lee side of the macroforms interpreted by us as mouth-bars, which also was a characteristic observed by Lang et al. (2021a) in their recent study. We propose that these transformations from a momentum-dominated flow to an underflow are the mechanism that allows these bedforms to be deposited in the area. We also verify the presence of climbing ripples (fig. 11C) in the study area, which are attributed to the passage from a supercritical to a subcritical flow during the deposition of the underflows (Hoyal et al., 2003; Lang et al., 2021a). However, the ripples could also be generated by the transition of the jet from a supercritical to a subcritical flow regime, as observed by other authors (Russell and Arnott, 2003; Hornung et al., 2007; Winsemann et al., 2009; Lang and Winsemann, 2013; Aquino et al., 2016; Lang et al., 2017).

In our analysis, the occurrence of tool marks at the base of some massive sandstone beds (Sm facies) (fig. 11A, 11B) could help us to understand if any factor could act as a facilitator for the loss of momentum from the jets. According to Peakall et al. (2020), the deposition of these marks occurs when the flow loses turbulence almost entirely, containing only a turbulent base capable of transport the coarser sediment (gravel) in their basal portion. This turbulence loss is attributed to the incorporation of mud in the flow, which results in a flow less turbulent and more cohesive (Baas and Best, 2008; Peakall et al., 2020). Nevertheless, the beds of

massive sandstone beds contain several mudstone intraclasts, which corroborates the hypothesis of mud incorporation during the flow evolution. So, we suggest that these mud incorporation during the flow evolution could help in the loss of velocity and turbulence during their development, which implicates the complete loss of momentum of the flow and their transformation to underflows distally.

Despite the deposition of the jets (concentrated, hyperconcentrated, and underflows) and the occurrence of debris flows, other processes developed along with the sedimentation of the glacial margin on the study area. The description of oversized lonestones (fig. 10A) deposited internally to massive diamictite beds suggests that ice-rafted debris could be sedimented from icebergs in proximal settings of the glacial margin (Eyles et al., 1985; Thomas and Connell, 1985; Powell, 1990; Lønne, 1995; Powell and Alley, 1997). We also observed the deposition of heterolithes (fig. 6E, 6F) that are disposed of between packages of coarse-grained facies. In our interpretation, these fine-grained facies could be related to low-density flows deposited during intervals where the jet sedimentation is lesser active on the glacial margin (Lowe, 1982; Mulder and Alexander, 2001).

In our view, the sedimentation of the ESFD is directed linked to a glacial source due to several characteristics observed at the succession: 1) Occurrence of striated, faceted, and polished clasts inside conglomerates and diamictites, which corroborates a glacial source to the sediments; 2) Deposition of oversized boulders on the basal portion attributed to grounding-zone sedimentation (subglacial conduit); 3) Description of metric lonestones inside massive diamictite beds deposited by ice-rafting; 4) Deposition of conglomerates and sandstones that represent the deposition of a jet-efflux model that could be directed linked to grounding-line fan sedimentation. Therefore, our study of the ESFD deposits disagrees with the previous interpretation for these deposits. Previous studies suggest that the sedimentation of this succession could be related to slope sedimentation fed by a non-glaciated coast, with a glacial source inside the continent (Schemiko et al., 2019). However, the faciological features described in the ESFD association support a glacial marginal system where the glacial source is close to the depositional site. About the slope setting propose by several authors for this system (Castro, 1980; Canuto, 1993; Schemiko et al., 2019), we agree in some way with this interpretation. However, in our understanding, the slope sedimentation at the study area has some specific

characteristics, which need to be discussed. Some authors have argued that when grounding-line fans are deposited in contact with a submarine slope (which seems to be or setting), they could develop bimodal sedimentation. This style is composed of hyperpycnal turbidites (concentrated and hyperconcentrated flows in Mulder and Alexander (2001) sense) and debris flow (Cofaigh et al., 2018; Bellwald et al., 2020). These ice-contact fans are called trough-mouth fans (Tripsanas and Piper, 2008; Cofaigh et al., 2018; Bellwald et al., 2020). In our understanding, the facies described in our system are very similar to this style of deposition. Furthermore, we don't identify studies that discuss flow transformation in a jet model in a glaciogenic slope context, so these could be the first facies-based work to deal with these settings.

Above the deposits of the ESFD association, we describe mainly massive sandstones and diamictites (where some are deformed) and some clast-supported conglomerates that represent the LSFD deposits (fig. 12). These deposits comprehend a change in the dynamics of the fan. The main difference between these deposits to the ESFD association is that we don't observe bedforms that could give us any information about the flow regime. Here, we keep that the density flows which originated the sandy and gravelly beds are mainly concentrated flows, with some hyperconcentrated being responsible for the genesis of clast-supported conglomerates. Despite that, the origin of the diamictites has differences from the deposition of the ESFD. According to the muddy fabric of the diamictites, we observe that the process which generated them is probably related to upwelling plumes (Powell and Molnia, 1989; Powell, 1990; Lønne, 1995). However, similar sandy beds of the diamictites of the ESFD are also observed in the LSFD association. Due to these characteristics, we also suggest that debris flow with a hydroplaning component could be acted on the deposition of the diamictites (Mohrig et al., 1998; Sohn, 2000).

In the upper portion of LSFD, we observed that the beds of sandstones and diamictites present resedimentation features. The main features that are kept in the deformed facies of the LSFD are deformed beds of sandstones that present a fluidized aspect and can be mixed with the diamictite beds. In our interpretation, these deformed facies marks start the collapse of the fan. In our view, these deformed sediments are probably related to MTD (mainly slumps) due to the

character of the deformed facies (Dott, Jr, 1963; Nardin et al., 1979; Martinsen, 1994; Posamentier and Martinsen, 2011). Analyzing these deformation features together with the uppermost diamictites of the SCD association, we suggest that these deposits could result from a progressive deformation and homogenization of the previous fan deposits (Dott, Jr, 1963; Nemec, 1990; Martinsen, 1994; Eyles and Eyles, 2000; Strachan, 2008; Rodrigues et al., 2020).

In our perception, these deformations occur in a submarine slope. This proposition follows our sedimentary model to deposition the ESFD and LSFD deposits of a grounding-line fan set up in the slope break. The occurrence of MTD is common in these settings (Cofaigh et al., 2018). High meltwater discharges linked with the deposition of the sediments directly above the submarine slopes could trigger the collapse of the fan and the accumulation of the MTD. In our view, these MTD present three different stages of deformation and homogenization. Firstly, the uppermost deposits in the LSFD. We observe just a deformation of the sandstone and diamictite beds in these facies, but we can still see the original planes of deposition in most of the record. In our model, these facies represent the most proximal portion of the MTD (Nemec, 1990; Martinsen, 1994; Moscardelli et al., 2006; Posamentier and Martinsen, 2011). Above these deformed sandstones and diamictites, we observe the second facies representing the collapse of the fan, the heterogeneous ressedimented diamictites (Dm(r-ht) facies). In these facies, the MTD starts to present processes of mixing and desegregation, showing different levels of matrix content inside the diamictite (Nemec, 1990; Martinsen, 1994; Eyles and Eyles, 2000; Strachan, 2008; Rodrigues et al., 2020). In the heterogeneous diamictites, the level of matrix content is directly related to the size of basinal clasts (sandstones and conglomerates). According to some authors, this reduction in the size of basinal clasts is related to processes of mixing and desegregation, where more homogeneous diamictites are directly related to the actions of these processes (Martinsen, 1994; Eyles and Eyles, 2000; Strachan, 2008; Rodrigues et al., 2020). We interpreted these diamictites as an intermediate portion of the collapse of the fan deposits. In our model, the processes of mixing and desegregation continue to act along the MTD, which leads to the deposition of homogeneous diamictites (Dm(r-hm) facies) in the last portion of the MTD. The progressive mixing and desegregation of the basinal clasts result in a homogenized product in the distal

portion of the MTD (Eyles and Eyles, 2000; Strachan, 2008; Rodrigues et al., 2020). This homogenization is marked by the high matrix content and the significant reduction of the size of the intrabasinal clasts, which are restricted only to sheared sandstone beds with a centimetric size.

In summary, the system's evolution is represented by four stages of sedimentation controlled by different processes. I) A glacial advance over a marine environment deforming the previous deposits and generating a glaciotectonized substrate (fig. 16). II) The early-stage of deposition of a glacial environment (fig. 16) containing a subglacial portion (grounding-zone wedge) and the deposition of a grounding line fan in the subaquatic portion. In the subaquatic environment, we interpret the domination of processes (concentrated and hyperconcentrated flows) related to a jet-efflux model. At these processes, we identify facies since the hydraulic jump (scour-fills, backsets, and clast segregation) in the most proximal portion of the fan; the deposition of supercritical bedforms (lenticular antidunes); the transition to subcritical flow (humpback dunes); and the establishment of a subcritical flow in a more distal portion (subcritical dunes). After that, the flow tends to lose momentum and transit to a gravity-dominated flow in the lee side of the mouth-bars. This transition leads to the deposition of sinusoidal antidunes and climbing ripples distally. We also observe that the sedimentation at the ice margin has a significant contribution of debris flows with a hydroplaning component, turbidity currents, and ice-rafting debris. III) The late stage of the fan (fig. 16) is controlled by concentrated (and some hyperconcentrated) flows at the ice margin. But here, we cannot identify any bedforms that provide any information about the flow regime. We also verify that upwelling plumes, debris flow, and ice-rafting debris are essential components of this fan stage. IV) The last stage is marked by the ressedimentation of the fan deposits as MTD in a submarine slope (fig. 16). These mass-flows present different internal deformation and homogenization stages marked by the progressive increment in the mixing and desegregation of the initial protolith.

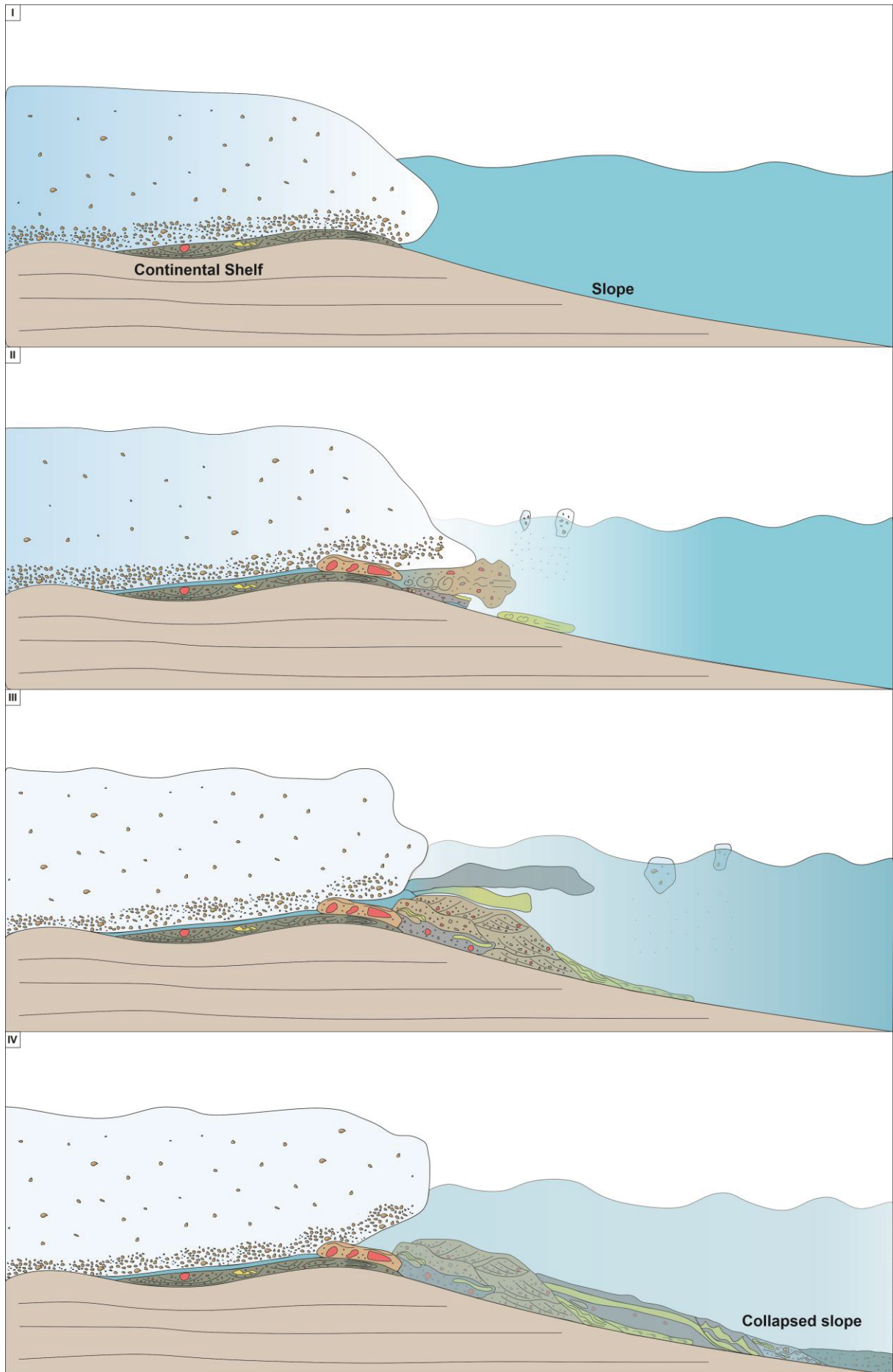


Figure 16 – Schematic depositional model proposed for the evolution of the grounding-line fan system at the Presidente Getúlio region (out of scale).

4.6.2 Depositional events and sediment source

During the fan deposition, we observe a complex architecture built up by several processes related mainly to a wall jet dynamic (concentrated, hyperconcentrated density flows, and upwelling plumes) and debris flow. In our view, this dynamic is strictly controlled by discharges associated with the glacier dynamics. Some studies try to associate the depositional architecture of the fans with these dynamics (Russell and Arnott, 2003; Winsemann et al., 2009). In our opinion, the fan deposition is linked to multiple single-event floods rather than attributed to seasonal floods. During the fan sedimentation, we don't observe any deposit related to varves or even thick mudstone deposits that could suggest huge gaps during the system's deposition. Analyzing the architecture of the fan, we observe that two main mechanisms are responsible for the deposition of the system, the wall-jets and the debris flow. The dominance of these two processes at the fan records a bimodal sedimentation of the system that intercalates conglomerates and sandstones related to the wall-jets, and diamictites, which result from the debris flow deposition. In our view, this bimodality on the deposits results from multiple events of deposition, probably related to single flood events. To help with this analysis, we can compare our record with other similar deposits in the Pleistocene. If we analyze recent deposits, we will observe that the occurrence of small single-flood events or flood events of high magnitude will affect in a different way the facies tract observed in the resulting deposits. In records interpreted as multiple small flood events, the final deposits tend to have frequent vertical intercalation of the facies and their related bedforms (Hornung et al., 2007; Winsemann et al., 2009; Lang et al., 2017). However, if we compare with the records which associated the deposition of the fan with a single-flood event of high magnitude, we will verify that the vertical interbreeding of facies and bedforms is not frequent (Russell and Arnott, 2003; Lang and Winsemann, 2013). In these records, the bedforms vary more laterally, so to understand these records, we need to analyze multiple outcrops laterally, to understand the transition of the flow and their respective bedforms. Examining the deposition of the Presidente Getúlio grounding-line fan, we will observe that the bedforms vary not only laterally but vertically, as observed in the sedimentological logs (fig. 3) and the PT outcrop (fig. 7,8). This analysis suggests that the building of

the fans is composed of multiple single flood events according to these vertical variations.

We already recognize that the fan building is linked to multiple small floods. However, we also want to understand the source that fed sediments to the deposition of the system. Schemiko et al. (2019) made a paleocurrent analysis for the system previously that in their interpretation are related to the action of hyperpycnal flows in a submarine slope. Their data suggest a paleotransport trend that goes to SSE and SSW (Schemiko et al., 2019). In their view, this system was fed by glaciers located towards the north inside the continent (Mottin et al., 2018; Schemiko et al., 2019). Their interpretation is corroborated by Mottin et al. (2018), who interpreted a glacial source towards the north based on the paleocurrents of glacial and glacial-influenced deposits with a similar age in the north of Paraná state. However, our paleocurrent data suggest a different source to the deposition of the succession. Observing our rose diagrams (fig. 15), we can see a primary trend of paleotransport to NW. This trend is similar to several other glacial successions in the Santa Catarina state deposits of the Itararé Group (Barbosa, 1940; Carvalho, 1940; Rocha-Campos et al., 1988; Santos et al., 1992; Puigdomenech et al., 2014; Aquino et al., 2016; Rosa et al., 2016, 2021; Fallgatter and Paim, 2019). This direction suggests that the source of the glacial sediments that compose the fan are located toward SE.

In the southern portion of the African continent, we observe several glacial deposits deposited during the LPIA (Crowell and Frakes, 1975; Martin, 1981; Visser, 1987). In Namibia, authors observed proximal glacial facies deposited in paleovalleys where the paleoflow indicate that these glaciers flowed towards the north (Paraná Basin) (Martin, 1981; Visser, 1987; Santos et al., 1996). In our interpretation, these glaciers advance toward the Paraná Basin during the deposition of the middle portion of the Rio do Sul formation. Furthermore, based on our and other authors' data, we suggest that the advance of these glaciers towards the Paraná Basin occurs in a marine environment (Castro, 1980; Canuto, 1993; Puigdomenech et al., 2014; Fallgatter and Paim, 2019; Schemiko et al., 2019), this is arguable due to the facies deposited below, above and during the deposition of the Presidente Getúlio grounding-line fan.

4.7 Conclusions

- The foliated diamictites at the base of the succession are interpreted as a glaciotectonized substrated promoted by a glacier advance during the deposition of the Rio do Sul Formation;
- The deposition of the EFSD and LSFD associations represent a glacial-marginal system with a subglacial portion (grounding-zone wedge) and a subaquatic portion (grounding-line fan) deposited in the slope break;
- Our work was the first one to identify bedforms related to the action of supercritical flows in grounding-line fan settings at the LPIA;
- The bedforms deposited in the ESFD association are directly related to waxing (momentum dominated) and waning (underflows) concentrated and hyperconcentrated flows in a wall-jet context;
- The deposits of the ESFD represent a complete flow transition following a wall-jet model: the hydraulic jump (scour-fills, backsets, and clast clusters); the deposition of supercritical flow bedforms (lenticular antidunes); their transition to subcritical flow (humpback dunes); and the establishment of a genuine subcritical flow (subcritical dunes);
- We identify that distally the wall-jets deposits represent bedforms related to the transformation of momentum-dominated jets to underflows that also transit from supercritical to subcritical flows. These bedforms are sinusoidal antidunes, deposited in the lee side of the mouth-bar macroforms and climbing ripples;
- The occurrence of tool-marks and mud intraclasts in deposits of the ESFD suggest that the incorporation of mud could help the flow in the loss of momentum and consequently the transition from momentum-dominated to gravity-dominated flows;
- Debris flows are also great contributors to the fan building. It's common along with these cohesive flows the occurrence of hydroplaning at the head of the flows, which leads to the deposition of surge-like turbidites;
- Turbidity currents, ice-rafting, and upwelling-plumes also contribute to the deposition of the fan;

- The accumulation of deformed sandstones and diamictites of the LSFD and the deposition of heterogeneous and homogeneous diamictites of the SCD are interpreted as MTD, representing the fan's collapse;
- In our view, the progressive deformation starting from the deformed deposits of the LSFD to the homogenous diamictites of the SCD represent processes of mixing and desegregation during the evolution of the MTD in a submarine slope;
- The architecture of the fan represents a bimodal sedimentation controlled mainly by wall-jets and debris flows. We interpret that the vertical intercalation of facies and bedforms related to these two main processes is related to multiple single-flood events.
- According to our paleocurrent analysis, the sediments of the fan were provided by glaciers located towards the south-eastern (probably Namibia).
- Finally, the fan represents a new glacier advance towards the Paraná Basin during the last stages of deposition of the Itararé Group. Our data suggest that this advance took place in a marine environment.

5. CONSIDERAÇÕES FINAIS

A metodologia aplicada neste estudo se mostrou satisfatória para melhorar o conhecimento acerca de sistemas glácio-marginais do Paleozoico superior da Bacia do Paraná. Dentro deste trabalho, conseguimos visualizar e caracterizar formas de leito que antes não haviam sido relatadas para este tipo de sistema deposicional em todo o registro da Glaciação Neopaleozoica. A caracterização de formas de leito de fluxo supercrítico neste contexto, mostra que ainda podemos avançar na compreensão dos processos atuantes nestes sistemas deposicionais e em um melhor entendimento de como transitam os regimes de fluxo em sucessões Neopaleozoicas.

Verificamos também, que este tipo de sistema deposicional pode ter uma sedimentação dinâmica, representada por múltiplos processos de deposição como os *wall-jets*, fluxos de detritos, *underflows*, decantação por gelo flutuante, plumas de detritos, fluxos de massa, etc. Estudar essa diversidade de processos em outras sucessões pode nos auxiliar em uma melhor compreensão dos eventos de

deposição e em como as descargas de água de degelo podem controlar a dinâmica do ambiente deposicional, evidenciando ciclos de deglaciação.

Por fim, sugerimos que sejam propostos mais trabalhos com enfoque nas transições de fluxo em sistemas glácio-marginais e glácio influenciados depositados durante a GNP. A realização desses trabalhos é essencial para que possamos compreender com mais clareza se depósitos glácio influenciados depositados durante esse período, são controlados por múltiplos eventos de descarga ou por eventos únicos. Além disso, a caracterização destes depósitos pode nos auxiliar em uma melhor compreensão da sazonalidade das descargas glaciais durante a GNP.

REFERÊNCIAS

- Aquino, C.D., Buso, V.V., Faccini, U.F., Milana, J.P., Paim, P.S.G., 2016. Facies and depositional architecture according to a jet efflux model of a late Paleozoic tidewater grounding-line system from the Itararé Group (Paraná Basin), southern Brazil. *J. South Am. Earth Sci.* 67, 180–200. <https://doi.org/10.1016/j.jsames.2016.02.008>
- Baas, J.H., Best, J.L., 2008. The dynamics of turbulent, transitional and laminar clay-laden flow over a fixed current ripple. *Sedimentology* 55, 635–666. <https://doi.org/10.1111/j.1365-3091.2007.00916.x>
- Barbosa, O., 1940. Estrias produzidas por gelo permo-carbonífero. *Mineração e Metal.* 4, 272–273.
- Batchelor, C.L., Dowdeswell, J.A., 2015. Ice-sheet grounding-zone wedges (GZWs) on high-latitude continental margins. *Mar. Geol.* 363, 65–92. <https://doi.org/https://doi.org/10.1016/j.margeo.2015.02.001>
- Bellwald, B., Planke, S., Becker, L.W.M., Myklebust, R., 2020. Meltwater sediment transport as the dominating process in mid-latitude trough mouth fan formation. *Nat. Commun.* 11, 1–10. <https://doi.org/10.1038/s41467-020-18337-4>
- Boulton, G., 1979. Processes of Glacier erosion on Different Substrata. *J. Glaciol.* 23, 15–38. <https://doi.org/doi:10.3189/S0022143000029713>
- Brennand, T., 1994. Macroforms, large bedforms and rhythmic sedimentary sequences in subglacial eskers, south-central Ontario: implications for esker genesis and meltwater regime. *Sediment. Geol.* 91, 9–55. [https://doi.org/10.1016/0037-0738\(94\)90122-8](https://doi.org/10.1016/0037-0738(94)90122-8)
- Canuto, J., 1993. Fácies e ambientes de sedimentação da Formação Rio do Sul (Permiano), Bacia do Paraná, na região de Rio do Sul, Estado de Santa Catarina. *Inst. Geociências da USP.*
- Carling, P.A., 1990. Particle over-passing on depth-limited gravel bars. *Sedimentology* 37, 345–355. <https://doi.org/10.1111/j.1365-3091.1990.tb00963.x>
- Cartigny, M.J.B., Ventra, D., Postma, G., van Den Berg, J.H., 2014. Morphodynamics and sedimentary structures of bedforms under supercritical-flow conditions: New insights from flume experiments. *Sedimentology* 61, 712–748. <https://doi.org/10.1111/sed.12076>
- Carvalho, P.F., 1940. Estrias glaciais em granodiorito sobposto ao Gondwana de Santa Catarina. *Mineração e Metal.* 4, 271–272.
- Castro, J.C., 1980. Fácies, ambientes e seqüências deposicionais das formações Rio do Sul e Rio Bonito, leste de Santa Catarina., in: *Anais Do XXXI Congresso Brasileiro de Geologia*. Camboriú, pp. 283–299.
- Cofaigh, C.O., Hogan, K.A., Jennings, A., Callard, S.L., Dowdeswell, J.A., Noormets,

R., Evans, J., 2018. The role of meltwater in high-latitude trough-mouth fan development: The Disko Trough-Mouth Fan, West Greenland. *Mar. Geol.* 402, 17–32. <https://doi.org/10.1016/j.margeo.2018.02.001>

Crowell, J.C., Frakes, L.A., 1970. Phanerozoic glaciation and the causes of ice ages. *Am. J. Sci.* 268, 193–224.

Crowell, J.C., Frakes, L.A., 1975. The Late Paleozoic Glaciation, in: Campbell, K.S. (Ed.), *Godwana Geology*. Australian National University Press, Canberra, pp. 313–331.

Dietrich, P., Hofmann, A., 2019. Ice-margin fluctuation sequences and grounding zone wedges: The record of the Late Palaeozoic Ice Age in the eastern Karoo Basin (Dwyka Group, South Africa). *Depos. Rec.* 5, 247–271. <https://doi.org/10.1002/dep2.74>

Dott, Jr, R.H., 1963. Dynamics of Subaqueous Gravity Depositional Processes. *Am. Assoc. Pet. Geol. Bull.* 47, 104–128. <https://doi.org/10.1306/bc743973-16be-11d7-8645000102c1865d>

Eyles, C.H., Eyles, N., 2000. Subaqueous mass flow origin for Lower Permian diamictites and associated facies of the Grant Group, Barrow Terrace, Canning Basin, Western Australia. *Sedimentology* 47, 343–356. <https://doi.org/10.1046/j.1365-3091.2000.00295.x>

Eyles, C.H., Eyles, N., França, A.B., 1993. Glaciation and tectonics in an active intracratonic basin: the Late Palaeozoic Itararé Group, Paraná Basin, Brazil. *Sedimentology* 40, 1–25. <https://doi.org/10.1111/j.1365-3091.1993.tb01087.x>

Eyles, C.H., Eyles, N., Gostin, V.A., 1998. Facies and allostratigraphy of high-latitude, glacially influenced marine strata of the Early Permian southern Sydney Basin, Australia. *Sedimentology* 45, 121–162. <https://doi.org/10.1046/j.1365-3091.1998.00138.x>

Eyles, C.H., Eyles, N., Miall, A.D., 1985. Models of glaciomarine sedimentation and their application to the interpretation of ancient glacial sequences. *Palaeogeogr. Palaeoclimatol. Palaeoecol.* 51, 15–84. [https://doi.org/10.1016/0031-0182\(85\)90080-X](https://doi.org/10.1016/0031-0182(85)90080-X)

Eyles, N., Eyles, C.H., McCabe, A.M., 1989. Sedimentation in an ice-contact subaqueous setting: The mid-Pleistocene “North Sea Drifts” of Norfolk, U.K. *Quat. Sci. Rev.* 8, 57–74. [https://doi.org/10.1016/0277-3791\(89\)90021-8](https://doi.org/10.1016/0277-3791(89)90021-8)

Fallgatter, C., Paim, P.S.G., 2019. On the origin of the Itararé Group basal nonconformity and its implications for the Late Paleozoic glaciation in the Paraná Basin, Brazil. *Palaeogeogr. Palaeoclimatol. Palaeoecol.* 531, 108225. <https://doi.org/10.1016/j.palaeo.2017.02.039>

Fedorchuk, N.D., Isbell, J.L., Griffis, N.P., Vesely, F.F., Rosa, E.L.M., Montañez, I.P., Mundil, R., Yin, Q.Z., Iannuzzi, R., Roesler, G., Pauls, K.N., 2019. Carboniferous

glaciotectonized sediments in the southernmost Paraná Basin, Brazil: Ice marginal dynamics and paleoclimate indicators. *Sediment. Geol.* 389, 54–72. <https://doi.org/10.1016/j.sedgeo.2019.05.006>

Franca, A.B., Potter, P.E., 1988. Estratigrafia, ambiente deposicional e análise de reservatório do Grupo Itararé (Permocarbonífero), Bacia do Paraná (Parte 1). *Bol. Geociências - Petrobras* 2, 147–191.

Goscombe, B.D., Passchier, C.W., Hand, M., 2004. Boudinage classification: End-member boudin types and modified boudin structures. *J. Struct. Geol.* 26, 739–763. <https://doi.org/10.1016/j.jsg.2003.08.015>

Hornung, J.J., Asprion, U., Winsemann, J., 2007. Jet-efflux deposits of a subaqueous ice-contact fan, glacial Lake Rinteln, northwestern Germany. *Sediment. Geol.* 193, 167–192. <https://doi.org/10.1016/j.sedgeo.2005.11.024>

Hoyal, D.C.J.D., Van Wagoner, J.C., Adair, N.L., Deffenbaugh, M., Li, D., Sun, T., Huh, C., Giffin, D.E., 2003. Sedimentation from jets: a depositional model for clastic deposits of all scales and environments. *Search Discov. Artic.* 40082 (Online-Journal; AAPG/ Datapages, Inc., 1444 South Boulder, Tulsa, OK, 74119, USA).

Isbell, J.L., Henry, L.C., Gulbranson, E.L., Limarino, C.O., Fraiser, M.L., Koch, Z.J., Ciccioli, P.L., Dineen, A.A., 2012. Glacial paradoxes during the late Paleozoic ice age: Evaluating the equilibrium line altitude as a control on glaciation. *Gondwana Res.* 22, 1–19. <https://doi.org/10.1016/j.gr.2011.11.005>

Isbell, J.L., Miller, M.F., Wolfe, K.L., Lenaker, P.A., 2003. Timing of late Paleozoic glaciation in Gondwana: Was glaciation responsible for the development of northern hemisphere cyclothems? *Spec. Pap. Geol. Soc. Am.* 370, 5–24. <https://doi.org/10.1130/0-8137-2370-1.5>

Ives, L.R.W., Isbell, J.L., 2021. A lithofacies analysis of a south polar glaciation in the early Permian: Pagoda formation, Shackleton Glacier Region, Antarctica. *J. Sediment. Res.* 91, 611–635. <https://doi.org/10.2110/jsr.2021.004>

Koch, Z.J., Isbell, J.L., 2013. Processes and products of grounding-line fans from the Permian Pagoda Formation, Antarctica: Insight into glacial conditions in polar Gondwana. *Gondwana Res.* 24, 161–172. <https://doi.org/10.1016/j.gr.2012.10.005>

Lang, J., Fedele, J.J., Hoyal, D.C.J.D., 2021a. Three-dimensional submerged wall jets and their transition to density flows: Morphodynamics and implications for the depositional record. *Sedimentology* 68, 1297–1327. <https://doi.org/10.1111/sed.12860>

Lang, J., Le Heron, D.P., Van den Berg, J.H., Winsemann, J., 2021b. Bedforms and sedimentary structures related to supercritical flows in glacial settings, *Sedimentology*. <https://doi.org/10.1111/sed.12776>

Lang, J., Sievers, J., Loewer, M., Igel, J., Winsemann, J., 2017. 3D architecture of cyclic-step and antidune deposits in glacial subaqueous fan and delta settings:

Integrating outcrop and ground-penetrating radar data. *Sediment. Geol.* 362, 83–100. <https://doi.org/10.1016/j.sedgeo.2017.10.011>

Lang, J., Winsemann, J., 2013. Lateral and vertical facies relationships of bedforms deposited by aggrading supercritical flows: From cyclic steps to humpback dunes. *Sediment. Geol.* 296, 36–54. <https://doi.org/10.1016/j.sedgeo.2013.08.005>

Limarino, C.O., Césari, S.N., Spalletti, L.A., Taboada, A.C., Isbell, J.L., Geuna, S., Gulbranson, E.L., 2014. A paleoclimatic review of southern South America during the late Paleozoic: A record from icehouse to extreme greenhouse conditions. *Gondwana Res.* 25, 1396–1421. <https://doi.org/10.1016/j.gr.2012.12.022>

Long, D., Rajaratnam, N., Steffler, P.M., Smy, P.R., 1991. Structure of flow in hydraulic jump. *J. Hydraul. Res.* 29, 207–218. <https://doi.org/10.1080/00221689109499004>

Long, D., Steffler, P.M., Rajaratnam, N., 1990. LDA study of flow structure in submerged hydraulic jump. *J. Hydraul. Res.* 28, 437–460. <https://doi.org/10.1080/00221689009499059>

Lønne, I., 1995. Sedimentary facies and depositional architecture of ice-contact glaciomarine systems. *Sediment. Geol.* 98, 13–43. [https://doi.org/10.1016/0037-0738\(95\)00025-4](https://doi.org/10.1016/0037-0738(95)00025-4)

Lowe, D., 1975. Water escape structures in coarse-grained sediments. *Sedimentology* 22, 157–204. <https://doi.org/10.1111/j.1365-3091.1975.tb00290.x>

Lowe, D., 1982. Sediment gravity flows: II. Depositional models with special reference to the deposits of high-density turbidity currents. *J. Sediment. Petrol.* 52, 279–297.

Martin, H., 1981. The Late Palaeozoic Dwyka Group of the South Kalahari Basin in Namibia and Botswana and the subglacial valleys of the Kaokoveld in Namibia, in: Hambrey, M., Harland, W. (Eds.), *Earth's Pre-Pleistocene Glacial Record*. Cambridge University Press, pp. 61–66.

Martinsen, O.J., 1989. Styles of soft-sediment deformation on a Namurian (Carboniferous) delta slope, Western Irish Namurian Basin, Ireland. *Geol. Soc. Spec. Publ.* 41, 167–177. <https://doi.org/10.1144/GSL.SP.1989.041.01.13>

Martinsen, O.J., 1994. Mass movements, in: Maltman, A. (Ed.), *The Geological Deformation of Sediments*. London, pp. 127–165. [https://doi.org/10.1016/0040-1951\(95\)00204-9](https://doi.org/10.1016/0040-1951(95)00204-9)

McCarroll, D., Rijdsdijk, K.F., 2003. Deformation styles as a key for interpreting glacial depositional environments. *J. Quat. Sci.* 18, 473–489. <https://doi.org/10.1002/jqs.780>

Milani, E.J., Melo, J.H.G., P.A., S., Fernandes, L., França, A.B., 2007. Bacia do paran . *Bol. Geociencias da Petrobras* 15, 265–287.

Mohrig, D., Whipple, K.X., Hondzo, M., Ellis, C., Parker, G., 1998. Hydroplaning of

subaqueous debris flows. *Bull. Geol. Soc. Am.* 110, 387–394. [https://doi.org/10.1130/0016-7606\(1998\)110<0387:HOSDF>2.3.CO;2](https://doi.org/10.1130/0016-7606(1998)110<0387:HOSDF>2.3.CO;2)

Moscardelli, L., Wood, L., Mann, P., 2006. Mass-transport complexes and associated processes in the offshore area of Trinidad and Venezuela. *Am. Assoc. Pet. Geol. Bull.* 90, 1059–1088. <https://doi.org/10.1306/02210605052>

Mottin, T.E., Vesely, F.F., de Lima Rodrigues, M.C.N., Kipper, F., de Souza, P.A., 2018. The paths and timing of late Paleozoic ice revisited: New stratigraphic and paleo-ice flow interpretations from a glacial succession in the upper Itararé Group (Paraná Basin, Brazil). *Palaeogeogr. Palaeoclimatol. Palaeoecol.* 490, 488–504. <https://doi.org/10.1016/j.palaeo.2017.11.031>

Mulder, T., Alexander, J., 2001. The physical character of subaqueous sedimentary density flow and their deposits. *Sedimentology* 48, 269–299. <https://doi.org/10.1046/j.1365-3091.2001.00360.x>

Nardin, T.R., Hein, F.J., Gorsline, D.S., Edwards, B.D., 1979. A review of mass movement processes, sediment and acoustic characteristics, and contrasts in slope and base-of-slope systems versus canyon-fan-basin floor systems. *SEPM Spec. Publ.* 27, 61–73. <https://doi.org/10.2110/pec.79.27.0061>

Nemec, W., 1990. Aspects of Sediment Movement on Steep Delta Slopes, in: *Coarse-Grained Deltas*. pp. 29–73. <https://doi.org/10.1002/9781444303858.ch3>

Peakall, J., Best, J., Baas, J.H., Hodgson, D.M., Clare, M.A., Talling, P.J., Dorrell, R.M., Lee, D.R., 2020. An integrated process-based model of flutes and tool marks in deep-water environments: Implications for palaeohydraulics, the Bouma sequence and hybrid event beds. *Sedimentology* 67, 1601–1666. <https://doi.org/10.1111/sed.12727>

Phillips, E.R., 2018. Glacitectonics, in: Menzies, J., van der Meer, J. (Eds.), *Past Glacial Environments: Second Edition*. Elsevier, Amsterdam, pp. 467–502. <https://doi.org/10.1016/B978-0-08-100524-8.00014-2>

Posamentier, H., Martinsen, O.J., 2011. The Character and Genesis of Submarine Mass-Transport Deposits: Insights from Outcrop and 3D Seismic Data. *SEPM Spec. Publ.* 7–38. <https://doi.org/10.2110/sepm.096.007>

Powell, R.D., 1990. Glacimarine processes at grounding-line fans and their growth to ice-contact deltas. *Geol. Soc. Spec. Publ.* 53, 53–73. <https://doi.org/10.1144/GSL.SP.1990.053.01.03>

Powell, R.D., Alley, R.B., 1997. Grounding-Line Systems: Processes, Glaciological Inferences and the Stratigraphic Record, in: *Geology and Seismic Stratigraphy of the Antarctic Margin*. pp. 169–187. <https://doi.org/10.1029/ar071p0169>

Powell, R.D., Molnia, B.F., 1989. Glacimarine sedimentary processes, facies and morphology of the south-southeast Alaska shelf and fjords. *Mar. Geol.* 85, 359–390. [https://doi.org/10.1016/0025-3227\(89\)90160-6](https://doi.org/10.1016/0025-3227(89)90160-6)

Puigdomenech, C.G., Carvalho, B., Paim, P.S.G., Faccini, U.F., 2014. Lowstand turbidites and delta systems of the Itararé group in the Vidal Ramos region (SC), southern Brazil. *Brazilian J. Geol.* 44, 529–544. <https://doi.org/10.5327/Z23174889201400040002>

Rajaratnam, N., Subramanyan, S., 1986. Plane turbulent denser wall jets and jumps: Jets parietaux et ressauts plans en régime turbulent dans les milieux moins denses. *J. Hydraul. Res.* 24, 265–280. <https://doi.org/10.1080/00221688609499306>

Roberts, P.J., Maile, K., Daviero, G., 2001. Mixing in stratified jets. *J. Hydraul. Eng.* 127, 194–200. [https://doi.org/https://doi.org/10.1061/\(ASCE\)0733-9429\(2001\)127:3\(194\)](https://doi.org/https://doi.org/10.1061/(ASCE)0733-9429(2001)127:3(194))

Rocha-Campos, A.C., Machado, L.C.R., Santos, P.R., Canuto, J.R., Castro, J.C., 1988. Pavimento estriado da Glaciação Neopaleozoica em Alfredo Wagner, Santa Catarina, Brasil. *Bol. Geociências da USP* 19, 39–46. [https://doi.org/10.1637/1933-5334\(2007\)2](https://doi.org/10.1637/1933-5334(2007)2)

Rodrigues, M.C., Trzaskos, B., Alsop, I., Vesely, F., 2020. Making a homogenite: An outcrop perspective into the evolution of deformation within mass-transport deposits. *Mar. Pet. Geol.* 112, 104033. <https://doi.org/10.1016/j.marpetgeo.2019.104033>

Rosa, E.L., Vesely, F.F., França, A.B., 2016. A review on late Paleozoic ice-related erosional landforms in the Paraná Basin: Origin and paleogeographical implications. *Brazilian J. Geol.* 46, 147–166. <https://doi.org/10.1590/2317-4889201620160050>

Rosa, E.L., Vesely, F.F., Isbell, J.L., Fedorchuk, N.D., 2021. As geleiras carboníferas no sul do Brasil. *Bol. Parana. Geociências* 78, 1–20. <https://doi.org/10.5380/geo.v75i0.46519>

Rosa, E.L.M., Vesely, F.F., Isbell, J.L., Kipper, F., Fedorchuk, N.D., Souza, P.A., 2019. Constraining the timing, kinematics and cyclicity of Mississippian-Early Pennsylvanian glaciations in the Paraná Basin, Brazil. *Sediment. Geol.* 384, 29–49. <https://doi.org/10.1016/j.sedgeo.2019.03.001>

Russell, A.J., 2007. Controls on the sedimentology of an ice-contact jökulhlaup-dominated delta, Kangerlussuaq, west Greenland. *Sediment. Geol.* 193, 131–148. <https://doi.org/10.1016/j.sedgeo.2006.01.007>

Russell, H.A.J., Arnott, R.W.C., 2003. Hydraulic-Jump and Hyperconcentrated-Flow Deposits of a Glacigenic Subaqueous Fan: Oak Ridges Moraine, Southern Ontario, Canada. *J. Sediment. Res.* 73, 887–905. <https://doi.org/10.1306/041103730887>

Santos, P.R., Rocha-Campos, A.C., Canuto, J.R., 1992. Estruturas de arrasto de icebergs em ritmo do Subgrupo Itararé (Neopaleozoico), Trombudo Central, SC. *Bol. I-G USP* 23, 1–18.

Santos, P.R., Rocha-Campos, A.C., Canuto, J.R., 1996. Patterns of late Palaeozoic deglaciation in the Parana Basin, Brazil. *Palaeogeogr. Palaeoclimatol. Palaeoecol.*

125, 165–184. [https://doi.org/10.1016/S0031-0182\(96\)00029-6](https://doi.org/10.1016/S0031-0182(96)00029-6)

Schemiko, D.C.B., Vesely, F.F., Rodrigues, M.C.N.L., 2019. Deepwater to fluvio-deltaic stratigraphic evolution of a deglaciated depocenter: The early Permian Rio do Sul and Rio Bonito formations, southern Brazil. *J. South Am. Earth Sci.* 95, 102260. <https://doi.org/10.1016/j.jsames.2019.102260>

Schneider, R.L., Muhlmann, H., Tommasi, E., Medeiros, R.A., Daemon, R.F., Nogueira, A.A., 1974. Revisão estratigráfica da Bacia do Paraná, in: *Anais Do XXVIII Congresso Brasileiro de Geologia*. pp. 41–65.

Sohn, Y.K., 2000. Depositional processes of submarine debris flows in the miocene fan deltas, Pohang Basin, SE Korea with special reference to flow transformation. *J. Sediment. Res.* 70, 491–503. <https://doi.org/10.1306/2DC40922-0E47-11D7-8643000102C1865D>

Strachan, L.J., 2008. Flow transformations in slumps: A case study from the Waitemata Basin, New Zealand. *Sedimentology* 55, 1311–1332. <https://doi.org/10.1111/j.1365-3091.2007.00947.x>

Thomas, G.S.P., Connell, R.J., 1985. Iceberg drop, dump, and grounding structures from Pleistocene glacio-lacustrine sediments, Scotland. *J. Sediment. Petrol.* 55, 243–249. <https://doi.org/10.1306/212f8689-2b24-11d7-8648000102c1865d>

Tripsanas, E.K., Piper, D.J.W., 2008. Glaciogenic Debris-Flow Deposits of Orphan Basin, Offshore Eastern Canada: Sedimentological and Rheological Properties, Origin, and Relationship to Meltwater Discharge. *J. Sediment. Res.* 78, 724–744. <https://doi.org/10.2110/jsr.2008.082>

Valdez Buso, V., Milana, J.P., di Pasquo, M., Paim, P.S.G., Philipp, R.P., Aquino, C.D., Cagliari, J., Junior, F.C., Kneller, B., 2020. Timing of the Late Palaeozoic glaciation in western Gondwana: New ages and correlations from Paganzo and Paraná basins. *Palaeogeogr. Palaeoclimatol. Palaeoecol.* 544, 109624. <https://doi.org/10.1016/j.palaeo.2020.109624>

Van der Wateren, D.M., 2002. Processes of glaciotectonism, in: Menzies, J. (Ed.), *Modern and Past Glacial Environments*. Butterworth-Heinemann, Oxford, pp. 417–443. <https://doi.org/10.1016/b978-075064226-2/50017-9>

Vesely, F.F., 2001. Análise de sequências em sucessões glaciais: estudo de caso no Grupo Itararé (C-P), nordeste do estado do Paraná. Univesidade Estadual Paulista.

Vesely, F.F., Assine, M.L., 2004. Seqüências e tratos de sistemas deposicionais do Grupo Itararé, norte do estado o Paraná. *Rev. Bras. Geociências* 34, 219–230. <https://doi.org/10.25249/0375-7536.2004342219230>

Vesely, F.F., Assine, M.L., 2006. Deglaciation sequences in the Permo-Carboniferous Itararé Group, Paraná Basin, southern Brazil. *J. South Am. Earth Sci.* 22, 156–168. <https://doi.org/10.1016/j.jsames.2006.09.006>

Vesely, F.F., Kraft, R.P., Mattos, T.R., Schemiko, D.C.B., Berton, F., Monteiro, L.B., Yamassaki, H.G., 2021. Os primeiros turbiditos do Brasil. *Bol. Parana. Geociências* 78, 110–129.

Vesely, F.F., Trzaskos, B., Kipper, F., Assine, M.L., Souza, P.A., 2015. Sedimentary record of a fluctuating ice margin from the Pennsylvanian of western Gondwana: Paraná Basin, southern Brazil. *Sediment. Geol.* 326, 45–63. <https://doi.org/10.1016/j.sedgeo.2015.06.012>

Visser, J.N.J., 1987. The palaeogeography of part of southwestern Gondwana during the Permo-Carboniferous glaciation. *Palaeogeogr. Palaeoclimatol. Palaeoecol.* 61, 205–219. [https://doi.org/10.1016/0031-0182\(87\)90050-2](https://doi.org/10.1016/0031-0182(87)90050-2)

Winsemann, J., Asprion, U., Meyer, T., Schramm, C., 2007. Facies characteristics of Middle Pleistocene (Saalian) ice-margin subaqueous fan and delta deposits, glacial Lake Leine, NW Germany. *Sediment. Geol.* 193, 105–129. <https://doi.org/10.1016/j.sedgeo.2005.11.027>

Winsemann, J., Hornung, J.J., Meinsen, J., Asprion, U., Polom, U., Brandes, C., Bußmann, M., Weber, C., 2009. Anatomy of a subaqueous ice-contact fan and delta complex, Middle Pleistocene, North-west Germany. *Sedimentology* 56, 1041–1076. <https://doi.org/10.1111/j.1365-3091.2008.01018.x>

Winsemann, J., Lang, J., Polom, U., Loewer, M., Igel, J., Pollok, L., Brandes, C., 2018. Ice-marginal forced regressive deltas in glacial lake basins: geomorphology, facies variability and large-scale depositional architecture. *Boreas* 47, 973–1002. <https://doi.org/10.1111/bor.12317>

Zalán, P. V., Wolff, S., Conceição, J.C.J., Astolfi, M.A.M., Vieira, I.S., Appi, V.T., Zanotto, O.A., 1987. Tectonics and sedimentation of the Paraná Basin, in: *Atas Do III Simpósio Sul-Brasileiro de Geologia*. pp. 441–477.